

University of Szeged
Faculty of Pharmacy
Department of Pharmaceutical Technology and Regulatory Affairs
Head: Prof. Dr. Ildikó Csóka

Ph.D. Thesis

Investigation of new innovative techniques for modeling skin
permeation

By
Dr. Stella Zsikó
Pharmacist

Supervisors:
Dr. habil. Szilvia Berkó Ph.D.
Dr. habil. Erzsébet Csányi Ph.D.

Szeged
2021

PUBLICATIONS RELATED TO THE SUBJECT OF THE THESIS

- I. **Stella Zsikó**; Kendra Cutcher; Anita Kovács; Mária Budai-Szűcs; Attila Gácsi; Gabriella Baki; Erzsébet Csányi; Szilvia Berkó
Nanostructured Lipid Carrier Gel for the Dermal Application of Lidocaine: Comparison of Skin Penetration Testing Methods
PHARMACEUTICS 11: 7 Paper: 310, 11 p. (2019) Q1, IF: 4.421
- II. **Stella Zsikó**; Erzsébet Csányi; Anita Kovács; Mária Budai-Szűcs; Attila Gácsi; Szilvia Berkó
Methods to Evaluate Skin Penetration *In Vitro*
SCIENTIA PHARMACEUTICA 87: 3 Paper: 19, 21 p. (2019) Q2, IF: -
- III. **Stella Zsikó**; Erzsébet Csányi; Anita Kovács; Mária Budai-Szűcs; Attila Gácsi; Szilvia Berkó
Novel *In Vitro* Investigational Methods for Modeling Skin Permeation: Skin PAMPA, Raman Mapping
PHARMACEUTICS 12: 9 Paper: 803, 10 p. (2020) Q1, IF: 4.421

PUBLICATIONS NOT RELATED TO THE SUBJECT OF THE THESIS

- I. Szilvia Berkó; **Stella Zsikó**; Gábor Deák; Attila Gácsi; Anita Kovács; Mária Budai-Szűcs; László Pajor; Zoltán Bajory; Erzsébet Csányi
Papaverine hydrochloride containing nanostructured lyotropic liquid crystal formulation as a potential drug delivery system for the treatment of erectile dysfunction
DRUG DESIGN DEVELOPMENT AND THERAPY 12 pp. 2923-2931. 9 p. (2018) Q1, IF: 3.216

PRESENTATIONS RELATED TO THE SUBJECT OF THE THESIS

- I. **Stella Zsikó**; Kendra Cutcher; Gyöngyi Samu; Erzsébet Csányi; Szilvia Berkó
Investigation of Lidocaine-Loaded Nanostructured Lipid Carrier for Dermal Delivery
Medical Conference for PhD Students and Experts of Clinical Sciences, Pécs, 2018 (PP)
- II. **Zsikó Stella**
A humán bőrpenetráció modellezésének lehetőségei
SZTE Orvos- és Gyógyszeréstudományok doktori iskolák II. PhD szimpóziuma, Szeged, 2018 (VP)
- III. **Zsikó Stella**
Az *in vivo* humán bőrpenetráció modellezésének lehetősége a hármas megközelítés módszerrel
XIII. Clauder Ottó Emlékverseny, Budapest, 2018 (VP)
- IV. **Stella Zsikó**; Szilvia Berkó; Erzsébet Csányi
Skin penetration investigational methods
I. Symposium of Young Researchers on Pharmaceutical Technology, Biotechnology and Regulatory Science, Szeged, 2019 (VP)
- V. **Stella Zsikó**; Kendra Cutcher; Anita Kovács; Mária Budai-Szücs; Attila Gácsi; Gabriella Baki; Erzsébet Csányi; Szilvia Berkó
Lidokain tartalmú nanostruktúrált lipid hordozó vizsgálata, különböző bőrpenetrációs mérési módszerek összehasonlítása
Gyógyszertechnológiai és Ipari Gyógyszerészeti Konferencia, Siófok, 2019 (PP)
- VI. **Stella Zsikó**; Erzsébet Csányi; Szilvia Berkó
Study of Skin Penetration Testing Methods
II. Symposium of Young Researchers on Pharmaceutical Technology, Biotechnology and Regulatory Science, Szeged, 2020 (VP)
- VII. Szilvia Berkó; **Stella Zsikó**; Erzsébet Csányi
New perspectives of skin penetration investigational methods for dermal preparations
XVI. Congressus Pharmaceuticus Hungaricus, Debrecen, 2020 (VP)
- VIII. **Stella Zsikó**; Szilvia Berkó; Erzsébet Csányi
New perspectives of skin penetration testing methods

Symposium of Young Researchers on Pharmaceutical Technology, Biotechnology and Regulatory Science, Szeged, 2020 (VP)

- IX. **Stella Zsikó**; Anita Kovács; Mária Budai-Szűcs; Attila Gácsi; Erzsébet Csányi; Szilvia Berkó

Comparison Study of Skin Penetration Testing Methods

12th World Meeting on Pharmaceutics, Biopharmaceutics and Pharmaceutical Technology, Vienna, 2021 (PP)

- X. **Zsikó Stella**, Csányi Erzsébet, Berkó Szilvia

Bőrimitáló membrán vizsgálata félszilárd gyógyszerkészítmények bőrpenetrációs tulajdonságainak jellemzésére

IV. Fiatal technológusok fóruma, 2021 (VP)

PRESENTATIONS NOT RELATED TO THE SUBJECT OF THE THESIS

- I. **Zsikó Stella**

Papaverin-hidroklorid tartalmú topikális készítmény fejlesztése és vizsgálata

XXXIII. Országos Tudományos Diákköri Konferencia, Pécs, 2017 (VP)

- II. **Stella Zsikó**; Gábor Deák; Attila Gácsi; Anita Kovács; Erzsébet Csányi; Szilvia Berkó

Development and investigation of papaverine hydrochloride containing nanostructured systems for the treatment of erectile dysfunction

12th Central European Symposium on Pharmaceutical Technology and Regulatory Affairs, Szeged, 2018 (PP)

TABLE OF CONTENTS

1. INTRODUCTION.....	1
2. LITERATURE BACKGROUND.....	2
2.1. Structure and Function of the Skin.....	2
2.2. Modifying Factors of Skin Permeation.....	3
2.3. General Guidelines of Skin Permeation Testing.....	5
2.4. Techniques for Modelling Permeation through Human Skin.....	6
2.4.1. Diffusion Cells.....	6
2.4.1.1. Types and Properties of Diffusion Cells.....	7
2.4.1.2. Diffusion Test Types.....	8
2.4.1.3. Membranes for Release and Permeation Measurements in Franz Diffusion tests.....	9
2.4.2. Skin Parallel Artificial Membrane Permeability Assay.....	10
2.4.3. The Most Important Experimental Considerations in the Case of Quantitative Methods.....	11
2.4.4. Spectroscopic Methods.....	13
3. EXPERIMENTAL AIMS.....	15
4. MATERIALS AND METHODS.....	16
4.1. Materials.....	16
4.1.1. Lidocaine Containing Nanostructured Lipid Carrier Gel.....	16
4.1.2. Diclofenac Sodium Containing Formulations.....	16
4.1.3. Synthetic and Biological Membranes.....	16
4.2. Methods.....	17
4.2.1. Preparation of the Lidocaine Containing Nanostructured Lipid Carrier Gel (LID-NLC gel).....	17

4.2.2. Preparation of the Diclofenac Sodium Containing Formulations.....	17
4.2.3. Drug Release and Permeation Studies.....	18
4.2.4. Investigation of Skin Permeation with Raman Spectroscopy.....	21
4.2.5. Statistical Analysis.....	21
5. RESULTS AND DISCUSSION.....	22
5.1. Experimental part 1.....	22
5.2. Experimental part 2.....	25
5.2.1. Investigation of Different Semisolid Formulations by Quantitative Methods.....	25
5.2.2. Semiquantitative study: RAMAN Mapping.....	31
6. CONCLUSION.....	33

ABBREVIATIONS

API	active pharmaceutical ingredient
CA	cellulose acetate
DFNa	diclofenac sodium
ECETOC	European Centre for Ecotoxicology and Toxicology of Chemicals
EFSA	European Food Safety Agency
EMA	European Medicines Agency
HSE	heat-separated human epidermis
IVPT	<i>in vitro</i> permeation test
IVRT	<i>in vitro</i> release test
LID	lidocaine
NLC	nanostructured lipid carrier
OECD	Organization for Economic Cooperation and Development
PAMPA	Parallel Artificial Membrane Permeability Assay
PBS	phosphate buffer solution
SC	stratum corneum
USEPA	United States Environmental Protection Agency
WHO/IPCS	World Health Organization International Programme on Chemical Safety

1. INTRODUCTION

Dermal and transdermal formulations are commonly used for carrying drugs to the skin and the underlying tissue, or through the skin for systemic action. In recent years, the number of dermal and transdermal formulations has increased. According to a business study carried out in 2016, the profits from transdermal preparations will rise dramatically by 2024 [1]. The main reason for their popularity is that they have a lot of advantages. For example, avoiding the first pass metabolism of the liver, gastrointestinal tract protection and non-invasive application. The growing market demands require an integrated regulatory environment that can easily identify and evaluate the product properties anywhere in the world and facilitate the research of drug optimization of the penetration through human skin.

Modeling of permeation through the skin is a complex challenge. There are various *in vitro* and *in vivo* methods. The different methods, along with the properties of the product, influence how the system can be tested most effectively. The investigational method is greatly influenced by the predictive ability, time, and labor requirements of the given method and its cost.

In vitro permeation studies using well-defined diffusion cells, skin models and membranes can be useful tools in the design and optimization of skin formulations [2–4]. The most commonly used quantitative method for measuring *in vitro* skin permeation is the use of Franz diffusion cell described by numerous directives [5–9]. In this method the test formulation is placed on the surface of a skin model, which is positioned as a barrier between the donor compartment and the receptor compartment of the Franz diffusion cell [10]. Advantages of the Franz cell method are that measurements can be carried out on human skin samples among other potential membranes; multiple tests can be performed; several formulations can be tested at the same time; there is no need for radio-labelling of the test material; and there are no ethical issues.

Human skin examinations give the most appropriate information, but, because of their high cost, it is a commonly accepted way to choose simpler *in vitro* methods in the early stages of formulation development. In addition to pharmaceutical research, these investigations also help other industries. In agrochemistry, pesticides and insect repellents are involved, and the veterinary and cosmetic industries also rely on these methods [4,11].

2. LITERATURE BACKGROUND

2.1. Structure and Function of the Skin

The skin, the largest organ of the human body, provides an easily accessible surface area for the possible administration of drugs, making it an attractive route for both topical and systemic drug delivery [12]. It is a multilayer tissue, and its main function is to guard the body against external circumstances by functioning as an effective barrier to the absorption of exogenous particles [13–15]. Dermal drug delivery is, therefore, a major challenge due to its barrier function [16–18]. Since the 1960s, several researchers have been studying the clarity of the skin structure, particularly in relation to this special barrier function [19–24].

The skin consists of three main layers: the epidermis, the dermis, and the subcutaneous tissue. The epidermis, excluding the stratum corneum, which is its outside layer, is a viable tissue. The epidermis does not have vascularization, and nutrients diffuse from the dermo-epidermal junction to maintain its viability. There are five layers that describe the different steps of cell life in the epidermis (Figure 1) [25]. These sublayers are the following, beginning from the non-viable stratum corneum (SC): Stratum lucidum (clear layer), stratum granulosum (granular layer), stratum spinosum (spinous or prickle layer), and stratum germinativum (basal layer). Providing mechanical protection, the skin prevents the body from drying as well as from the absorption of toxic chemicals and microorganisms. Stratum corneum serves as a crucial part of the barrier mechanism for the permeation of topical medications. Various models have been recommended for SC mimicking. The most simplistic model is defined as a “brick and mortar” structure; the stratum corneum includes corneocytes (the “bricks”) and an intercellular lipid matrix (the “mortar”), which is essentially responsible for the barrier function [22]. The SC cells are named corneocytes. There are 15 to 20 layers of corneocytes with a thickness of 10 to 15 μm , but when hydrated, the stratum corneum considerably grows, and its thickness may reach up to 40 μm , showing extended permeability. These cells are dense, functionally dead and anucleated. The lipids surround the corneocytes and form bilayers. The intercellular lipid (Figure 1) consists of a mixture of fatty acids, ceramides, cholesterol, cholesterol esters and a small fraction of cholesterol sulfate producing a special ordered structure [13,26,27]. These properties should be taken into account when modeling permeation during the development of artificial membranes.

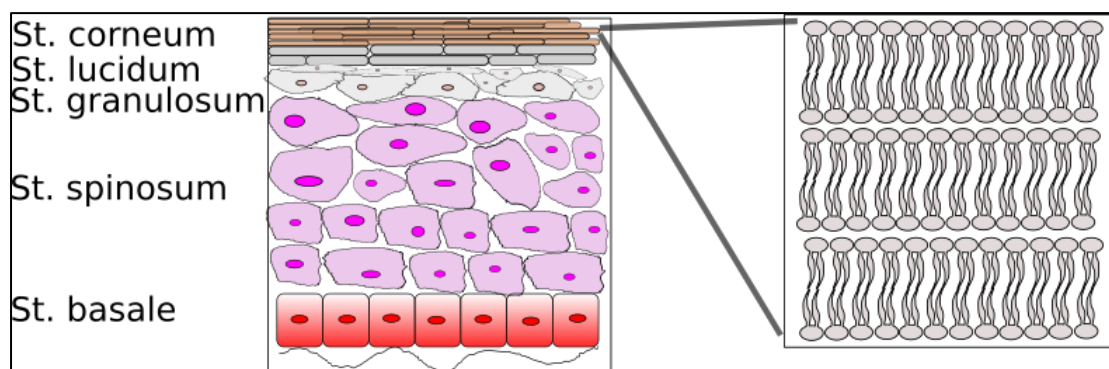


Figure 1 Structure of the epidermis and the intercellular lipid matrix.

There are three major routes of permeation for the passive diffusion of molecules through the cutaneous barrier (Figure 2). The first pathway is the intercellular pathway of permeation, which has been the most relevant for several years. About 15 years ago, the follicular permeation pathway was also established as a second important pathway. The transcellular permeation pathway, where the materials pass through both the corneocytes and the lipid layers, seems to be unimportant at present [26,28,29].

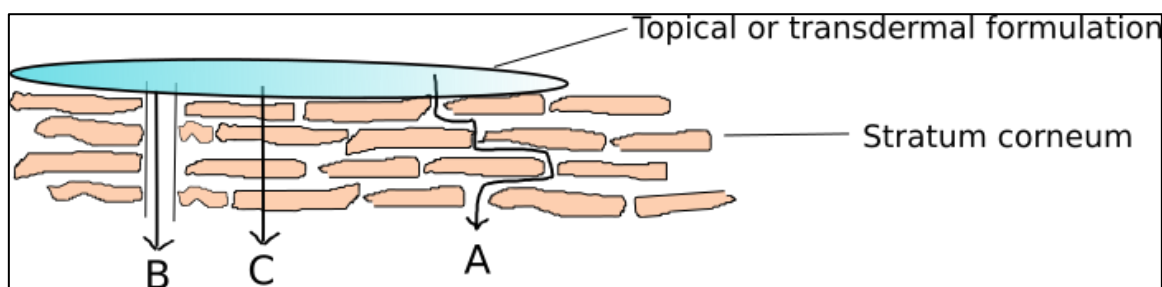


Figure 2 Routes of permeation. A: Intercellular permeation pathway, B: Follicular permeation pathway, C: Transcellular permeation pathway.

2.2. Modifying Factors of Skin Permeation

The liberation of an active pharmaceutical ingredient (API) from a pharmaceutical product applied to the skin and its transport to the different skin layers and systemic circulation is a multistep process which includes (a) the release of API from the preparation, (b) drug partitioning into the stratum corneum, (c) drug diffusion toward the stratum corneum, (d) drug partitioning from the stratum corneum into viable epidermis layers, (e) diffusion through the viable epidermis layers into the dermis, (f) drug absorption by vessels, (g) reaching systemic circulation (Figure 3).

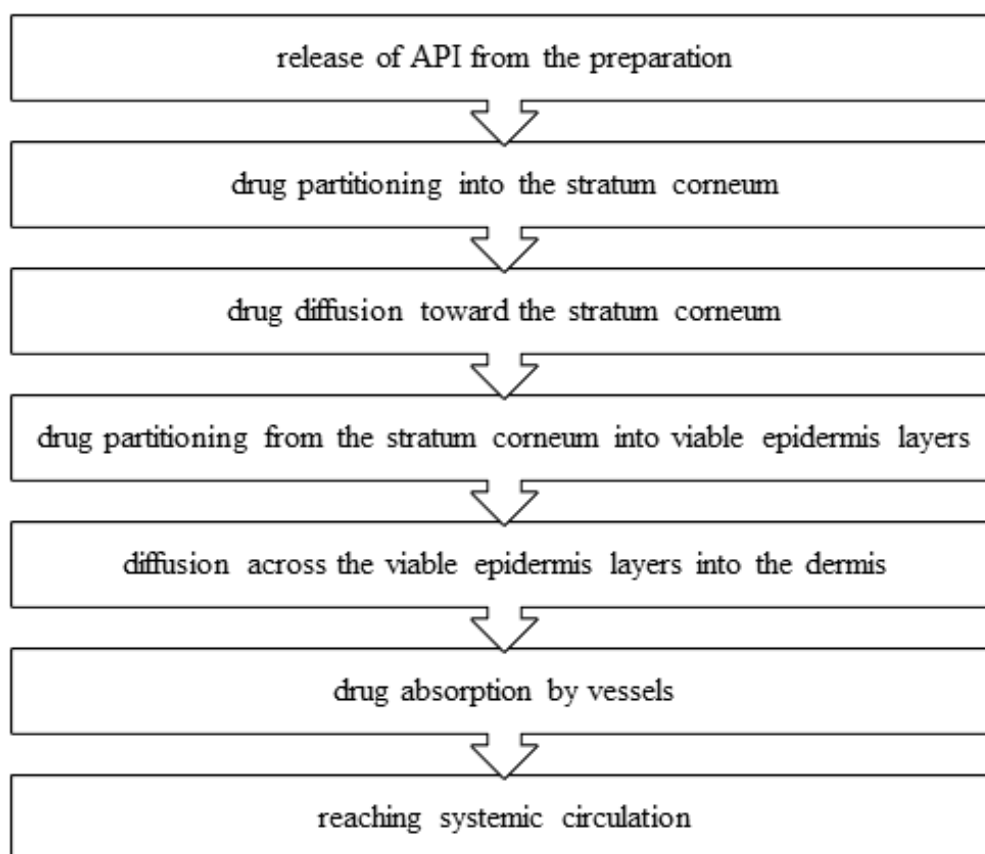


Figure 3 Drug transport through the skin.

This multistep process is affected by the properties of API, vehicle, skin and their interactions [22–25]. The selection of APIs for dermal delivery must be based on many factors, including physicochemical characteristics, drug-membrane interactions, vehicle, and pharmacokinetic aspects. The ideal physicochemical characteristics of a drug chosen for cutaneous administration are low molecular weight (<600 Da); low melting point (<200 °C), which is related to appropriate solubility; a high but stable partition coefficient; and solubility in water and oils to achieve a proper concentration gradient and increase the diffusion force over the skin [30–37].

Percutaneous permeation is also impaired by biological factors. Basic heterogeneity in the skin barrier is due to factors such as skin hydration, age, gender, skin surface area, disease or damage malformations and previous therapy [16,38–41]. In order to provide the skin with a safe barrier function, the hydration level of the skin needs to be balanced, and a proper amount of water is required. Permeability is increased if hydration improves [42]. Age has an impact on permeation into the skin. Baby skin and damaged skin have higher permeability.

The permeability of the drug through the stratum corneum is modulated by the carrier/vehicle, too. A vehicle can improve the physical state and permeability of the skin by the hydration effect or an alteration of the lipid bilayer structure.

2.3. General Guidelines of Skin Permeation Testing

Recently, the regulation of dermal and transdermal preparations has received increasing attention. More and more documents are available for dermal permeation and absorption studies from Europe and the United States. These documents promote a harmonized road to conducting dermal and transdermal studies. The Organization for Economic Cooperation and Development published several issues about this topic, including

- Guidance Notes on Dermal Absorption (No. 156) [9],
- Test Guideline 427 (*in vivo* methods) [7]
- Test Guideline 428 (*in vitro* methods) [8], and
- Guidance Document for the Conduct of Skin Absorption Studies [6].

There are some other documents such as

- World Health Organization International Programme on Chemical Safety (WHO/IPCS) Environmental Health Criteria 235 [43],
- European Centre for Ecotoxicology and Toxicology of Chemicals (ECETOC) Monograph 20 [44],
- United States Environmental Protection Agency (USEPA) report on dermal exposure assessment [45],
- European Food Safety Agency (EFSA) Guidance on dermal absorption for plant protection products [9], and
- the latest European Medicines Agency (EMA) document, Draft Guideline on Quality and Equivalence of Topical Products [46].

These documents present rules and descriptions of how to perform dermal permeation assays, however, the measurements are not properly regulated. There are two suggested methods. One is the widely used diffusion cell and the other is the tape stripping method. However, in the scientific literature there are new type of measurements, such as skin PAMPA or different spectroscopic and microscopic methods, which may complete the suggested tests.

2.4. Techniques for Modeling Permeation through Human Skin

There are two major types of techniques. Quantitative approaches include the use of different diffusion cells and skin Parallel Artificial Membrane Permeability Assay (PAMPA). Qualitative or semi-quantitative approaches are various microscopic and spectroscopic approaches and their combinations (Figure 4).

Quantitative *in vitro* tests are regularly performed to measure the amount of API permeated through a membrane over time in relation to the diffusion area related to the collected quantity of API in an acceptor chamber [13,32,33,47–52].

In the case of qualitative techniques, the aim is usually to follow the active substance in the skin. The presence or relative quantity of the active ingredient in the various layers of the skin can be determined. The use of several approaches combined will complement each other well, making the regulatory approval process simpler.

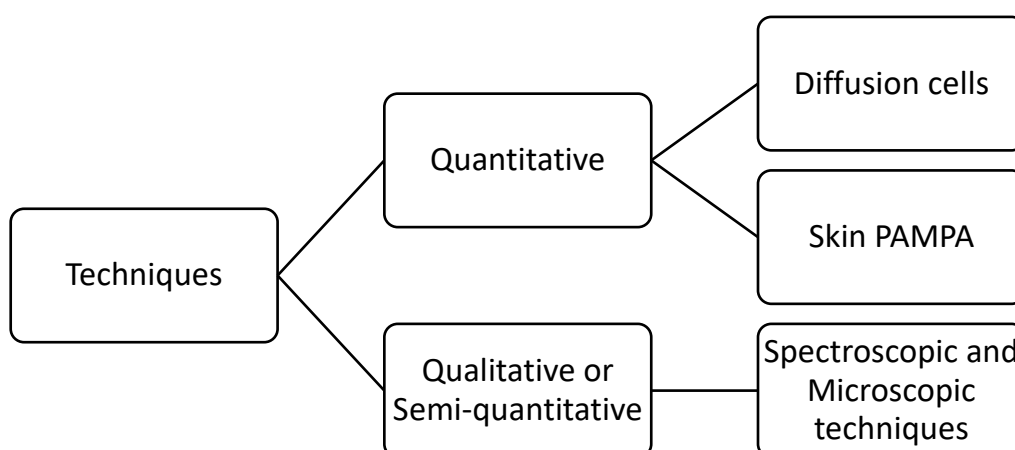


Figure 4 The main methods for following up skin permeation.

2.4.1. Diffusion Cells

Diffusion tests working with human skin have become the “gold-standard” model due to the pioneering work of Dr. Thomas J. Franz, who developed the “Franz cell” in 1970. It determines important relationships between skin, API, and formulation [53–55]. This tool always consists of a cell that holds a chamber for drug application, a membrane through which the drug may diffuse, and an acceptor media chamber from which samples may be investigated [53]. Cells are made unique by different arrangements and membranes used.

2.4.1.1. Types and Properties of Diffusion Cells

Diffusion cells can be categorized into two main classes, static (classic Franz diffusion cell) and flow-through cells. In the case of a static cell, the acceptor phase is not totally changed during the measurement. A fresh acceptor phase is continuously flowing in the flow-through cell.

The donor, the membrane, and the acceptor may be placed either vertically, as in the popular classic Franz diffusion cell (Figure 5) and in the flow-through cell or horizontally as in the side-by-side cell (Figure 6) [53]. There are two main types of vertical Franz cells, open and closed cells. When the cell is opened from above, the measurement runs on atmospheric pressure which better models the real-world conditions. However, most of the cells can be closed from the top. If the instrument is connected to an automatic sampler and it is closed, this will result in higher pressure and, therefore, its predicting higher permeation values. Nowadays, the "hand-sampler" Franz diffusion cells have been replaced by systems connected to an automated sampler. Sampling systems facilitate the work of researchers and reduce the errors of human sampling.

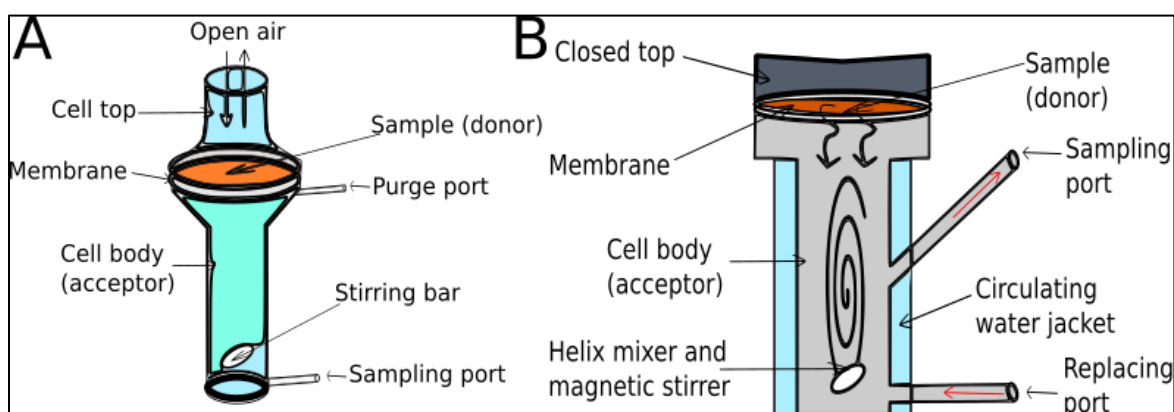


Figure 5 Open (A) and closed (B) vertical static Franz diffusion cells.

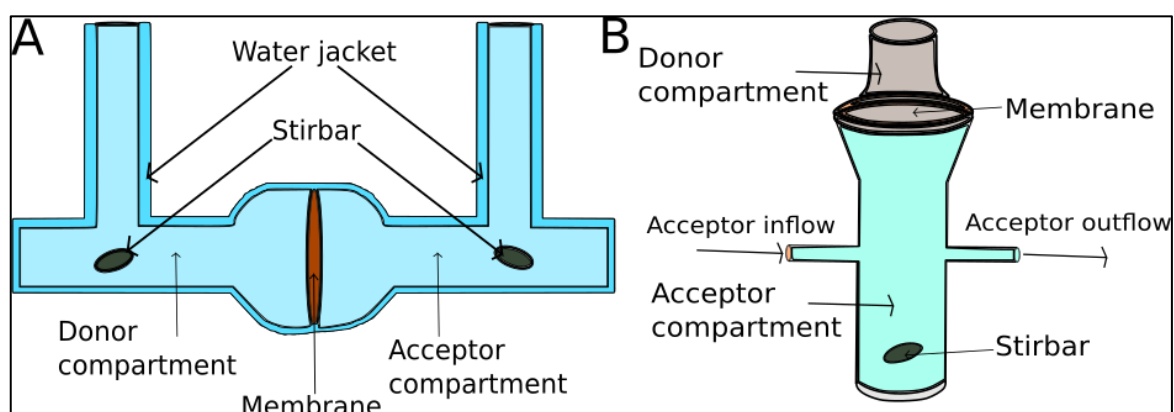


Figure 6 Side-by-side cell (A) and flow-through cell (B).

2.4.1.2. Diffusion Test Types

In the latest European Medicines Agency (EMA, 2018) document (Draft Guideline on Quality and Equivalence of Topical Products) diffusion tests are grouped as follows. There are *in vitro* release tests (IVRT) and *in vitro* skin permeation tests (IVPT).

An IVRT with pseudo-infinite dosing using diffusion cells evaluates the rate and extent of release of an active substance in the proposed formulation. In the case of IVRT, synthetic membrane (lipid-based or non-lipid-based model membranes) should be used. The IVRT study shows the release rate. IVRT is well established for characterizing and evaluating the performance of semi-solid dosage forms. IVRT can be a sensitive and discriminating method that is generally responsive to physicochemical changes in semisolid drug products. IVRT serves as a valuable tool for the demonstration of comparative *in vitro* drug release rates between the test and reference products. IVRT is not expected to correlate with or be predictive of *in vivo* bioavailability or bioequivalence.

Determining the characteristic permeation profile of a drug product using an IVPT is an acceptable method. The sample dose is recommended to be finite (2 to 15 mg/cm²). The IVPT study shows the flux profile, and the detected quantities (in the pg to ng range). Therefore, an IVPT study is recommended for comparing the cutaneous pharmacokinetics of a drug from the test and reference products using excised human skin with a competent skin barrier mounted on a qualified diffusion cell system.

In the early stages of development, IVRT should be used, thereafter, IVPT can be used for promising formulations [56]. IVRT is specific to the formulation, while *in vitro-in vivo* correlation is expected for IVPT. The main differences are summarized in Table 1.

Table 1 *In vitro* release tests (IVRT) and *in vitro* skin permeation tests (IVPT).

IVRT	IVPT
Synthetic membrane	Human skin
Infinite dose	Finite dose
Release rate	Flux profile
µg to mg range	pg to ng range
Relative consistency	Donor variability
Specific to the formulation	<i>in vitro</i> – <i>in vivo</i> correlation

In the development of dermal formulations, it is not sufficient to perform IVRT measurements that show the amount of drug released and diffused across a membrane of given pore size. It is also essential to introduce biological permeation studies (IVPT), as this is the only way to study the interaction of the drug with the skin and the possible reservoir function.

2.4.1.3. Membranes for Release and Permeation Measurements in Franz Diffusion Tests

In IVRT, different synthetic membranes can be used to test the formulations under development. Synthetic, commercially available membranes generally consist of layers of polymeric macromolecules that determine the diffusion of drugs through them. Several types of synthetic membranes are available for example silicon, polyethersulfone, cellulose, polytetrafluoroethylene, and mixtures and derivatives thereof. The aspects of membrane selection, properties expected from the membrane are the following:

- inert, low binding capacity to the drug,
- compatibility with the release medium
- compatibility with the test product.

The membrane structure should remain constant until the end of the experiment.

One of the synthetic membranes used in IVRT in the last decade is cellulose acetate (CA) membranes [31,33,57–61]. CA is a basic, porous (0.45 μm ; 0.25 μm) synthetic membrane used to test the efficiency of the topical formulation without a rate-limiting property. The disadvantage of CA as a porous membrane is that it does not fully correlate to the properties of the human skin barrier so it can demonstrate incorrect drug permeability. Thus, it can only be used for IVRT tests [62].

In IVPT, human skin is the most important model for testing the delivery of drugs from different formulations. However, it has a lot of limitations:

- ethical permission (in some countries);
- variability;
- different sources: age, sex, race, plastic surgery, amputation, cadaver;
- different anatomical parts: abdomen, thigh, breast, back;
- storage [42,63,64].

Because of the limitations of human skin, there is a need for new innovative synthetic membranes specifically created to be used as a substitute for human skin models in *in vitro* permeation studies [2,62,65,66]. There is an effort to develop new types of so-called skin-mimic membranes that do not belong to the classical synthetic membranes.

Strat-M membrane is one newly introduced synthetic membrane to predict drug permeation with better human skin correlation. As a synthetic test model with low variability and no special storage or hydration requirements, Strat-M membrane simplifies experimental design and data analysis. Like human skin, the Strat-M membrane has multiple layers with different diffuseness. The membrane consists of two layers of polyethersulfone (PES, more resistant to diffusion) on top of one layer of polyolefin (more open and diffuse). These polymeric layers form a porous structure with a gradient across the membrane in terms of pore size and diffuseness [62,67–72]. Previous findings are promising, but there is not enough literature data to confirm its applicability.

2.4.2. Skin Parallel Artificial Membrane Permeability Assay

The skin parallel artificial membrane permeability assay method appeared as a new type of permeation test in addition to the classic diffusion cell methods. It is not included in official guides, but more and more research is being done with it. The results so far are encouraging, but more data are needed to properly evaluate the method.

The Parallel Artificial Membrane Permeability Assay is a 96-well plate-based method for the fast determination of passive membrane permeability of molecules. There are different PAMPA models and one especially for skin permeation testing. This technique is based on a sandwich of two 96-well microtiter plates that fit into each other, with the upper one containing an approximately 45 μm pore-size PVDF filter (~membrane) at its bottom [73]. It is a promising method because of its low cost and high throughput. The skin model published earlier combines silicone oil and isopropyl myristate [74,75].

Sinkó et al. have developed the skin PAMPA method for the prediction of skin permeation *in vitro* [76]. Skin PAMPA has been created to imitate the characteristics of the stratum corneum using cholesterol, free fatty acid, and a ceramide-analogue compounds [16,18]. The experimental design is shown in Figure 7.

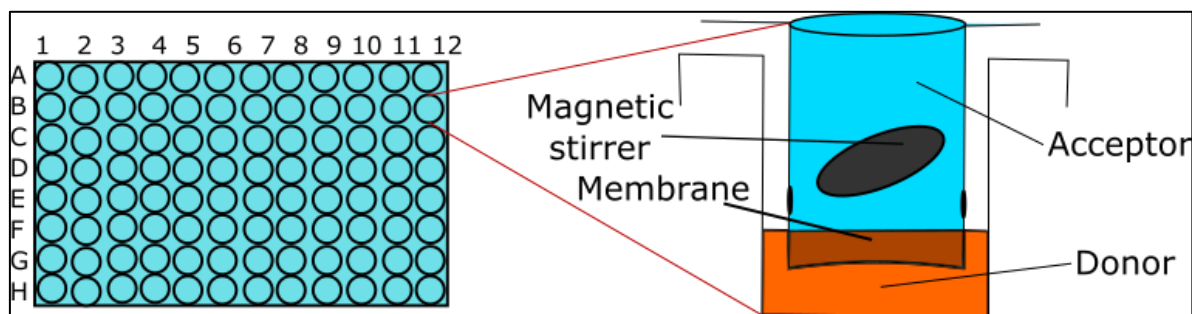


Figure 7 Experimental design of the skin PAMPA method.

2.4.3. The Most Important Experimental Considerations in the Case of Quantitative Methods

In order to obtain reliable dermal permeability data, several parameters have to be considered for the design of the test system:

- the sink condition,
- the incubation time,
- the incubation temperature,
- the mixing,
- the hydration of the membrane,
- the amount of dose [77].

Ueda and colleagues have determined the sink condition: to reach sink conditions, the receptor medium must have a sufficiently high capacity to dissolve or take away the drug, and at the end of the test, the receptor medium does not exceed 10 w/w% drug solubility in the releasing matrix [78]. In the case of molecules with low water solubility, it is not so easy to create the sink condition. By changing the composition and the pH of the acceptor and donor phases, a suitable sink condition can be created. Alternatively, the sink condition can be achieved using surfactants in the acceptor phase. A further solution is the use of serum albumin because it is capable of binding lipophilic components, thereby keeping the free concentration of the molecule lower. The advantage of using albumin is that it is a sufficiently large molecule to not permeate through the skin.

The duration of the IVRT should be sufficient to characterize the release profile, ideally releasing at least 70% of the active substance used. The minimum duration of IVPT testing is 24 hours. If the duration of the test is longer than 24 hours, the integrity of the membrane must be demonstrated. In the case of incubation time, it is important to consider the fact that the structure of the skin or the artificial membrane should remain unchanged until the end of the experiment. To avoid the overestimation of dermal permeation, different skin integrity tests are needed to eliminate the use of damaged skin preparations. This test should ensure the exclusive use of skin-derived data with an appropriate barrier function in the assays. Several methods can be used to examine skin integrity. Widely used methods are the measurement of tritium water permeability, the measurement of transepidermal water loss, and the determination of transepidermal electrical resistance. A relatively new method is the use of the tritium-labeled internal reference standard, where integrity testing is performed simultaneously with the

measurement [73–75,79–82]. For each method, it can be stated that the measurements are different and not properly regulated. Different labs use different limits and measure under different conditions. In the future, the proper regulation of integrity testing and the clear definition of limit values for the proper evaluation of dermal formulations will be essential.

The incubation temperature affects both the permeability of the compounds and the rheological properties of the product studied. Usually, the temperature should be stable at $32\pm1^{\circ}\text{C}$.

The selected mixing speed should guarantee enough mixing of the acceptor phase during the test [18].

Hydration of the skin affects, among other things, the barrier function of the stratum corneum. Therefore, the creation of an optimal hydration state is essential [83]. The state of hydration is also important for synthetic membranes. It is important to follow the manufacturer's instructions.

Depending on the amount of sample in the test cells, two types of experiments can be distinguished: finite and infinite dose measurements. In the case of the infinite dose, the amount of sample used is in large excess, hence the donor phase (the sample itself) cannot be emptied under normal circumstances. As a result, when examining a permeability-time profile in this case, the straight line usually rises with a constant slope without experiencing a plateau phase. The opposite of the infinite dose is the finite dose. When finite doses are used, a limited amount of sample (donor phase) is applied to the skin or to the surface of the artificial membrane. It should be noted that the latter experimental circumstance is much closer to the condition when the patient applies a given preparation onto his or her own skin. Based on the recommendation of the OECD a finite dose for a solution-phase sample is recommended if the applied dose does not exceed $10\text{ }\mu\text{L}/\text{cm}^2$ or is in the range of 1 to $10\text{ mg}/\text{cm}^2$ for a semisolid sample [83]. The EMA guide recommends 2 to $15\text{ mg}/\text{cm}^2$ for finite dose measurements. Certainly, it is more advantageous to design the measurement conditions to approach the finite dose requirements as much as possible [81].

There are some measurement parameters which affect drug permeation, such as occlusive or non-occlusive application [79]. Dermal and transdermal drug delivery can be performed after occlusive or non-occlusive (open) application. Occlusion can be achieved by covering the skin by impermeable films or others, such as strips, gloves, diapers, textiles, garments, wound dressings, or transdermal therapeutic systems [77, 84].

2.4.4. Spectroscopic methods

Spectroscopic methods can produce molecular information about the spatial distribution of drugs in the different layers of the skin.

The tape stripping method is listed in the official recommendations of skin permeation methods. The tape stripping method is used to model the permeation into the stratum corneum. This method is time-consuming, semi-destructive, and difficult to reproduce, and only the stratum corneum can be examined. This enables chemically selective and non-destructive sample analysis with high spatial resolution in three dimensions and allows multiple components to be monitored at the same time.

Nowadays, Raman spectroscopy is a new powerful technique to properly understand skin structure and percutaneous drug delivery too [85–88]. Raman spectroscopy is a promising spectroscopic method based on discovering the characteristic vibrational energy levels of a molecule excited by a laser ray and it gives information about the molecular structure of tissue components, including the permeated quantity of API without the use of fluorescent labels or chemical stains [85,89–91]. Confocal Raman spectroscopy can be used to investigate topical formulations *in vitro* and *in vivo* [92,93]. Therefore, this method is promising to follow the permeation of APIs and it is suitable for monitoring the permeation of exogenous materials into the skin layers [31,94]. The method is mentioned in the latest EMA recommendation. In the future, if there is enough favorable investigation, it might be recommended by all authorities.

Permeation through the skin can be explored by chemical mapping (Figure 8). Raman Spectrometry is highly selective, with a fingerprint spectrum that allows clear molecular identification. The irradiating light can be focused on a very small point ($\sim 1 \mu\text{m}^2$) with suitable microscope lens, so reliable chemical information can also be obtained from a microscopic area of the sample. The spatial distribution of the fundamental components of the sample can be determined by the spectra that make up the map. Chemical maps contain a huge quantity of data. Although these can be controlled by methods commonly used in spectroscopy, the huge amount of data can be utilized more efficiently by using appropriate mathematical (multivariate data analysis) techniques. Thanks to these advantages, the technology has enormous potential in various applications: from the analysis of the distribution of the physiological components of the skin and tissues through the diagnosis of pathological conditions to biopharmaceutical studies, such as drug permeation kinetics [16,25,93,95].

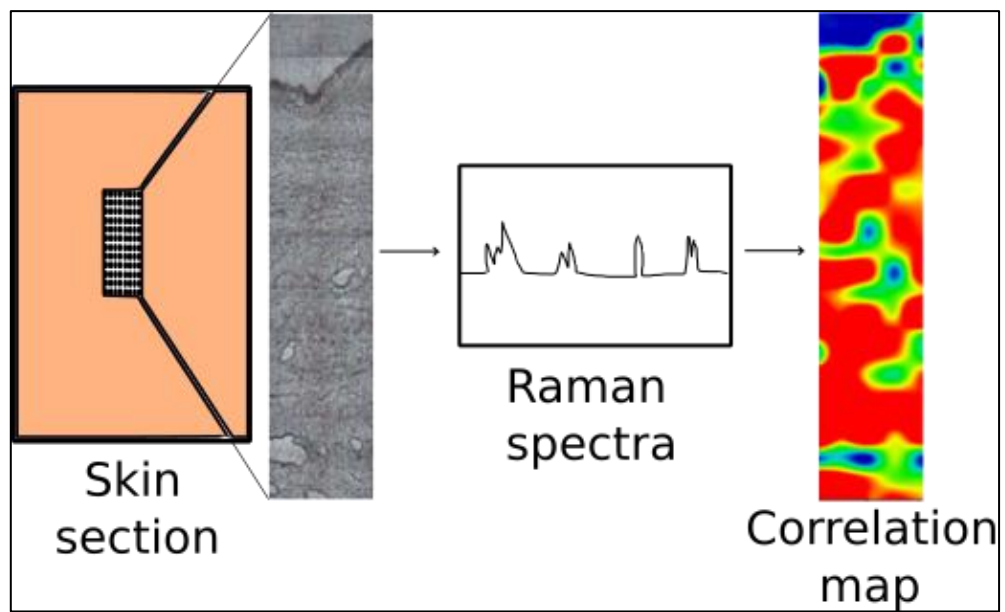


Figure 8 Raman chemical mapping.

3. EXPERIMENTAL AIMS

The aim of this research was to investigate the applicability and substitutability of traditionally used and new, innovative and promising methods for modeling skin permeation. During the work we aimed to:

- compare the Hanson Franz cell and the Logan Franz cell and their substitutability;
- examine the applicability of different membranes, in particular whether the human epidermis can be replaced by a synthetic membrane;
- examine the applicability of Skin PAMPA method;
- investigate Raman mapping as a semiquantitative method; and
- examine the sensitivity of the methods to detect differences between different formulations.

Dermal preparations such as a hydrogel, different types of creams and a nanostructured lipid carrier gel were investigated to compare different methods. The following steps were set.

In the first part of my Ph.D. work (Experimental part 1), different quantitative skin permeation modeling methods were used to study drug release and permeation. Two types of vertical Franz diffusion cells (Logan, Hanson) were compared by three different membranes, including cellulose, Strat-M and the gold-standard heat-separated human epidermis. Next, these cells were compared to the Skin PAMPA method, as well.

During the second part of my work (Experimental part 2), I aimed to investigate whether there is correlation between the findings of quantitative experiments and semiquantitative spectroscopic measurements. Logan Franz cell, skin PAMPA and Raman spectroscopic methods were compared. Another aim was also to determine how selective these methods are in order to be able to demonstrate the differences between different compositions. A hydrogel and two types of creams were investigated as these are the most generally used dermal preparations.

4. MATERIALS AND METHODS

4.1. Materials

4.1.1. Lidocaine Containing Nanostructured Lipid Carrier Gel

Lidocaine base and glycerol were obtained from Hungaropharma Ltd. (Budapest, Hungary). Miglyol® 812 N (caprylic/capric triglyceride) was a gift from Sasol GmbH (Hamburg, Germany). Cremophor® RH 60 (PEG-60 Hydrogenated Castor Oil; HLB value: 15–17) was kindly supplied by BASF SE Chemtrade GmbH (Ludwigshafen, Germany). Apifil® (PEG-8 Beeswax) was a gift from Gattefossé (St. Priest, France). Methocel™ E4M (hydroxypropyl methylcellulose) was from Colorcon (Budapest, Hungary). The water used was purified and deionized with the Milli-Q system from Millipore (Milford, MA, USA).

4.1.2. Diclofenac Sodium Containing Formulations

Diclofenac sodium, ethanol 96 w/w%, cetostearyl alcohol, liquid paraffin, white petrolatum, white beeswax, wool fat, oleyl oleate and castor oil were obtained from Hungaropharma Ltd. (Budapest, Hungary). Polysorbate 60 was obtained from Sigma-Aldrich (Budapest, Hungary). Methocel™ E4M (hydroxypropyl methylcellulose) was purchased from Colorcon (Budapest, Hungary). The water used has been filtered and deionized using the Millipore (Milford, MA, USA) Milli-Q method.

4.1.3. Synthetic and Biological Membranes

The cellulose acetate membrane (Porafil membrane filter, cellulose acetate, pore diameter: 0.45 µm) was obtained from Macherey-Nagel GmbH & Co. KG (Düren, Germany). The Strat-M membrane (Strat-M Membrane, Transdermal Diffusion Test Model, 25 mm) was from Merck KGaA (Darmstadt, Germany). Excised human skin was obtained from Caucasian female patients by a routine plastic surgery procedure in the Department of Dermatology and Allergology, University of Szeged. The *in vitro* skin permeation test does not need ethical permission, and patient's consent according to the Act CLIV of 1997 on health, Section 210/A in Hungary. The local ethical committee (Ethical Committee of the University of Szeged, Albert Szent-Györgyi Clinical Center) was informed about the *in vitro* skin permeation studies (Human Investigation Review Board license number: 83/2008). The skin PAMPA sandwiches (P/N: 120657), hydration solution (P/N: 120706) and stirring bars (P/N: 110066) were purchased from Pion, Inc (Woburn, MA, USA). The UV plates (UV-star micro plate, clear, flat bottom, half area) were from Greiner Bio-one (Kremsmünster, Austria).

4.2. Methods

4.2.1. Preparation of the Lidocaine Containing Nanostructured Lipid Carrier Gel (LID-NLC gel)

NLCs are colloidal carriers which were introduced in the early 1990s. They are derived from o/w emulsions by replacing the liquid lipid with a solid lipid at room temperature. The lipophilic phase of NLC included Apifil, Cremophor RH 60 and Miglyol 812 N, which were melted at 60 °C under controlled stirring. Then lidocaine was added to the melted lipid phase under similar conditions. Then warm purified water was added to the lipid phase to form the pre-emulsion. The pre-emulsion was ultrasonicated using a Hielscher UP200S compact ultrasonic homogenizer (Hielscher Ultrasonics GmbH, Teltow, Germany) for 10 min at 70 w/w% amplitude. At the end, the sample was cooled in ice to obtain the solid lipid particles (LID-NLC) [38]. For dermal application, a concentrated gel was formed at room temperature with glycerol and Methocel E4M. In the last step, the NLC dispersion was added to the gel (LID-NLC gel) to form the final composition (5 w/w% of lidocaine). A blank-NLC and blank-NLC gel were also prepared using the same procedure, but without adding lidocaine. Table 2 summarizes the formulations.

Table 2 Compositions of the test preparations.

LID-NLC	LID-NLC Gel
Apifil	LID-NLC
Cremophor RH60	Glycerol
Miglyol 812N	Methocel E4M
Purified water	
Lidocaine	

4.2.2. Preparation of the Diclofenac Sodium Containing Formulations

Three different semisolid preparations were formulated (Table 3.).

The conventional hydrogel was prepared with 1 w/w% DFNa dissolved in the mixture of purified water and ethanol 96 w/w%, then Methocel E4M and microbiological preservative were added. In the case of the o/w cream, the oily phase consisting of cetostearyl alcohol, liquid paraffin, white petrolatum and Polysorbate 60 was heated up to 60 °C. Then, hot water was added to the oily phase under agitation. DFNa was dispersed in the preparation and it was homogenized until the mixture was cooled.

Finally, the microbiological preservative was added. In the case of the w/o cream, the oily phase consisting of white beeswax, wool fat, oleyl oleate and castor oil was heated up to 60 °C. Then, hot water was added to the oily phase under agitation. Finally, DFNa was dispersed in the preparation and it was homogenized.

Table 3 Compositions of the diclofenac sodium containing formulations.

hydrogel	o/w cream	w/o cream
Diclofenac sodium	Diclofenac sodium	Diclofenac sodium
Methocel E4M	Cetostearyl alcohol	White beeswax
Ethanol 96 w/w%	Liquid paraffin	Wool fat
Purified water	Purified water	Purified water
Microbiological preservative	White petrolatum	Castor oil
	Polysorbate 60	Oleyl oleate
	Microbiological preservative	

4.2.3. Drug Release and Permeation Studies

Three different methods were used to model and compare drug release and diffusion through the membrane and permeation through the skin from different formulations (Table 4.). The methods included two types of vertical Franz diffusion cells, namely Hanson Microette TM Topical & Transdermal Diffusion Cell System, and Logan Automated Dry heat sampling system. The third method used was the skin PAMPA method. In the Franz cells, the donor and acceptor phases were separated by either a synthetic membrane cellulose acetate and Strat-M membrane or a biological membrane: heat-separated human epidermis (HSE). The heat-separation method was applied to isolate the epidermis. The excised human fat-free subcutaneous skin was put in a water bath (60 ± 0.5 °C, 1 minute), and separated the epidermis from the dermis. A 0.300 g of sample was placed in the donor chamber on the membrane. Thermostated phosphate buffer solution (PBS pH 7.4 ± 0.15), made in-house, kept at 32 ± 0.5 °C was used as the acceptor phase. Membrane diffusion and skin permeation experiments lasted for 24 h (sampling times: 0.5; 1; 2; 3; 4; 5; 6; 8; 10; 12; 16; 20; and 24 h). The concentration of the drug was measured spectrophotometrically with a Thermo Scientific Evolution 201 spectrometer with Thermo Insight v1.4.40 software package (Thermo Fisher Scientific, Waltham, MA, USA) at a wavelength of 262 (LID) and 275 (DFNa) nm.

The skin PAMPA sandwiches were used after a 24-hour hydration period (Hydration Solution, Pion, Inc., Billerica, MA, USA). 70 μ L of the preparation were applied to the well of the formulation plate as the donor phase. Phosphate buffer solution (PBS pH 7.4 ± 0.15), made in-house, was used as the acceptor phase. The top plate was filled with 250 μ L of fresh acceptor solution, and a stirring bar was also used in each well. The Gut-Box™ from Pion, Inc. was used for stirring; the resultant sandwich was incubated at 32 °C for six hours. The skin PAMPA membrane is not designed for 24-h measurements, the membrane can provide relevant values for a shorter time. Therefore, the acceptor solution was examined after 0.5, 1, 2, 3, 4, 5 and 6 h of incubation. The quantity of the API was determined by UV spectroscopy at 262 (LID) and 275 (DFNa) nm using a Synergy HT UV plate reader by KC4 (BIO-TEK Instruments, Inc., Winooski, VT, USA) software.

Permeation profiles of dermal formulations were obtained. The cumulative amount (Q) of drug permeated per cm^2 at final time point was calculated. The flux (J) was the slope of the cumulative amounts of API ($\mu\text{g}/\text{cm}^2$) permeated versus time (h) profiles. Time point correlations between the amounts of drug permeated through heat-separated human epidermis and skin PAMPA membrane were shown and correlation coefficients (R^2) were calculated.

Table 4 *The experimental design of drug diffusion and permeation studies.*

	Hanson Microette TM Topical&Transdermal Franz Diffusion Cell System	LOGAN Automated Dry Heat Sampling System	Skin PAMPA
Static or dynamic cell	static	static	static
Number of cells	6	6	96
Cell properties	closed (under pressure)	open	open
Permeation surface area	1.76 cm ²	1.76 cm ²	0.3 cm ²
Amount of acceptor phase	7 ml	9 ml	250 µl
Acceptor phase	Phosphate buffer solution pH 7.4	Phosphate buffer solution pH 7.4	Phosphate buffer solution pH 7.4
Donor phase	0.30 g	0.30 g	70 µl
Membrane	Synthetic <ul style="list-style-type: none"> • cellulose • Strat-M Biological <ul style="list-style-type: none"> • HSE 	Synthetic <ul style="list-style-type: none"> • cellulose • Strat-M Biological <ul style="list-style-type: none"> • HSE 	Skin PAMPA membrane
Temperature	32 °C	32°C	32°C
Sampling	automatic	automatic	by hand
Time of measurement	6 or 24 h	6 or 24 h	6 h
Determination of active substance	Spectrophotometry	Spectrophotometry	Spectrophotometry

4.2.4. Investigation of Skin Permeation with Raman Spectroscopy

Excised human subcutaneous fat-free skin (epidermis and dermis) was used. It was obtained from Caucasian female patients who underwent abdominal plastic surgery. 1 cm² of the skin surface was treated with the formulations for 3 h at 32 °C. The treated skins were frozen and sectioned (10-µm-thick cross-sections) with a Leica CM1950 cryostat (Leica Biosystems GmbH, Wetzlar, Germany). The microtomed skin samples were placed on an aluminum surface with the SC towards the top of the plate. Raman spectroscopic measurements were made with a Thermo Fisher DXR Dispersive Raman Spectrometer (ThermoFisher Scientific Inc., Waltham, MA, USA) equipped with a CCD camera and a diode laser. A laser light source of 780 nm wavelength was used, with a maximum power of 24 mW, which is the best source for studying biological samples. With the use of this type of laser source, fluorescence had less effect. The microscopic lens used for the measurements was magnified by 50 × and the pinhole aperture was 25 µm. A 200 to 1.800 µm area was explored in the case of chemical mapping; the step size was 50 µm vertically and horizontally. 205 spectra were observed, 16 scans were reported to accumulate each spectrum, and the exposure period was 2 s. When analyzing the treated vs. untreated skin samples, the different spectra of each component of the formulations and drug were used as reference points. A laser light of 532 nm was used to record the different spectra of the components and formulations. 32 scans were registered for each spectrum, with an exposure time of 6 s. The optics magnitude in the Raman microscope was 10 with a 25 µm slit aperture. Data acquisition and analysis were accomplished using OMNICTM8.2 for Dispersive Raman software package (ThermoFisher Scientific Inc., Waltham, MA, USA) [24,27].

4.2.5. Statistical Analysis

Data analysis, statistics and graphs were performed from the experimental data via Microsoft® Excel® (Microsoft Office Professional Plus 2013, Microsoft Excel 15.0.5023.100, Microsoft Corporation, Washington, USA), OriginPro® 8.6 software (OriginLab® Corporation, Northampton, Massachusetts, USA). Prism for Windows (GraphPad Software Inc., La Jolla, CA, USA) was used to conduct statistical data analysis using two-way ANOVA variance analysis (Bonferroni post-test). Differences were regarded as significant if * $p < 0.05$, ** $p < 0.01$, *** $p < 0.001$ and **** $p < 0.0001$ versus the control.

5. RESULTS AND DISCUSSION

5.1. Experimental part 1

Experimental part 1 contains the comparison of two types of Franz cells using different membranes and comparison of Franz cells method to skin PAMPA method. The 5 w/w% lidocaine containing NLC gel was used as test preparation. The amount of lidocaine released/permeated *in vitro* from the LID-NLC gel through the two synthetic and one biological membrane was calculated in terms of mean cumulative amount in $\mu\text{g}/\text{cm}^2 \pm \text{SD}$ by 24 h.

Cellulose acetate membrane was used for IVRT and heat-separated human epidermis was used for IVPT. The findings of both approaches were compared with the Strat-M membrane, which is a synthetic membrane specifically designed for skin penetration tests.

The findings are shown in Figure 9, which demonstrates the results obtained after 24 hours. There was a significant difference between the results of the two cells in the case of the cellulose membrane and significant difference was observed in the case of Strat-M and HSE membranes, too. The drug release through the synthetic cellulose membrane is significantly higher than permeation through the biological HSE membrane. It is important to know the extent of release (IVRT), but this does not provide relevant information for permeation. It is very important to examine the permeation process through the skin (IVPT) to know not only the released amount of drug, but also to see the interactions between the drug or the drug delivery system and the skin. However, it is promising that the results of synthetic Strat-M membrane are very close to the result of HSE.

For skin PAMPA measurements, we found that the integrity of the membrane was insufficient for 24-hour measurements, that is why skin PAMPA measurements were only run for a maximum of 6 hours.

The *in vitro* released/permeated amount of lidocaine from the LID-NLC gel through the two synthetic and one biological membrane and skin PAMPA were calculated in terms of mean cumulative amount in $\mu\text{g}/\text{cm}^2 \pm \text{SD}$ by 6 h.

The results were compared with the 6 h data obtained on Franz cells (Figure 10). There was no significant difference between the results of the skin PAMPA membrane, Logan Strat-M and Logan HSE membrane.

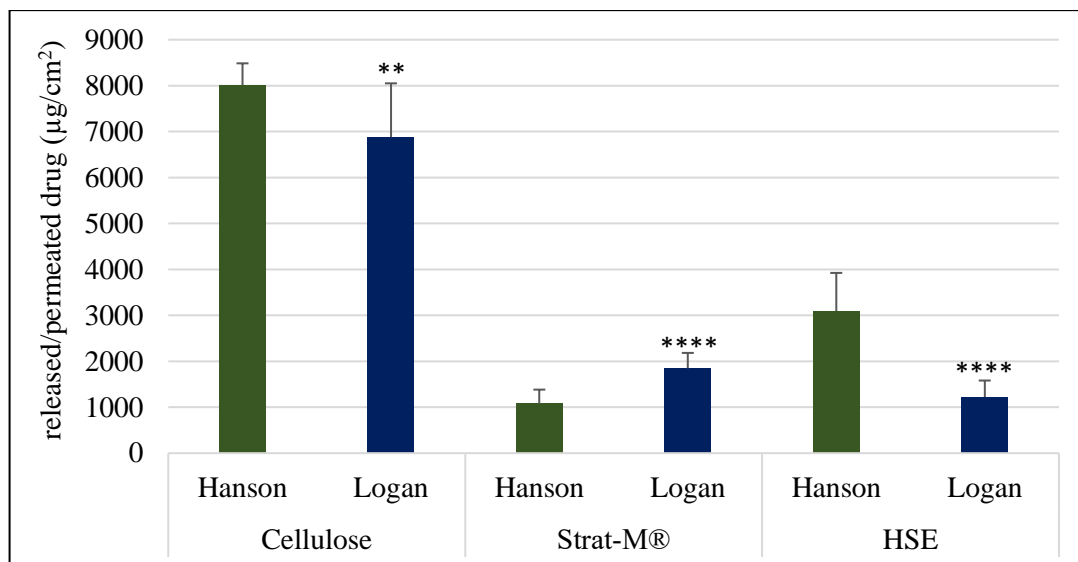


Figure 9 Comparison of diffusion cells and membranes.

(**** $p < 0.0001$, ** $p < 0.01$)

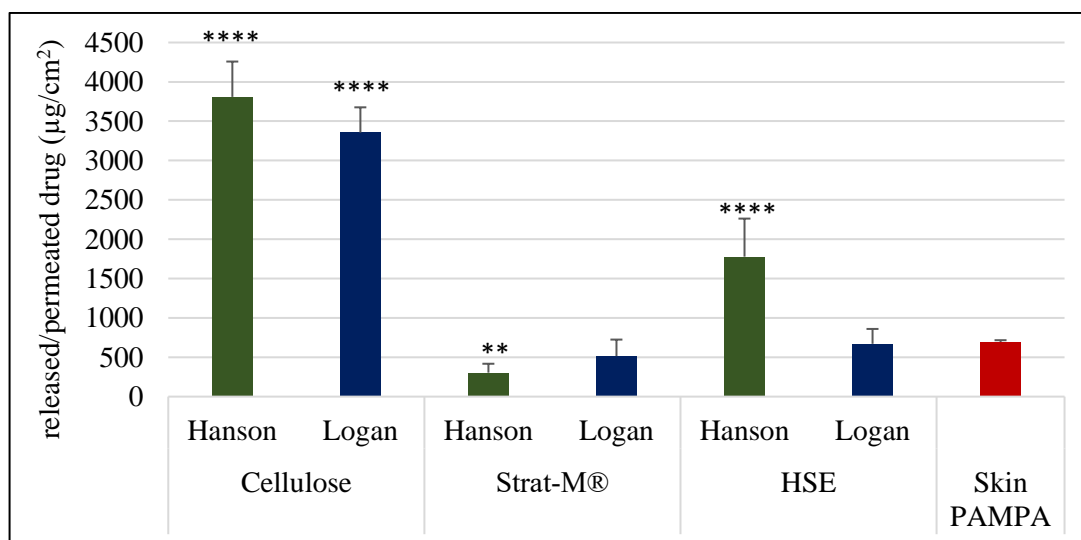


Figure 10 Comparison of skin PAMPA membrane results with Franz cell measurements.

(** $p < 0.01$, **** $p < 0.0001$ vs skin PAMPA)

The following figures illustrate the results evaluated separately on the Hanson and Logan cells (Figure 11-12). The analysis of relevance for the HSE membrane, the Strat-M membrane and the skin PAMPA membrane did not show a significant difference in the Logan cell. Significantly, more drugs pass through the cellulose membrane over 6 hours. The results obtained from the Hanson instrument showed a higher standard

deviation. Compared to the HSE membrane, the findings of all three other membranes showed a significant difference at the end of the 6-hour study.

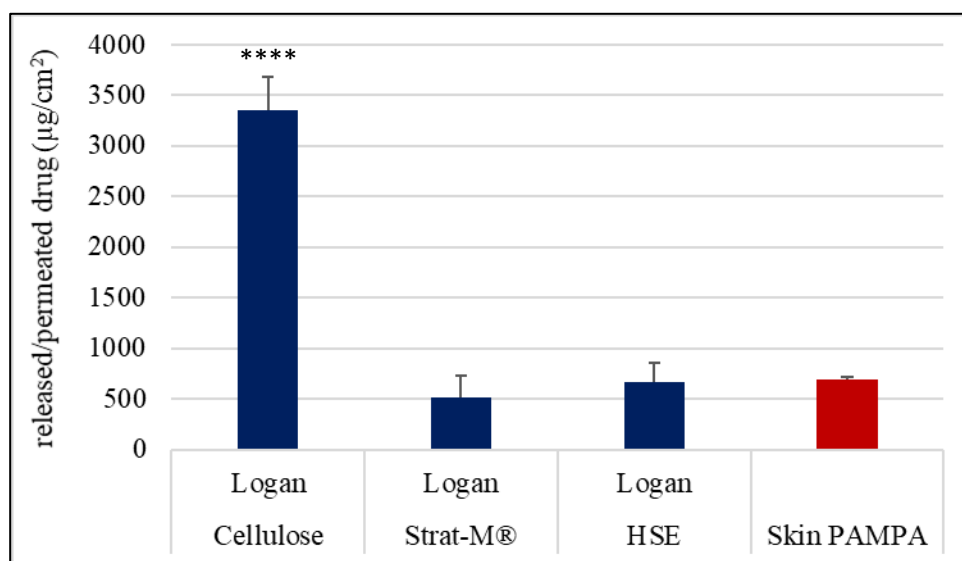


Figure 11 Results of Logan cell and skin PAMPA.

(**** $p < 0.0001$ vs Logan HSE)

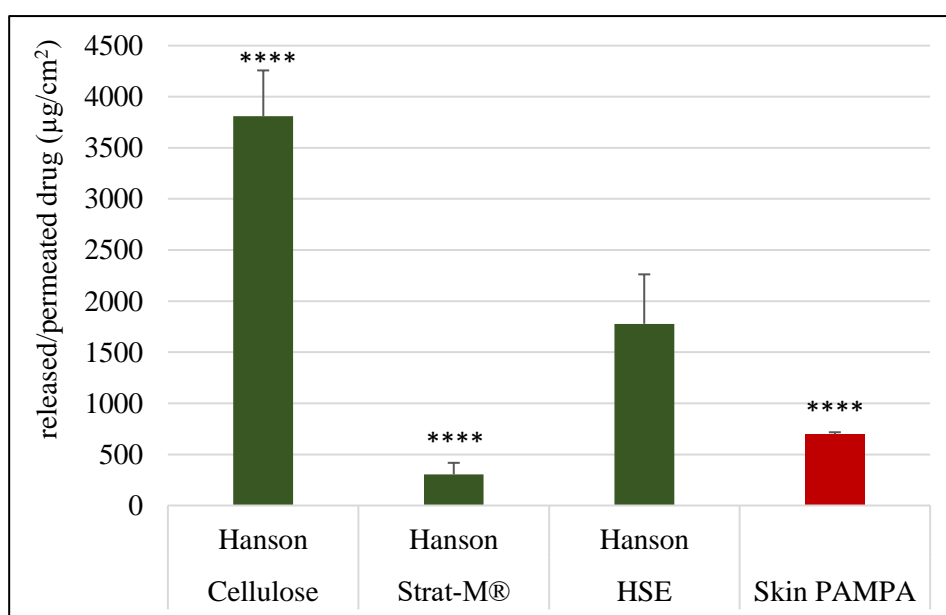


Figure 12 Results of Hanson cell and skin PAMPA.

(**** $p < 0.0001$ vs Hanson HSE)

Summary of experimental part 1

A lidocaine-loaded, NLC gel were used to study *in vitro* release and skin permeation. Two types of Franz cell equipment were compared to each other. Logan and Hanson Franz cells provided different results.

Different membranes were compared, as well. Both the new special skin PAMPA membrane and new synthetic Strat-M membranes correlated well with the HSE membrane and the Strat-M membranes showed the most similar drug permeability profile to the *in vitro* human skin membrane.

Based on the results, it can be stated that the IVPT tests approved in the guidelines (penetration of the human epidermis) can be better replaced with a Strat-M membrane patterned on a Logan cell and a skin PAMPA device. The results of the Hanson cell showed a significant difference between the different membranes and the skin PAMPA. In our work, further investigations were performed on the Logan cell.

5.2. Experimental part 2

In experimental part 2, Logan Franz cell and skin PAMPA methods were compared to Raman spectroscopy. Logan Franz cell and skin PAMPA are quantitative, while Raman spectroscopy is semiquantitative. The sensitivity of these methods was also tested by the investigation of different semisolid preparations.

Three most commonly used dermal formulations were compared: a hydrogel, an o/w and a w/o cream each of them containing 1 w/w% of DFNa.

5.2.1. Investigation of Different Semisolid Formulations by Quantitative Methods

The Franz cell and skin PAMPA methods are based on the quantitative measurement of drug permeation through a skin-mimicking membrane. Figures 13 and 14 show the cumulative amount of drug passing through the different membranes from the different types of formulations in 6 h in $\mu\text{g}/\text{cm}^2$.

In Figure 13 different formulations were compared. In the case of cellulose membrane, the hydrogel showed the highest drug release values. The hydrogel is an aqueous-based system where the drug is in dissolved form, and diffusion through the synthetic membrane is high. The highest permeation from the o/w cream was observed in HSE, Strat-M and skin PAMPA measurements because DFNa is in the outer aqueous phase of the cream, and the emulsifier content of the cream promotes permeation through human skin and special skin-mimicking membranes. The release and permeation of DFNa from the w/o cream were extremely low in all measurements. The drug is presumably in

the inner phase of the cream, and the low diffusion and permeation can be explained by the fact that the diffusion of DFNa through the oil phase limits the release of the drug.

In the case of the hydrogel and o/w cream, the other membranes showed a significant difference compared to the result of HSE, but the result of the Strat-M membrane was closest to that of the human epidermis. In the case of the w/o cream, there was no significant difference between the results of HSE and Strat-M membrane.

In Figure 14, we examined the different compositions on the different membranes. Through the cellulose membrane, the hydrogel showed the best results, followed by the o/w cream and finally the w/o cream. There was a significant difference in drug release between the formulations. Penetration through the human epidermis changed the order, the best result was given by the o/w cream, followed by the hydrogel and then the w/o cream. A possible explanation is that the emulsifiers in the o/w cream have a penetration enhancing effect, which facilitated the penetration of the active ingredient. On the Strat-M membrane and skin PAMPA membrane, the sequence followed the results obtained on the HSE. It can be concluded that the PAMPA membrane, containing the compounds of the stratum corneum, and the Strat-M skin-mimic membrane correlates well with the HSE.

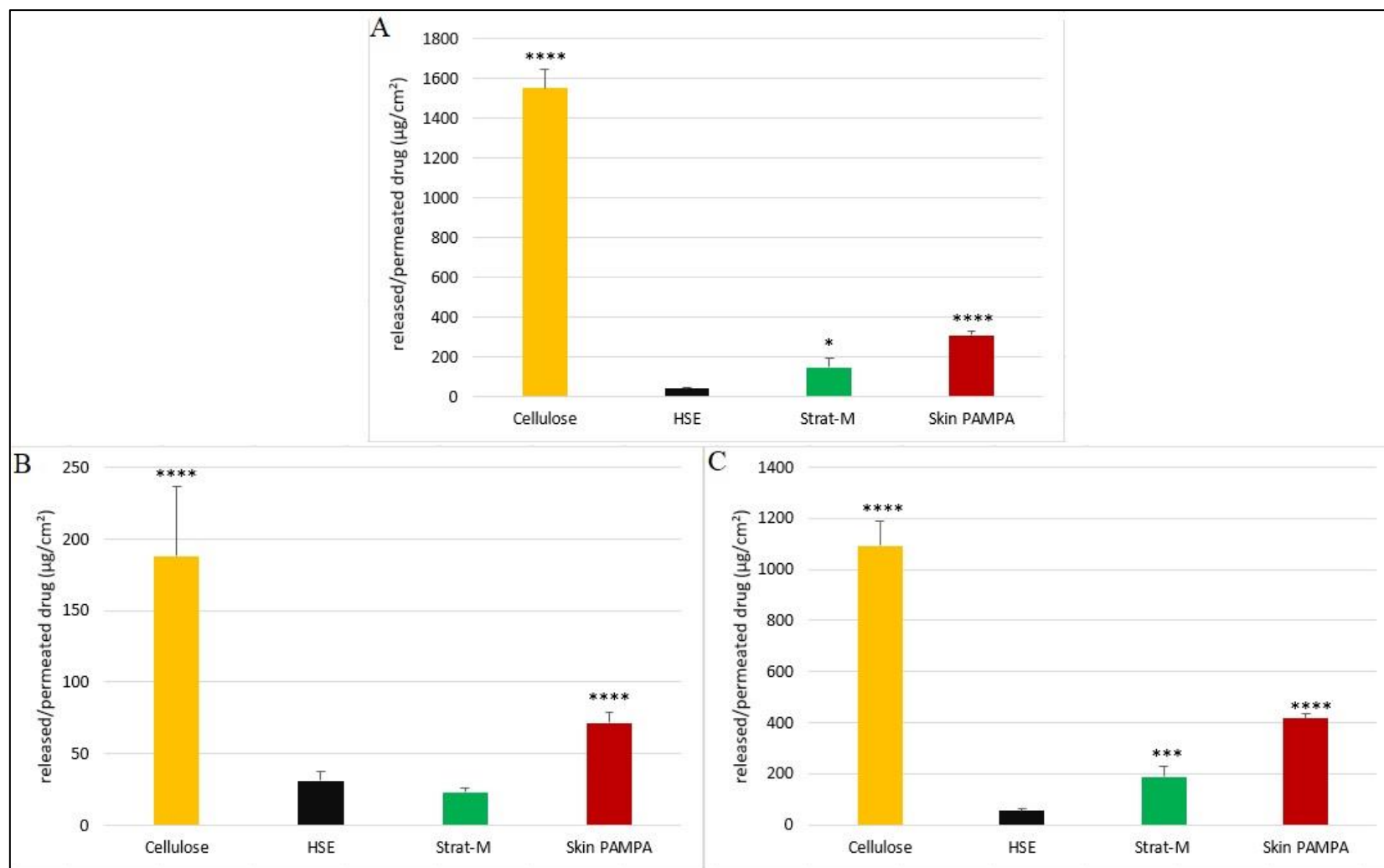


Figure 13 **A:** Results of drug released and penetrated from the hydrogel **B:** Results of drug released and penetrated from w/o cream **C:** Results of drug released and penetrated from o/w cream.
 (**** $p < 0.0001$, *** $p < 0.001$, * $p < 0.05$ vs HSE)

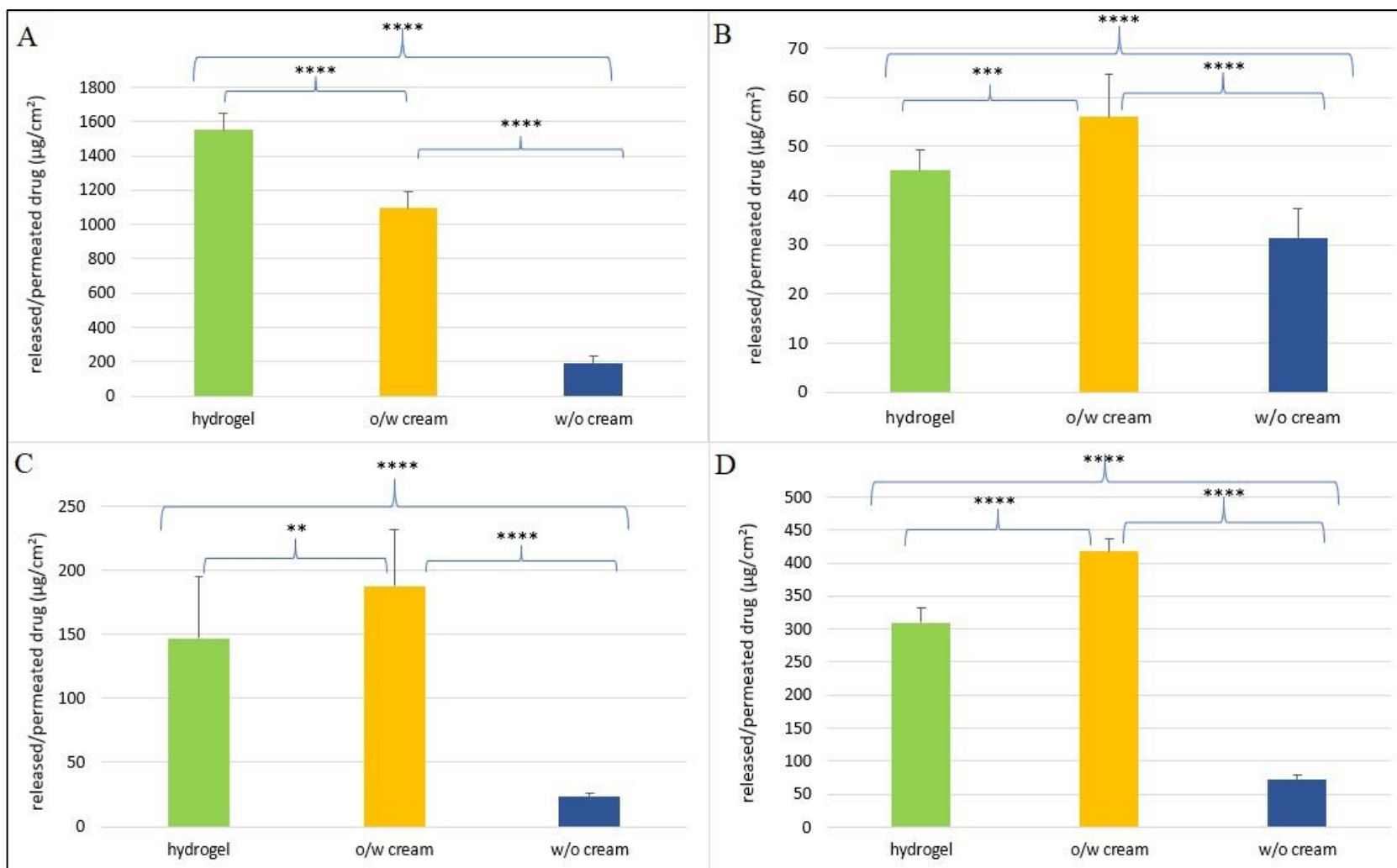


Figure 14 **A:** Results of drug diffusion through cellulose membrane **B:** Results of drug penetration through the HSE membrane **C:** Results of drug penetration through Strat-M membrane **D:** Results of drug penetration through skin PAMPA membrane.
 (**** $p < 0.0001$, *** $p < 0.001$, ** $p < 0.01$)

The mathematical evaluation of the results is shown in Table 5. Permeation parameters (Q, and J) show the differences between the methods and formulations. All methods have good sensitivity to show significant differentiation between the different formulations, so it is a very good tool in the preformulation phase to find the best suited one for the purpose of use.

Table 5 Permeation parameters of diclofenac sodium through cellulose membrane, Strat-M membrane, heat-separated human epidermis and PAMPA membrane after 6 h.

Formulation	Q, 6 h ($\mu\text{g}/\text{cm}^2$)	J ($\mu\text{g}/\text{cm}^2/\text{h}$)
cellulose		
hydrogel	1552.0 \pm 98.9	76.03
o/w cream	1092.9 \pm 98.4	179.13
w/o cream	188.2 \pm 48.8	31.36
Strat-M		
hydrogel	146.83 \pm 47.94	23.593
o/w cream	187.68 \pm 44.33	29.966
w/o cream	23.17 \pm 3.04	3.3194
HSE		
hydrogel	45.18 \pm 4.15	7.32
o/w cream	56.1 \pm 8.6	8.37
w/o cream	31.4 \pm 6.0	4.50
skin PAMPA		
hydrogel	310.1 \pm 21.4	52.59
o/w cream	417.6 \pm 19.7	68.51
w/o cream	71.5 \pm 7.1	11.85

Q, cumulative amount of diclofenac sodium permeated per cm^2 at 6 h (mean \pm SD, $n=6$); **J**, flux determined from the slope of the cumulative amounts of diclofenac sodium permeated ($\mu\text{g}/\text{cm}^2$) versus time (h) profiles

Figures 15 and 16 show the correlation of the skin PAMPA and Strat-M membrane to HSE. Both synthetic membranes demonstrate high correlation to HSE in this study. The time point correlation between the synthetic membranes and HSE was in the range of 0.93–0.99.

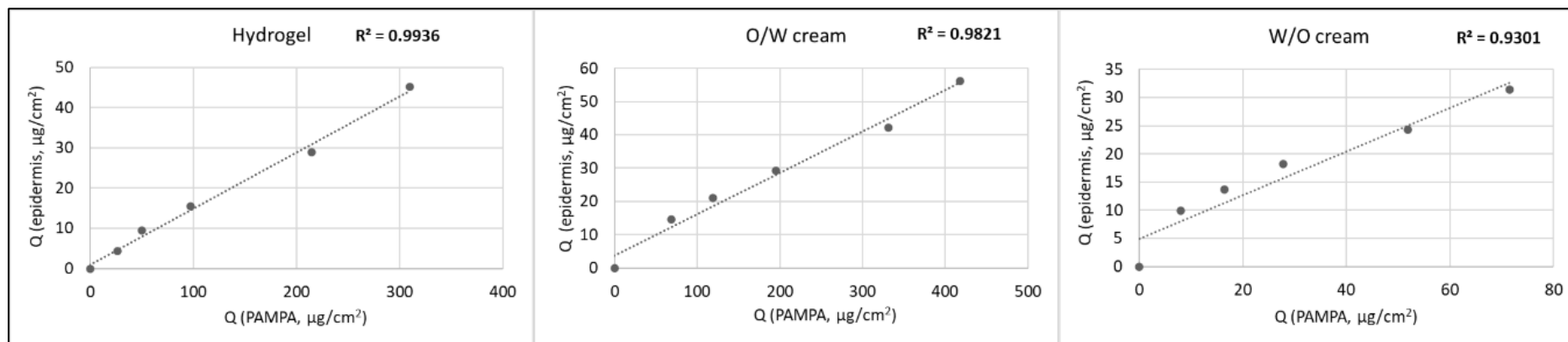


Figure 15 Diclofenac sodium permeation, time point correlations between the amounts of drug permeated through heat-separated human epidermis and skin PAMPA.

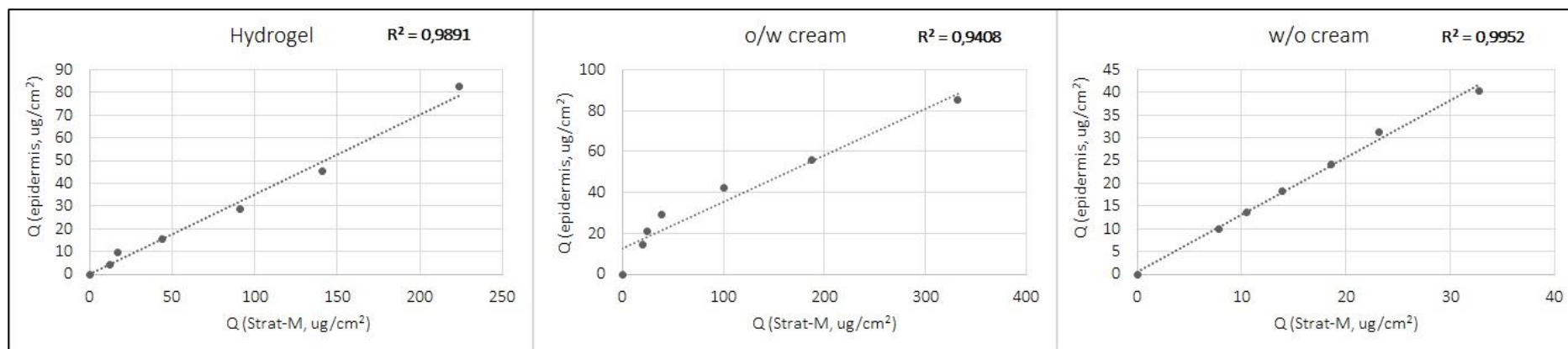


Figure 16 Diclofenac sodium permeation, time point correlations between the amounts of drug permeated through heat-separated human epidermis and Strat-M membrane.

5.2.2. Semiquantitative study: RAMAN Mapping

The Raman correlation map proves the presence of the permeated drug formulations in the different regions of the human skin, from the skin surface to the lower layers of the dermis after treatment with the different compositions. The Raman spectra of the skin are really diverse and consist of numerous bands originating from different skin segments (e.g., nucleic acids, lipids, proteins) [86,96,97]. Several bands are overlapping with the spectra of the examined preparations. During the Raman experiments, the differences in the localization of the formulations in the skin regions were determined and compared with the Franz cell and skin PAMPA results.

The correlation maps, which showed the distribution of DFNa, were produced by fitting the appropriate spectra to the spectra of the treated skin. DFNa is easily determined from the formulations but the intensities of the characteristic DFNa peaks are very low. Therefore, the spectra of the pure API could not be used to make an acceptable correlation map. In this case, we had to use the spectrum of the whole preparation to make the skin distribution correlation maps, which indicates the presence of DFNa as well. The spectral maps were resolved in order to verify the presence of the formulation in the different regions of the human skin. The fingerprint region of the preparation spectra was related to the spectra of human skin being tested and untreated. The similarity was shown as intensity. The distribution profiles describing the relationship between the map spectra (treated skin specimen) and the defined reference spectrum (fingerprint region) were created. The resulting correlation intensity values of the map spectra are similar to the match values of the reference spectra. A more powerful intensity rate means a higher correlation with the reference spectrum.

The Raman chemical maps of the preparations are shown in Figure 17. In the case of the hydrogel, the most permeated drugs are found in the upper layers of the skin, the epidermis and the upper dermis. The o/w cream mostly permeated into the deeper layers of the skin. This is due to the emulsifier, which increases permeation. In the case of the w/o cream, most of the composition could be found only in the stratum corneum region, and deeper permeation was blocked. This is due to its really high oil content in the external phase, which cannot pass through the hydrophilic layer of the epidermis.

These results correlate well with the results of HSE and skin PAMPA. In correlation with these results, the o/w cream shows the most effective permeation results where the formulation could be found in the dermis, followed by hydrogel, where the formulation

passed through the regions of the epidermis and dermis. The permeation of the w/o cream was the lowest with all the methods during the time of the experiment.

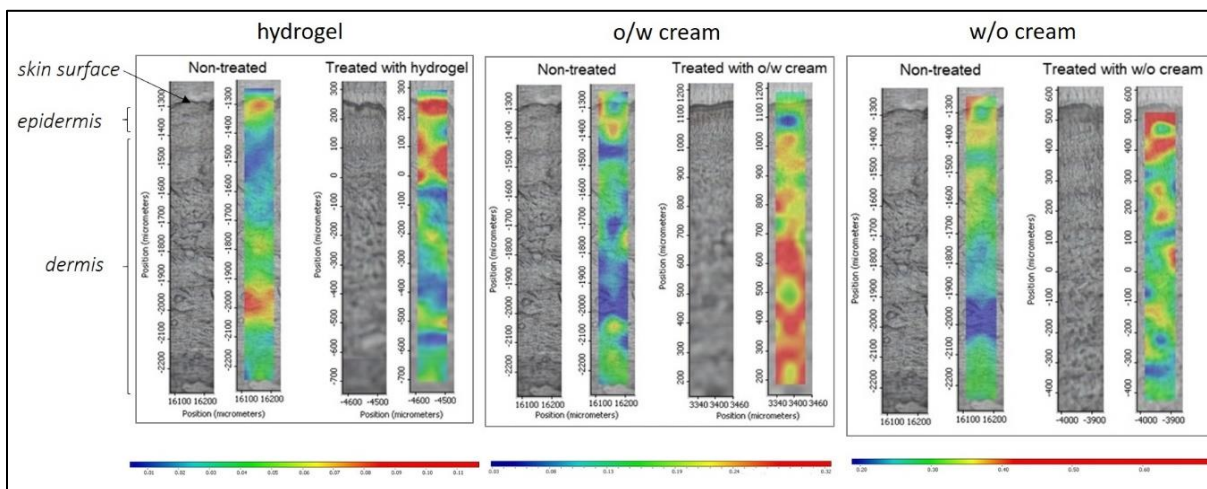


Figure 17 Raman correlation maps for the distribution of diclofenac sodium in human skin after treatment with hydrogel, o/w cream and w/o cream. Untreated skin is also displayed as a control in all cases.

Color coding of drug formulation content: red > yellow > green > blue.

Summary of experimental part 2

The investigations proved the applicability of the Strat-M membrane and the skin PAMPA method in skin permeation tests. Both methods correlated highly with the HSE membrane the permeation of different dermal formulations was compared. However, the quantity of the permeated drug from different formulations was different.

The comparison of the results indicates that the skin PAMPA and Strat-M method were closer to the gold standard HSE (IVPT) method. Its use before IVPT tests may be beneficial as it shows differences between formulations in the same way as HSE.

This part of the work also highlights the capability of Raman spectroscopy as a non-destructive technique for studying skin distribution of active ingredients and following the active ingredient in the skin layers. It could semi-quantitatively estimate the relative amounts of preparations permeated into the different skin layers. It is important to understand how different formulations influence the permeation of active agents into/through the skin as this presents relevant information for formulation developers. In the current study, the results of Raman mapping have high correlation with the results of Strat-M, skin PAMPA and IVPT methods.

6. CONCLUSION

Modeling drug permeation through the skin is a complex challenge. Although there are many quantitative and qualitative methods for following-up skin penetration/permeation, the different techniques are not fully equivalent but complement each other. The advantages and disadvantages of the different methods are summarized in Table 6.

Table 6 *Advantages and disadvantages of previously discussed methods.*

	Advantages	Disadvantages
Franz Diffusion	<ul style="list-style-type: none">• accepted by authorities• quantitative• automated (can be)• various synthetic and biological membranes• repeated dosing (open cell)	<ul style="list-style-type: none">• differences between research labours• different types of cells• application requires practice
Skin PAMPA	<ul style="list-style-type: none">• fast, several preparations can be tested at the same time• small space and instrument demand• quantitative	<ul style="list-style-type: none">• not automated• sampling by hand• synthetic membrane only• limited time
Raman Spectroscopy	<ul style="list-style-type: none">• high resolution• <i>in vitro</i> (sometimes <i>in vivo</i>)• non-invasive• semi-destructive• highly selective	<ul style="list-style-type: none">• difficult to reproduce• expensive lasers are needed• only qualitative (or semiquantitative)• usually, the time of measurement is long

For the evaluation of drug permeation, pharmaceutical technologists must decide those properly suited to their examinations. These models make a rapid screening and faster optimization of product possible. The success of topical and transdermal therapy correlates with the techniques used for the evaluation of preparations, which facilitates the optimization of the skin penetration of the API that is why sufficient API penetration is possible at the therapeutic site.

This work has proven that the new Strat-M membrane, the skin PAMPA method and the Raman mapping technique have the potential to be used as a screening tool to choose the best dermal formulation in the pharmaceutical, cosmetic, and personal care industries. The development of methodologies to improve the throughput of formulation testing will help to promote a better understanding of preparation variables and mechanisms of skin permeation. Future studies in this field are still needed to examine and compare the different methods. Other types of formulations and active substances should also be tested. It would also be useful to study different drug concentrations for the same formulations to support the suitability of the method for monitoring dermal permeation. Therefore, it is essential to highlight that the investigated *in vitro* models provide important tools for screening a series of drug formulations, evaluation of skin permeation and mechanism of action of the carrier systems, and evaluation of rank of skin transport. Thus, in pharmaceutical development, less effective preparations can be excluded quickly and cheaply from many formulations.

Based on our results, the conclusions suggest that all early screening examinations can be performed with model tools such as IVRT and skin PAMPA using cheaper synthetic membranes. The final formulations should be examined with IVPT to collect permeation data supplemented with semiquantitative methods like Raman mapping using human skin.

THESIS FINDINGS

I. Comparative study of diffusion cells

- There was significant difference between the results of the two types of Franz cell devices.
- The amount of drug permeated on each device was dependent on the membrane. For devices alone, no general correlation can be created.
- These findings should be considered for official assessment and authorization.

II. Investigation of Strat-M synthetic membrane

- The Strat-M membrane findings were compared to the already well-defined cellulose membrane and heat-separated human epidermis.
- Based on the results, significantly less active substance passed through the innovative synthetic Strat-M membrane compared to the cellulose membrane. The Strat-M membrane showed almost the same result as the values measured on HSE due to its special skin-mimic properties. Examining the 24-hour cumulative amounts measured on the HSE, the Strat-M membrane also showed a good correlation with the human epidermis in formulations of different compositions. The penetration-enhancing effect of the o/w cream, which is well detectable on HSE, could be well modeled by the Strat-M membrane.
- Based on these results, the synthetic Strat-M membrane can be recommended for IVPT measurements to replace the human epidermis, thus eliminating the disadvantageous properties of the biological membrane.

III. Investigation of Skin PAMPA method

- Compared to the cellulose membrane, significantly less drug was permeated on the skin PAMPA membrane, but significantly more drug was permeated compared to the tests performed on HSE. The skin PAMPA membrane proved to be more permeable in terms of cumulative amount of drug than the Strat-M membrane.
- In the case of different formulations, the skin PAMPA membrane, like the Strat-M membrane, well modeled the results obtained at HSE. It was able to differentiate between each formulation.
- It can be concluded that the skin PAMPA method may also be suitable to replace the HSE membrane, with the limitation that only a shorter 6-hour test period is recommended to ensure membrane integrity.

IV. Investigation of Raman spectroscopy

- The Raman spectroscopy with chemical mapping was studied, which allows for the examination of penetration across the whole skin. It was already mentioned in the most recent EMA guideline, so it is critical to investigate the method's applicability.
- The results confirmed that the method is suitable for detecting differences between preparations. The penetration enhancing effect was well detectable, too.
- Raman mapping may complement the results of quantitative methods of skin penetration.

REFERENCES

1. Transdermal Drug Delivery Systems Market - Industry Analysis, Market Size, Share, Trends, Application Analysis, Growth And Forecast 2019 - 2024 Available Online: <https://Industryarc.Com/Research/Transdermal-Drug-Delivery-Systems-Market-Research> (01.04.2019.).
2. Abd, E.; Yousuf, S.; Pastore, M.; Telaprolu, K.; Mohammed, Y.; Namjoshi, S.; Grice, J.; Roberts, M. Skin Models for the Testing of Transdermal Drugs. *Clin. Pharmacol. Adv. Appl.* **2016**, Volume 8, 163–176, doi:10.2147/CPAA.S64788.
3. Shah, V.P.; Yacobi, A.; Rădulescu, F.Ş.; Miron, D.S.; Lane, M.E. A science based approach to topical drug classification system (TCS). *Int. J. Pharm.* **2015**, 491, 21–25.
4. Wiedersberg, S.; Guy, R.H. Transdermal Drug Delivery: 30+ Years of War and Still Fighting! *J. Controlled Release* **2014**, 190, 150–156, doi:10.1016/j.jconrel.2014.05.022.
5. OECD Guidance Document for the Conduct of Skin Absorption Studies; OECD Series on Testing and Assessment, **2004**; ISBN 978-92-64-07879-6.
6. OECD. Guidance Notes on Dermal Absorption, Series on Testing and Assessment No. 156. **2011**, Paris.
7. OECD. Test Guideline 427: Skin Absorption: In Vivo Method. **2004**, Paris.
8. OECD. Test Guideline 428: Skin Absorption: In Vitro Method. **2004**, Paris.
9. European Food Safety Authority (EFSA); Buist, H.; Craig, P.; Dewhurst, I.; Hougaard Bennekou, S.; Kneuer, C.; Machera, K.; Pieper, C.; Court Marques, D.; Guillot, G.; et al. Guidance on Dermal Absorption. *EFSA J.* **2017**, 15, doi:10.2903/j.efsa.2017.4873.
10. Franz, T.J. Percutaneous Absorption. On the Relevance of in Vitro Data. *J. Invest. Dermatol.* **1975**, 64, 190–195, doi:10.1111/1523-1747.ep12533356.
11. So, J.; Ahn, J.; Lee, T.-H.; Park, K.-H.; Paik, M.-K.; Jeong, M.; Cho, M.-H.; Jeong, S.-H. Comparison of International Guidelines of Dermal Absorption Tests Used in Pesticides Exposure Assessment for Operators. *Toxicol. Res.* **2014**, 30, 251–260, doi:10.5487/TR.2014.30.4.251.
12. Groeber, F.; Holeiter, M.; Hampel, M.; Hinderer, S.; Schenke-Layland, K. Skin Tissue Engineering — In Vivo and in Vitro Applications. *Adv. Drug Deliv. Rev.* **2011**, 63, 352–366, doi:10.1016/j.addr.2011.01.005.
13. Anissimov, Y.G.; Jepps, O.G.; Dancik, Y.; Roberts, M.S. Mathematical and Pharmacokinetic Modelling of Epidermal and Dermal Transport Processes. *Adv. Drug Deliv. Rev.* **2013**, 65, 169–190, doi:10.1016/j.addr.2012.04.009.

14. Bo Forslind. A Domain Mosaic Model of the Skin Barrier. *Acta Derm Venereol* **1994**, 74, 1-6.
15. Godin, B.; Touitou, E. Transdermal Skin Delivery: Predictions for Humans from in Vivo, Ex Vivo and Animal Models. *Adv. Drug Deliv. Rev.* **2007**, 59, 1152–1161, doi:10.1016/j.addr.2007.07.004.
16. Dragicevic, N.; I. Maibach, H. Percutaneous Penetration Enhancers Drug Penetration Into/Through the Skin; *Springer Berlin Heidelberg*, **2017**; ISBN 978-3-662-53268-3.
17. Prausnitz, M.R.; Elias, P.M.; Franz, T.J.; Schmuth, M.; Tsai, J.-C.; Menon, G.K.; Holleran, W.M.; Feingold, K.R. Skin Barrier and Transdermal Drug Delivery. *Medical Therapy*, **2012**, 10
18. Ueda, C.T.; Shah, V.P.; Derdzinski, K.; Ewing, G.; Flynn, G.; Maibach, H.; Marques, M.; Rytting, H.; Shaw, S.; Thakker, K.; et al. Topical and Transdermal Drug Products. *Dissolution Technol.* **2010**, 17, 12–25, doi:10.14227/DT170410P12.
19. Feldmann, R.J.; Maibach, H.I. Absorption of Some Organic Compounds Through the Skin in Man. *J. Invest. Dermatol.* **1970**, 54, 399–404, doi:10.1111/1523-1747.ep12259184.
20. Blank, I.H. Factors Which Influence the Water Content of the Stratum Corneum. *J. Invest. Dermatol.* **1952**, 18, 433–440, doi:10.1038/jid.1952.52.
21. Vinson, L.J.; Singer, E.J.; Koehler, W.R.; Lehman, M.D.; Masurat, T. The Nature of the Epidermal Barrier and Some Factors Influencing Skin Permeability. *Toxicol. Appl. Pharmacol.* **1965**, 7, 7–19, doi:10.1016/0041-008X(65)90107-9.
22. Elias, P.M. The Permeability Barrier in Mammalian Epidermis. *J. Cell Biol.* **1975**, 65, 180–191, doi:10.1083/jcb.65.1.180.
23. Sweeney, T.M.; Downing, D.T. The Role of Lipids in the Epidermal Barrier to Water Diffusion. *J. Invest. Dermatol.* **1970**, 55, 135–140, doi:10.1111/1523-1747.ep12291678.
24. Hadgraft, J. Skin Deep. *Eur. J. Pharm. Biopharm.* **2004**, 58, 291–299, doi:10.1016/j.ejpb.2004.03.002.
25. Ruela, A.L.M.; Perissinato, A.G.; Lino, M.E. de S.; Mudrik, P.S.; Pereira, G.R. Evaluation of Skin Absorption of Drugs from Topical and Transdermal Formulations. *Braz. J. Pharm. Sci.* **2016**, 52, 527–544, doi:10.1590/s1984-82502016000300018.
26. Jepps, O.G.; Dancik, Y.; Anissimov, Y.G.; Roberts, M.S. Modeling the Human Skin Barrier — Towards a Better Understanding of Dermal Absorption. *Adv. Drug Deliv. Rev.* **2013**, 65, 152–168, doi:10.1016/j.addr.2012.04.003.

27. Barry, B.W. Novel Mechanisms and Devices to Enable Successful Transdermal Drug Delivery. *Eur. J. Pharm. Sci.* **2001**, *14*, 101–114, doi:10.1016/S0928-0987(01)00167-1.
28. Patzelt, A.; Richter, H.; Knorr, F.; Schäfer, U.; Lehr, C.-M.; Dähne, L.; Sterry, W.; Lademann, J. Selective Follicular Targeting by Modification of the Particle Sizes. *J. Controlled Release* **2011**, *150*, 45–48, doi:10.1016/j.jconrel.2010.11.015.
29. Zsikó; Csányi; Kovács; Budai-Szücs; Gácsi; Berkó Methods to Evaluate Skin Penetration In Vitro. *Sci. Pharm.* **2019**, *87*, 19, doi:10.3390/scipharm87030019.
30. Namjoshi, S., Dabbaghi, M., Roberts, M.S., Grice, J.E., Mohammed, Y., Quality by Design: Development of the Quality Target Product Profile (QTPP) for Semisolid Topical Products. *Pharmaceutics*, **2020**, *12*, 287. doi:10.3390/pharmaceutics12030287.
31. Berkó, S.; Zsikó, S.; Deák, G.; Gácsi, A.; Kovács, A.; Budai-Szücs, M.; Pajor, L.; Bajory, Z.; Csányi, E. Papaverine Hydrochloride Containing Nanostructured Lyotropic Liquid Crystal Formulation as a Potential Drug Delivery System for the Treatment of Erectile Dysfunction. *Drug Des. Devel. Ther.* **2018**, *Volume 12*, 2923–2931, doi:10.2147/DDDT.S168218.
32. Bakonyi, M.; Berkó, S.; Kovács, A.; Budai-Szücs, M.; Kis, N.; Erős, G.; Csóka, I.; Csányi, E. Application of Quality by Design Principles in the Development and Evaluation of Semisolid Drug Carrier Systems for the Transdermal Delivery of Lidocaine. *J. Drug Deliv. Sci. Technol.* **2018**, *44*, 136–145, doi:10.1016/j.jddst.2017.12.001.
33. Zsikó, S.; Csányi, E.; Kovács, A.; Budai-Szücs, M.; Gácsi, A.; Berkó, S. Novel In Vitro Investigational Methods for Modeling Skin Permeation: Skin PAMPA, Raman Mapping. *Pharmaceutics* **2020**, *12*, 803, doi:10.3390/pharmaceutics12090803.
34. Kalia, Y. Modeling Transdermal Drug Release. *Adv. Drug Deliv. Rev.* **2001**, *48*, 159–172, doi:10.1016/S0169-409X(01)00113-2.
35. Machado, A.C.H.R.; Lopes, P.S.; Raffier, C.P.; Haridass, I.N.; Roberts, M.; Grice, J.; Leite-Silva, V.R. Skin Penetration. In *Cosmetic Science and Technology*; Elsevier, **2017**; pp. 741–755 ISBN 978-0-12-802005-0.
36. Moser, K.; Kriwet, K.; Naik, A.; Kalia, Y.N.; Guy, R.H. Passive Skin Penetration Enhancement and Its Quantification in Vitro. *Eur. J. Pharm. Biopharm.* **2001**, *10*.
37. Delgado-Charro, M.B.; Guy, R.H. Effective Use of Transdermal Drug Delivery in Children. *Adv. Drug Deliv. Rev.* **2014**, *73*, 63–82, doi:10.1016/j.addr.2013.11.014.
38. Machado, M.; Hadgraft, J.; Lane, M.E. Assessment of the Variation of Skin Barrier Function with Anatomic Site, Age, Gender and Ethnicity: Assessment of the Variation

- of Skin Barrier Function. *Int. J. Cosmet. Sci.* **2010**, 32, 397–409, doi:10.1111/j.1468-2494.2010.00587.x.
39. Waller, J.M.; Maibach, H.I. Age and Skin Structure and Function, a Quantitative Approach (I): Blood Flow, PH, Thickness, and Ultrasound Echogenicity. *Skin Res. Technol.* **2005**, 11, 221–235, doi:10.1111/j.0909-725X.2005.00151.x.
 40. Behl, C.R.; Flynn, G.L.; Kurihara, T.; Smith, W.; Gatmaitan, O.; Higuchi, W.I.; Ho, N.F.H.; Pierson, C.L. Permeability of Thermally Damaged Skin: I. Immediate Influences of 60°C Scalding on Hairless Mouse Skin. *J. Invest. Dermatol.* **1980**, 75, 340–345, doi:10.1111/1523-1747.ep12531096.
 41. Behl, C.R.; Flynn, G.L.; Barrett, M.; Walters, K.A.; Linn, E.E.; Mohamed, Z.; Kurihara, T.; Ho, N.F.H.; Higuchi, W.I.; Pierson, C.L. Permeability of Thermally Damaged Skin II: Immediate Influences of Branding at 60°C on Hairless Mouse Skin Permeability. *Burns* **1981**, 7, 389–399, doi:10.1016/0305-4179(81)90125-X.
 42. Flaten, G.E.; Palac, Z.; Engesland, A.; Filipović-Grčić, J.; Vanić, Ž.; Škalko-Basnet, N. In Vitro Skin Models as a Tool in Optimization of Drug Formulation. *Eur. J. Pharm. Sci.* **2015**, 75, 10–24, doi:10.1016/j.ejps.2015.02.018.
 43. Kielhorn, J.; International Programme on Chemical Safety *Dermal Absorption*; Environmental health criteria; WHO: Geneva, **2006**; ISBN 978-92-4-157235-4.
 44. European Centre for Ecotoxicology and Toxicology of Chemicals. Percutaneous absorption, Monograph; No. 20; European Centre for Ecotoxicology and Toxicology of Chemicals: Bruxelles, Belgium, **1993**; ISSN 0773-6347-20.
 45. EPAU.S. Environmental Protection Agency (EPA). EPAU.S. Environmental Protection Agency (EPA). Dermal Exposure Assessment: A Summary of EPA Approaches. Available Online: [Http://Www.Epa.Gov/Ncea](http://www.epa.gov/ncea). (01.04.2019.).
 46. European Medicines Agency. FDA Draft Guideline on Quality and Equivalence of Topical Products EMA/CHMP/QWP/708282/2018; European Medicines Agency: Amsterdam, The Netherlands, **2018**.
 47. Anissimov, Y.G.; Roberts, M.S. Diffusion Modelling of Percutaneous Absorption Kinetics: 4. Effects of a Slow Equilibration Process Within Stratum Corneum on Absorption and Desorption Kinetics. *J. Pharm. Sci.* **2009**, 98, 772–781, doi:10.1002/jps.21461.
 48. Anissimov, Y.G.; Roberts, M.S. Diffusion Modeling of Percutaneous Absorption Kinetics. 1. Effects of Flow Rate, Receptor Sampling Rate, and Viable Epidermal

- Resistance for a Constant Donor Concentration. *J. Pharm. Sci.* **1999**, 88, 1201–1209, doi:10.1021/js990053i.
49. Anissimov, Y.G.; Roberts, M.S. Diffusion Modeling of Percutaneous Absorption Kinetics: 3. Variable Diffusion and Partition Coefficients, Consequences for Stratum Corneum Depth Profiles and Desorption Kinetics. *J. Pharm. Sci.* **2004**, 93, 470–487, doi:10.1002/jps.10567.
 50. Anissimov, Y.G.; Roberts, M.S. Diffusion Modeling of Percutaneous Absorption Kinetics: 2. Finite Vehicle Volume and Solvent Deposited Solids. *J. Pharm. Sci.* **2001**, 90, 504–520, doi:10.1002/1520-6017(200104)90:4<504::AID-JPS1008>3.0.CO;2-H.
 51. Todo, H.; Oshizaka, T.; Kadhum, W.; Sugibayashi, K. Mathematical Model to Predict Skin Concentration after Topical Application of Drugs. *Pharmaceutics* **2013**, 5, 634–651, doi:10.3390/pharmaceutics5040634.
 52. Crank, J. *The Mathematics of Diffusion*, 2nd ed.; Clarendon Press: Oxford, UK, **1975**; ISBN 978-0-19-853344-3.
 53. Franz, T.J. Percutaneous Absorption. On the Relevance of in Vitro Data. *J. Invest. Dermatol.* **1975**, 64, 190–195, doi:10.1111/1523-1747.ep12533356.
 54. Franz, T.J. The Finite Dose Technique as a Valid in vitro Model for the Study of Percutaneous Absorption in Man. In *Current Problems in Dermatology*; Simon, G.A., Paster, Z., Klingberg, M.A., Kaye, M., Eds.; S. Karger AG, **1979**; Vol. 7, pp. 58–68 ISBN 978-3-8055-2797-2.
 55. Sesto Cabral, M.E.; Ramos, A.N.; Cabrera, C.A.; Valdez, J.C.; González, S.N. Equipment and Method for *in Vitro* Release Measurements on Topical Dosage Forms. *Pharm. Dev. Technol.* **2015**, 20, 619–625, doi:10.3109/10837450.2014.908308.
 56. Bronaugh, R.L.; Stewart, R.F. Methods for In Vitro Percutaneous Absorption Studies IV: The Flow-Through Diffusion Cell. *J. Pharm. Sci.* **1985**, 74, 64–67, doi:10.1002/jps.2600740117.
 57. Barry, B.W.; Eini, D.I.D.E. Influence of Non-Ionic Surfactants on Permeation of Hydrocortisone, Dexamethasone, Testosterone and Progesterone across Cellulose Acetate Membrane. *J. Pharm. Pharmacol.* **1976**, 28, 219–227, doi:10.1111/j.2042-7158.1976.tb04134.x.
 58. Zsikó, S.; Cutcher, K.; Kovács, A.; Budai-Szűcs, M.; Gácsi, A.; Baki, G.; Csányi, E.; Berkó, S. Nanostructured Lipid Carrier Gel for the Dermal Application of Lidocaine: Comparison of Skin Penetration Testing Methods. *Pharmaceutics* **2019**, 11, 310, doi:10.3390/pharmaceutics11070310.

59. Bakonyi, M.; Gácsi, A.; Berkó, S.; Kovács, A.; Csányi, E. Stratum Corneum Lipid Liposomes for Investigating Skin Penetration Enhancer Effects. *RSC Adv.* **2018**, *8*, 27464–27469, doi:10.1039/C8RA04129F.
60. Csányi, E.; Sütő, B.; Berkó, S.; Kozma, G.; Kukovecz, Á.; Budai-Szűcs, M.; Erős, G.; Kemény, L.; Sztojkov-Ivanov, A.; Gaspar, R. Development of Ibuprofen-Loaded Nanostructured Lipid Carrier-Based Gels: Characterization and Investigation of in Vitro and in Vivo Penetration through the Skin. *Int. J. Nanomedicine* **2016**, 1201.
61. Csizmazia, E.; Erős, G.; Berkesi, O.; Berkó, S.; Szabó-Révész, P.; Csányi, E. Pénétration Enhancer Effect of Sucrose Laurate and Transcutol on Ibuprofen. *J. Drug Deliv. Sci. Technol.* **2011**, *21*, 411–415, doi:10.1016/S1773-2247(11)50066-8.
62. Haq, A.; Dorrani, M.; Goodyear, B.; Joshi, V.; Michniak-Kohn, B. Membrane Properties for Permeability Testing: Skin versus Synthetic Membranes. *Int. J. Pharm.* **2018**, *539*, 58–64, doi:10.1016/j.ijpharm.2018.01.029.
63. Atrux-Tallau, N.; Pirot, F.; Falson, F.; Roberts, M.S.; Maibach, H.I. Qualitative and Quantitative Comparison of Heat Separated Epidermis and Dermatomed Skin in Percutaneous Absorption Studies. *Arch. Dermatol. Res.* **2007**, *299*, 507–511, doi:10.1007/s00403-007-0789-y.
64. Madison KC. Barrier function of the skin: "la raison d'être" of the epidermis. *J Invest Dermatol.* **2003**, *121*(2):231-41. doi:10.1046/j.1523-1747.2003.12359.x.
65. Hennies H.C., Poumay Y. Skin Disease Models In Vitro and Inflammatory Mechanisms: Predictability for Drug Development. Organotypic Models in Drug Development. *Handbook of Experimental Pharmacology*, **2021**, 265. doi:10.1007/164_2020_428
66. Neupane, R.; Boddu, S.H.S.; Renukuntla, J.; Babu, R.J.; Tiwari, A.K. Alternatives to Biological Skin in Permeation Studies: Current Trends and Possibilities. *Pharmaceutics* **2020**, *12*, 152, doi:10.3390/pharmaceutics12020152.
67. Arce, F.J.; Asano, N.; See, G.L.; Itakura, S.; Todo, H.; Sugibayashi, K. Usefulness of Artificial Membrane, Strat-M®, in the Assessment of Drug Permeation from Complex Vehicles in Finite Dose Conditions. *Pharmaceutics* **2020**, *12*, 173, doi:10.3390/pharmaceutics12020173.
68. Bolla, P.K.; Clark, B.A.; Juluri, A.; Cheruvu, H.S.; Renukuntla, J. Evaluation of Formulation Parameters on Permeation of Ibuprofen from Topical Formulations Using Strat-M® Membrane. *Pharmaceutics* **2020**, *12*, 151, doi:10.3390/pharmaceutics12020151.

69. Haq, A.; Goodyear, B.; Ameen, D.; Joshi, V.; Michniak-Kohn, B. Strat-M® Synthetic Membrane: Permeability Comparison to Human Cadaver Skin. *Int. J. Pharm.* **2018**, *547*, 432–437, doi:10.1016/j.ijpharm.2018.06.012.
70. Kaur, L.; Singh, K.; Paul, S.; Singh, S.; Singh, S.; Jain, S.K. A Mechanistic Study to Determine the Structural Similarities Between Artificial Membrane Strat-M™ and Biological Membranes and Its Application to Carry Out Skin Permeation Study of Amphotericin B Nanoformulations. *AAPS PharmSciTech* **2018**, *19*, 1606–1624, doi:10.1208/s12249-018-0959-6.
71. Merck Millipore Strat-M membrane product brochure. Available Online: https://www.merckmillipore.com/HU/hu/product/Strat-M-Membrane-Transdermal-Diffusion-Test-Model-25mm,MM_NF-SKBM02560 (2021.05.10.)
72. Uchida, T.; Kadhum, W.R.; Kanai, S.; Todo, H.; Oshizaka, T.; Sugibayashi, K. Prediction of Skin Permeation by Chemical Compounds Using the Artificial Membrane, Strat-M™. *Eur. J. Pharm. Sci.* **2015**, *67*, 113–118, doi:10.1016/j.ejps.2014.11.002.
73. Lee, W.-R.; Hsiao, C.-Y.; Huang, T.-H.; Wang, C.-L.; Alalaiwe, A.; Chen, E.-L.; Fang, J.-Y. Post-Irradiation Recovery Time Strongly Influences Fractional Laser-Facilitated Skin Absorption. *Int. J. Pharm.* **2019**, *564*, 48–58, doi:10.1016/j.ijpharm.2019.04.043.
74. Kansy, M.; Senner, F.; Gubernator, K. Physicochemical High Throughput Screening: Parallel Artificial Membrane Permeation Assay in the Description of Passive Absorption Processes. *J. Med. Chem.* **1998**, *41*, 1007–1010, doi:10.1021/jm970530e.
75. Ottaviani, G.; Martel, S.; Carrupt, P.-A. Parallel Artificial Membrane Permeability Assay: A New Membrane for the Fast Prediction of Passive Human Skin Permeability. *J. Med. Chem.* **2006**, *49*, 3948–3954.
76. Sinkó, B.; Garrigues, T.M.; Balogh, G.T.; Nagy, Z.K.; Tsinman, O.; Avdeef, A.; Takács-Novák, K. Skin-PAMPA: A New Method for Fast Prediction of Skin Penetration. *Eur. J. Pharm. Sci.* **2012**, *45*, 698–707, doi:10.1016/j.ejps.2012.01.011.
77. Zhai, H.; Maibach, H.I. Occlusion vs. Skin Barrier Function: Occlusion versus Skin Barrier Function. *Skin Res. Technol.* **2002**, *8*, 1–6, doi:10.1046/j.0909-752x.2001.10311.x.
78. Escobar-Chavez, J.J.; Merino-Sanjuán, V.; López-Cervantes, M.; Urban-Morlan, Z.; Piñón-Segundo, E.; Quintanar-Guerrero, D.; Ganem-Quintanar, A. The Tape-Stripping Technique as a Method for Drug Quantification in Skin. *J. Pharm. Pharm. Sci.* **2008**, *11*, 104, doi:10.18433/J3201Z.

79. Soriano-Ruiz, J.L.; Suñer-Carbó, J.; Calpena-Campmany, A.C.; Bozal-de Febrer, N.; Halbaut-Bellowa, L.; Boix-Montañés, A.; Souto, E.B.; Clares-Naveros, B. Clotrimazole Multiple W/O/W Emulsion as Anticandidal Agent: Characterization and Evaluation on Skin and Mucosae. *Colloids Surf. B Biointerfaces* **2019**, *175*, 166–174, doi:10.1016/j.colsurfb.2018.11.070.
80. Serpe, L.; Muniz, B.V. Full-Thickness Intraoral Mucosa Barrier Models for In Vitro Drug- Permeation Studies Using Microneedles. *J. Pharm. Sci.* **2019**, *108*, 1756–1764.
81. Köllmer M, Mossahebi P, Sacharow E, Gorissen S, Gräfe N, Evers DH, Herbig ME. Investigation of the Compatibility of the Skin PAMPA Model with Topical Formulation and Acceptor Media Additives Using Different Assay Setups. *AAPS PharmSciTech.* **2019**, 20(2):89. doi:10.1208/s12249-019-1305-3.
82. Sinkó, B.; Pálfi, M.; Béni, S.; Kökösi, J.; Takács-Novák, K. Synthesis and Characterization of Long-Chain Tartaric Acid Diamides as Novel Ceramide-Like Compounds. *Molecules* **2010**, *15*, 824–833, doi:10.3390/molecules15020824.
83. Selzer, D.; Abdel-Mottaleb, M.M.A.; Hahn, T.; Schaefer, U.F.; Neumann, D. Finite and Infinite Dosing: Difficulties in Measurements, Evaluations and Predictions. *Adv. Drug Deliv. Rev.* **2013**, *65*, 278–294, doi:10.1016/j.addr.2012.06.010.
84. Zhai, H.; Maibach, H.I. Effects of Skin Occlusion on Percutaneous Absorption: An Overview. *Skin Pharmacol. Physiol.* **2001**, *14*, 1–10, doi:10.1159/000056328.
85. Binder, L.; SheikhRezaei, S.; Baierl, A.; Gruber, L.; Wolzt, M.; Valenta, C. Confocal Raman Spectroscopy: In Vivo Measurement of Physiological Skin Parameters – A Pilot Study. *J. Dermatol. Sci.* **2017**, *88*, 280–288, doi:10.1016/j.jdermsci.2017.08.002.
86. Ilchenko, O.; Pilgun, Y.; Makhnii, T.; Slipets, R.; Reynt, A.; Kutsyk, A.; Slobodianiuk, D.; Koliada, A.; Krasnenkov, D.; Kukharsky, V. High-Speed Line-Focus Raman Microscopy with Spectral Decomposition of Mouse Skin. *Vib. Spectrosc.* **2016**, *83*, 180–190, doi:10.1016/j.vibspec.2016.02.003.
87. Pyatski, Y.; Zhang, Q.; Mendelsohn, R.; Flach, C.R. Effects of Permeation Enhancers on Flufenamic Acid Delivery in Ex Vivo Human Skin by Confocal Raman Microscopy. *Int. J. Pharm.* **2016**, *505*, 319–328, doi:10.1016/j.ijpharm.2016.04.011.
88. dos Santos, L.; Téllez S, C.A.; Sousa, M.P.J.; Azoia, N.G.; Cavaco-Paulo, A.M.; Martin, A.A.; Favero, P.P. In Vivo Confocal Raman Spectroscopy and Molecular Dynamics Analysis of Penetration of Retinyl Acetate into Stratum Corneum. *Spectrochim. Acta. A. Mol. Biomol. Spectrosc.* **2017**, *174*, 279–285, doi:10.1016/j.saa.2016.11.042.

89. Chen, G.; Ji, C.; Miao, M.; Yang, K.; Luo, Y.; Hoptroff, M.; Collins, L.Z.; Janssen, H.-G. Ex-Vivo Measurement of Scalp Follicular Infundibulum Delivery of Zinc Pyrithione and Climbazole from an Anti-Dandruff Shampoo. *J. Pharm. Biomed. Anal.* **2017**, *143*, 26–31, doi:10.1016/j.jpba.2017.05.031.
90. Nakagawa, N.; Matsumoto, M.; Sakai, S. *In Vivo* Measurement of the Water Content in the Dermis by Confocal Raman Spectroscopy. *Skin Res. Technol.* **2010**, *16*, 137–141, doi:10.1111/j.1600-0846.2009.00410.x.
91. Sigurdsson, S.; Philipsen, P.A.; Hansen, L.K.; Larsen, J.; Gniadecka, M.; Wulf, H.C. Detection of Skin Cancer by Classification of Raman Spectra. *IEEE Trans. Biomed. Eng.* **2004**, *51*, 1784–1793, doi:10.1109/TBME.2004.831538.
92. Smith, G.P.S.; McGoverin, C.M.; Fraser, S.J.; Gordon, K.C. Raman Imaging of Drug Delivery Systems. *Adv. Drug Deliv. Rev.* **2015**, *89*, 21–41, doi:10.1016/j.addr.2015.01.005.
93. Franzen, L.; Windbergs, M. Applications of Raman Spectroscopy in Skin Research — From Skin Physiology and Diagnosis up to Risk Assessment and Dermal Drug Delivery. *Adv. Drug Deliv. Rev.* **2015**, *89*, 91–104, doi:10.1016/j.addr.2015.04.002.
94. Pezzotti, G.; Boffelli, M.; Miyamori, D.; Uemura, T.; Marunaka, Y.; Zhu, W.; Ikegaya, H. Raman spectroscopy of human skin: Looking for a quantitative algorithm to reliably estimate human age. *J. Biomed. Opt.* **2015**, doi:10.1117/1.JBO.20.6.065008
95. Balázs Vajna. Multivariate Curve Resolution and Regression Methods in Raman Chemical Imaging. Theses of Ph.D. Dissertation, Budapest University of Technology and Economics, Budapest, 30.11.2012.
96. Bakonyi, M.; Gácsi, A.; Kovács, A.; Szűcs, M.-B.; Berkó, S.; Csányi, E. Following-up Skin Penetration of Lidocaine from Different Vehicles by Raman Spectroscopic Mapping. *J. Pharm. Biomed. Anal.* **2018**, *154*, 1–6, doi:10.1016/j.jpba.2018.02.056.
97. Synytsya, A.; Alexa, P.; Besserer, J.; De Boer, J.; Froschauer, S.; Gerlach, R.; Loewe, M.; Moosburger, M.; Obstová, I.; Quicken, P.; et al. Raman Spectroscopy of Tissue Samples Irradiated by Protons. *Int. J. Radiat. Biol.* **2004**, *80*, 581–591, doi:10.1080/09553000412331283515.

ACKNOWLEDGEMENTS

I would like to express my sincere gratitude to the Head of the Institute of Pharmaceutical Technology and Regulatory Affairs **Prof. Dr. Ildikó Csóka** for providing me with the opportunity to work in this Department and complete my Ph.D. work under her expert guidance.

I would like to express my warmest thanks to my supervisors **Dr. habil. Erzsébet Csányi** associate professor and **Dr. habil. Szilvia Berkó** associate professor for their guidance, patience, motivation, and continuous support of my research.

I wish to thank **Dr. Attila Gácsi** for his immense help and co-operation, especially in Raman measurements.

I am very grateful to all of my co-authors for their kind collaboration.

I am deeply indebted to the members of the second research group of the Institute of Pharmaceutical Technology and Regulatory Affairs.

I wish to thank all members of the Institute of Pharmaceutical Technology and Regulatory Affairs for their help and friendship.

I also owe a very important debt to my friends and family for their encouragement, support and understanding; and for ensuring a peaceful background.

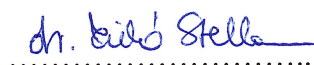
NYILATKOZAT SAJÁT MUNKÁRÓL

Név: Dr. Zsikó Stella

A doktori értekezés címe: Investigation of new innovative techniques for modeling skin permeation

Én, dr. Zsikó Stella teljes felelősségem tudatában kijelentem, hogy a Szegedi Tudományegyetem Gyógyszerésztudományok Doktori Iskolában elkészített doktori (Ph.D.) disszertációm saját kutatási eredményeimen alapulnak. Kutatómunkám, eredményeim publikálása, valamint disszertációm megírása során a Magyar Tudományos Akadémia Tudományetikai Kódexében lefektetett alapelvek és ajánlások szerint jártam el.

Szeged, 2021.06.10.



Dr. Zsikó Stella

ANNEX

I

Article

Nanostructured Lipid Carrier Gel for the Dermal Application of Lidocaine: Comparison of Skin Penetration Testing Methods

Stella Zsikó ¹, Kendra Cutcher ², Anita Kovács ¹, Mária Budai-Szűcs ¹, Attila Gácsi ¹, Gabriella Baki ², Erzsébet Csányi ¹ and Szilvia Berkó ^{1,*}

¹ Institute of Pharmaceutical Technology and Regulatory Affairs, Faculty of Pharmacy, University of Szeged, 6720 Szeged, Hungary

² Frederic and Mary Wolfe Center, College of Pharmacy and Pharmaceutical Sciences, University of Toledo, Toledo, OH 43614, USA

* Correspondence: berkosz@pharm.u-szeged.hu

Received: 6 May 2019; Accepted: 25 June 2019; Published: 2 July 2019



Abstract: The aim of this research was to investigate the stability of a lidocaine-loaded nanostructured lipid carrier dispersion at different temperatures, formulate a nanostructured lipid carrier gel, and test the penetration profile of lidocaine from the nanostructured lipid carrier gel using different skin penetration modeling methods. The formulations were characterized by laser diffraction, rheological measurements and microscopic examinations. Various in vitro methods were used to study drug release, diffusion and penetration. Two types of vertical Franz diffusion cells with three different membranes, including cellulose, Strat-M[®], and heat separated human epidermis were used and compared to the Skin-parallel artificial membrane permeability assay (PAMPA) method. Results indicated that the nanostructured lipid carrier dispersion had to be gelified as soon as possible for proper stability. Both the Skin-PAMPA model and Strat-M[®] membranes correlated favorably with heat separated human epidermis in this research, with the Strat-M[®] membranes sharing the most similar drug permeability profile to an ex vivo human skin model. Our experimental findings suggest that even when the best available in vitro experiment is selected for modeling human skin penetration to study nanostructured lipid carrier gel systems, relevant in vitro/in vivo correlation should be made to calculate the drug release/permeation in vivo. Future investigations in this field are still needed to demonstrate the influence of membranes and equipment from other classes on other drug candidates.

Keywords: dermal drug delivery; diffusion cell; Franz diffusion; Skin-PAMPA; Strat-M[®] membrane; nanocarrier

1. Introduction

Topical and transdermal formulations are widely used for delivering drugs to the skin and underlying tissue, or through the skin for systemic action. The vast majority of topically applied formulations are semisolids, including creams, ointments and gels, which offer suitable residence time on the skin, and are usually well accepted by the patients. Topical formulations deliver the active pharmaceutical ingredients (APIs) into different layers of the skin, thus enabling several diseases to be prevented and/or cured. The beginning, duration and strength of the therapeutic effect depend on the efficacy of three consecutive processes: (1) The release of the API from the carrier system; (2) penetration/diffusion of the API into the stratum corneum or other skin layers; (3) exertion of a pharmacological effect at the target point. All these effects determine the safety-efficacy profile of a product [1–3]. For most skin problems or diseases, the target point is the stratum corneum, viable epidermis or dermis.

Modeling of penetration through the skin is discussed by numerous directives [4–8]. The *in vitro* method for skin penetration modeling is included in OECD Guideline 428 [5]. Advantages of the *in vitro* method are that measurements can be carried out on human skin samples among other potential membranes; multiple tests can be performed on a skin sample from the same donor; several formulations can be tested at the same time; there is no need for radio-labelling the test material; and there are no ethical issues.

Topical semisolid products are complex formulations with a complex structure. Physical properties of the composition depend on several factors, including particle size of dispersed particles, surface tension between the phases, fractional distribution of the drug between the phases, and rheological behavior of the product. These properties collectively determine the *in vitro* dissolution profile, together with other characteristics. The amount of API released *in vitro* is an important quality characteristic of a product. Modeling of penetration through the skin is a complex challenge. The device and the membrane, along with the properties of the product influence how the system can be tested most effectively. There are various types of equipment with which the diffusion and penetration of drug carrier systems can be studied. Human skin tests give the most relevant information; however, because of the high cost, it is a generally accepted approach to choose simpler methods in the early stages of formulation development. Previously, several simple, reliable, reproducible and validated methods were described for drug liberation by a vertical diffusion cell (VDC) using a synthetic membrane [9–11]. *In vitro* drug release testing is a widely used and reliable tool for evaluating products.

The use of Franz diffusion cells to evaluate skin permeability has developed into a major research methodology. With Franz diffusion studies, diffusion and penetration of an API through the skin and the relationships among the skin, drug and formulation can be investigated [12–19]. Franz diffusion cells are available with multiple types of automatic sampler systems. A lot of different membranes, including artificial and biological membranes can be applied on the Franz cells. Artificial membranes provide a simple and reproducible alternative way to study the basic physicochemical mechanisms of the drug diffusion, including interactions between the carrier and the membrane. They are suitable for early-stage drug development studies [13]. The Strat-M[®] membrane, built by two polyether sulfone layers, was specifically designed for skin penetration studies. The layers are impregnated with a mixture of synthetic lipids, and a polyolefin layer is located underneath. Moving downwards into the membrane layers, the size of the pores increases [20]. Transdermal diffusion and safety of APIs, excipients, functional cosmetic ingredients, cosmetic active substances, and finished products can be tested using the Strat-M[®] membrane. Advantages include that its diffusion properties are highly correlated with human diffusion studies, and it is characterized by minimal variability. It is also long-lasting and requires no special storage conditions or preparation for its use [20–24]. In addition to synthetic membranes, human skin membranes can also be used to model skin penetration. In the development of dermal preparations, it is not sufficient to perform membrane diffusion studies. It is necessary to do permeation studies through the biological membrane since the interaction of the API and carrier system with the skin can also be investigated, and it can be determined whether and to what extent the skin acts as a reservoir for the API. Usually, skin sections are obtained from plastic surgery, and a heat-separated epidermis is used as a membrane [13,25,26].

The parallel artificial membrane permeability assay (PAMPA) is a device that is adapted to simulate penetration of a product into the skin. For Skin-PAMPA, the bottom part of the PAMPA sandwich is substituted by a special donor plate, which was designed to study semi-solid products. It contains synthetic ceramides and has similar penetration properties to full-thickness skin. Synthetic lipids are easier to store, and their stability is more favorable [27–30]. The biomimetic model is able to determine *in vitro* human skin data based on the tests and can be a good alternative to skin permeability testing [17,28,31].

Lidocaine is a commonly used numbing agent before local interventions. Delivering lidocaine to the skin from a specific vehicle provides a numbing/pain relief effect to that area. It is possible to localize the numbing effect onto a smaller skin area without reaching the muscle. By concentrating

the numbing effect to the skin, the patient is able to retain full motor function of the area to which lidocaine is applied.

Our research group previously formulated and compared different drug carrier systems for the dermal delivery of lidocaine, including a conventional hydrogel, an oleogel, a lyotropic liquid crystalline gel and nanostructured lipid carrier (NLC) gel. It was concluded that the penetration of lidocaine from the NLC gel was the most significant, and the skin hydrating and occlusive effect made it a favorable carrier system [25,32]. In addition, several articles in the literature featured lidocaine-filled NLCs or NLC gels [33–37]. Therefore, a lidocaine-loaded NLC and NLC gel was selected for the current investigations.

In this study, our aims were to investigate the stability of a lidocaine-loaded NLC dispersion at various storage temperatures, formulate an NLC gel, and evaluate the penetration profile of lidocaine from the NLC gel. Two types of vertical Franz diffusion cells with three different membranes, including a cellulose membrane, Strat-M[®] membrane, and heat separated human epidermis were used to study the drug release and permeation. Additionally, the NLC gels were evaluated using the Skin-PAMPA method, and the three methods were compared.

2. Materials and Methods

2.1. Materials

Lidocaine base and glycerol were obtained from Hungaropharma Ltd. (Budapest, Hungary). Miglyol[®] 812 N (caprylic/capric triglyceride) was a gift from Sasol GmbH (Hamburg, Germany). Cremophor[®] RH 60 (PEG-60 Hydrogenated Castor Oil; HLB value: 15–17) was kindly supplied by BASF SE Chemtrade GmbH (Ludwigshafen, Germany). Apifil[®] (PEG-8 Beeswax) was a gift from Gattefossé (St. Priest, France). Methocel[™] E4M (hydroxypropyl methylcellulose) was from Colorcon (Budapest, Hungary). The water used was purified and deionized with the Milli-Q system from Millipore (Milford, MA, USA). The cellulose acetate filter (Porafil membrane filter, cellulose acetate, pore diameter: 0.45 µm) was obtained from Macherey-Nagel GmbH & Co. KG (Düren, Germany). The Strat-M[®] membrane (Strat-M[®] Membrane, Transdermal Diffusion Test Model, 25 mm) was from Merck KGaA (Darmstadt, Germany). Excised human skin was obtained from a Caucasian female patient by routine plastic surgery procedure in the Department of Dermatology and Allergology, University of Szeged. The ex vivo skin penetration test does not need ethical permission, and patient's consent according to the Act CLIV of 1997 on health, Section 210/A in Hungary. The local ethical committee (Ethical Committee of the University of Szeged, Albert Szent-Györgyi Clinical Center) was informed about the ex vivo skin penetration studies (Human Investigation Review Board license number: 83/2008). The Skin-PAMPA sandwiches (P/N: 120657), hydration solution (P/N: 120706) and stirring bars (P/N: 110066) were purchased from Pion, Inc (Woburn, MA, USA). The UV plates (UV-star micro plate, clear, flat bottom, half area) were from Greiner Bio-one (Kremsmünster, Austria).

2.2. Methods

2.2.1. Preparation of the NLC

NLCs are colloidal carriers which were introduced in the early 1990s. They are derived from o/w emulsions by replacing the liquid lipid with a solid lipid at room temperature. The lipophilic phase of NLC included Apifil, Cremophor RH 60 and Miglyol 812 N, which were melted at 60 °C under controlled stirring. Then lidocaine was added to the melted lipid phase under similar conditions. Then purified water was added to the lipid phase to form the pre-emulsion. The pre-emulsion was ultrasonicated using a Hielscher UP200S compact ultrasonic homogenizer (Hielscher Ultrasonics GmbH, Teltow, Germany) for 10 min at 70% amplitude. At the end, the sample was cooled in ice to obtain the solid lipid particles (LID-NLC) [38]. For dermal application, a gel was formed at room temperature with glycerol and Methocel E4M. In the last step, the NLC dispersion was added to the

gel (LID-NLC gel). A blank-NLC and blank-NLC gel were also prepared using the same procedure, but without adding lidocaine. Table 1 summarizes the formulations. The NLC formulations were stored at different temperatures 7 °C (cold) and 25 °C (room temperature).

Table 1. Compositions of the test preparations.

LID-NLC	Blank NLC	LID-NLC Gel	Blank NLC-Gel
Apifil 11.8%	Apifil 11.8%	LID-NLC 89%	Blank NLC 89%
Cremophor RH 60.8%	Cremophor RH 60.8%	Glycerin 8%	Glycerin 8%
Miglyol 812 N 5%	Miglyol 812 N 5%	Methocel E4M 3%	Methocel E4M 3%
Purified water 69.2%	Purified water 75.2%		
Lidocaine 6%			

2.2.2. Laser Diffraction

Laser diffraction analysis was performed with a Malvern Mastersizer 2000 particle size analyzer provided with the Hydro SM wet dispersion unit (Malvern Instruments, Worcestershire, UK) to determine the particle size and stability of the NLC formulation at different temperatures (cold and room temperature). A few drops of the sample were placed inside the Hydro SM loaded with purified water, and the speed of the stirrer was set to 2000 rpm. Three values, namely $d(0.1)$, $d(0.5)$, and $d(0.9)$, were evaluated, indicating that 10%, 50%, and 90% of the analyzed particles were below a certain size (diameter). The span value describing the width of the particle size distribution curve $((d(0.9) - d(0.1))/d(0.5))$ was calculated as well.

2.2.3. Rheological Measurements

Rheological measurements were performed with a Physica MCR101 rheometer (Anton Paar GmbH, Graz, Austria), employing a parallel plate geometry PP25 with a measuring gap of 0.1 mm to verify the proper consistency of the LID-NLC gel system for topical application. The blank-NLC gel was studied as well. Flow curves, viscosity curves and frequency sweep tests were obtained. The shear rate was increased from 0.1 to 100 1/s (up-curve) and then decreased from 100 to 0.1 1/s (down-curve) in CR mode. The shearing time in was 300 s. The measurements were carried out at 25 °C [39].

2.2.4. Microscopic Examinations

The structure of the NLC samples was examined with a microscope (LEICA DM6 B, Leica Microsystems GmbH, Wetzlar, Germany) at room temperature. Magnifications were 100× and 200×.

2.2.5. pH Measurements

For pH measurement, 10 g of each sample (NLC dispersion and NLC gel) was placed in a beaker, and the surface pH was measured using a Testo 206 pH meter (Testo SE & Co. KGaA, Lenzkirch, Germany) with a pH2 probe. Three parallel measurements were carried out at room temperature.

2.2.6. Drug Diffusion and Penetration Studies

Three different methods were used to model and compare drug release and diffusion through the membrane and penetration into the skin from the LID-NLC gel (Table 2). The methods included two types of vertical Franz diffusion cells, namely Hanson Microette TM Topical & Transdermal Diffusion Cell System, and Logan Automated Dry heat sampling system. The third method used was the Skin-PAMPA method. On the Franz cells, the donor and acceptor phases were separated by either a synthetic cellulose acetate membrane, a Strat-M® membrane or heat-separated human epidermis (HSE). A 0.3 g portion of sample was placed in the donor chamber on the membrane. The human skin was placed in a water bath (60 ± 0.5 °C), and the epidermis was separated from the dermis. Thermostated phosphate buffer solution (PBS pH 7.4 ± 0.15), made in-house, kept at

32 ± 0.5 °C was used as the acceptor phase. Membrane diffusion and skin penetration experiments lasted 24 h (sampling times: 0.5; 1; 2; 3; 4; 5; 6; 8; 10; 12; 16; 20; and 24 h). The stirring speed was 400 rpm. The concentration of the drug was measured spectrophotometrically with a Thermo Scientific Evolution 201 spectrometer with Thermo Insight v1.4.40 software package (Thermo Fisher Scientific, Waltham, MA, USA) at a wavelength of 262 nm (analytical parameters: Slope: 0.001738 ± 0.000016; SE: 4.554 × 10^{−5}; SD: 0.0001205; LOD: 0.2339 µg/mL; LOQ: 0.7088 µg/mL). The Skin-PAMPA sandwiches were used after a 24-hour hydration period (Hydration Solution, Pion, Inc., Billerica, MA, USA). 70 µL of the NLC gels were applied to the well of the formulation plate as the donor phase. Phosphate buffer solution (PBS pH 7.4 ± 0.15), made in-house, was used as the acceptor phase. The top plate was filled with 250 µL of fresh acceptor solution, and a stirring bar was also used in each well. The Gut-Box™ from Pion, Inc. was used for stirring; the resultant sandwich was incubated at 32 °C for six hours. The Skin-PAMPA membrane is not designed for 24-h measurements, the membrane can provide relevant values for a shorter time. Therefore, the acceptor solution was examined after 0.5, 1, 2, 3, 4, 5 and 6 h of incubation. The quantity of the API was determined by UV spectroscopy at 262 nm using a Synergy HT UV plate reader by KC4 (BIO-TEK Instruments, Inc., Winooski, VT, USA) software. The quantity of the permeated API was expressed as µg/cm² units.

Table 2. The experimental design of drug diffusion and penetration studies.

Device	Hanson	Logan	Skin-PAMPA
Membrane	Cellulose acetate Strat-M® HSE	Cellulose acetate Strat-M® HSE	Skin-PAMPA membrane

2.2.7. Statistical Analysis

Two-way ANOVA analysis of variance (Bonferroni post-test), working with Prism for Windows software (GraphPad Software Inc., La Jolla, CA, USA), was used to analyze the statistical difference between the samples. Results are shown as average of six parallel experiments and standard deviation (SD). Variations were considered significant if $p < 0.05$ *, $p < 0.01$ ** and $p < 0.001$ *** versus the control.

3. Results and Discussion

3.1. Particle Size Analysis

Usually light scattering methods, such as photon correlation spectroscopy and/or laser diffraction (LD) are used for particle size determination of lipid nanoparticles. LD is a powerful method that has a wider detection spectrum (20 nm–2.000 µm), and it is considered a better option for lipid nanoparticles in the upper nanometer and micrometer size ranges.

All NLC dispersions were in the nanosize range, between 97 and 163 nm (d(0.5)). The particle size of LID-NLC stored at room temperature was the smallest (97 nm), and it was stable for three days (the values of d(0.5) and d(0.9) were below 200 nm). On the fourth day, the d(0.9) values showed a significant increase (41.749 µm). The particle size of the NLC dispersion stored in the refrigerator increased after one day. The reason for this instability was that lidocaine crystallized in the refrigerator, and the formulation was not stable under these conditions. The exact parameters are summarized in Table 3. According to the particle size analysis, the holding time of the preparation was three days at room temperature.

Table 3. Particle size of nanostructured lipid carrier (NLC) dispersions stored at different conditions.

Day	NLC Dispersion	d(0.1) μm	d(0.5) μm	d(0.9) μm	Span
1st day	Blank-NLC, room temperature	0.066	0.131	0.320	1.950
	Blank-NLC, cooled	0.066	0.130	0.302	1.821
	LID-NLC, room temperature	0.069	0.098	0.145	0.787
	LID-NLC, cooled	0.069	0.098	0.146	0.790
2nd day	Blank-NLC, room temperature	0.065	0.127	0.266	1.584
	Blank-NLC, cooled	0.065	0.127	0.266	1.587
	LID-NLC, room temperature	0.068	0.097	0.144	0.782
	LID-NLC, cooled	0.073	0.114	0.259	1.625
3rd day	Blank-NLC, room temperature	0.065	0.126	0.258	1.542
	Blank-NLC, cooled	0.065	0.126	0.262	1.564
	LID-NLC, room temperature	0.069	0.098	0.146	0.791
	LID-NLC, cooled	0.079	0.130	0.300	1.698
4th day	Blank-NLC, room temperature	0.065	0.128	0.289	1.746
	Blank-NLC, cooled	0.065	0.128	0.298	1.814
	LID-NLC, room temperature	0.090	0.163	41.749	255.201
	LID-NLC, cooled	-	-	-	-

3.2. Microscopic Study

Parallel to the particle size analysis, microscopic studies were performed as well on the NLC dispersions. As it can be seen in Figure 1, in cooled circumstances lidocaine crystals appeared on the second day, while at room temperature they appeared on the third day. Based on the microscopic examination, the holding time of the NLC dispersion was two days at room temperature.

The structure of the LID-NLC gel was examined with a polarized light microscope as well. The formula had a homogenous structure after two weeks, no API crystals were detected (Figure 2). It can be concluded based on these results that it is very important to gelify the NLC dispersion as soon as possible for proper stability.

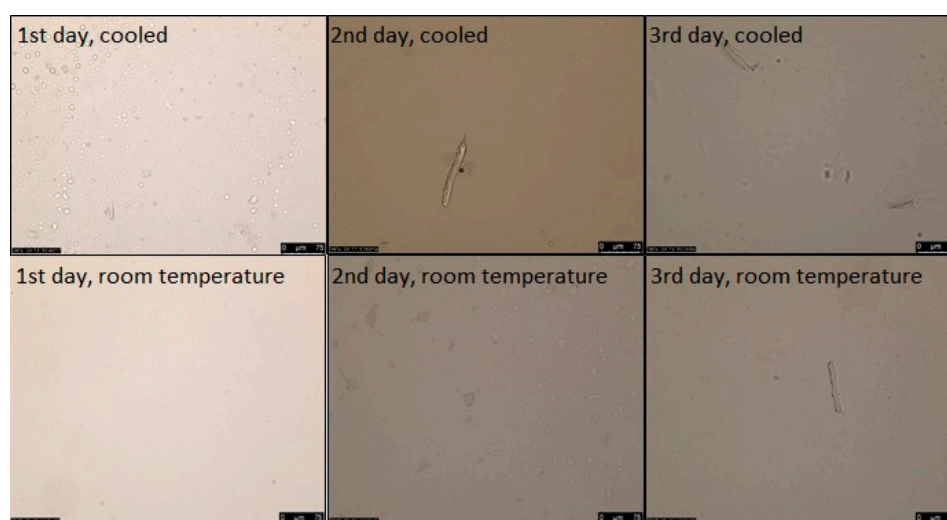


Figure 1. The NLC dispersions' stability over the course of three days at different storage conditions. (The magnification was 200 \times).

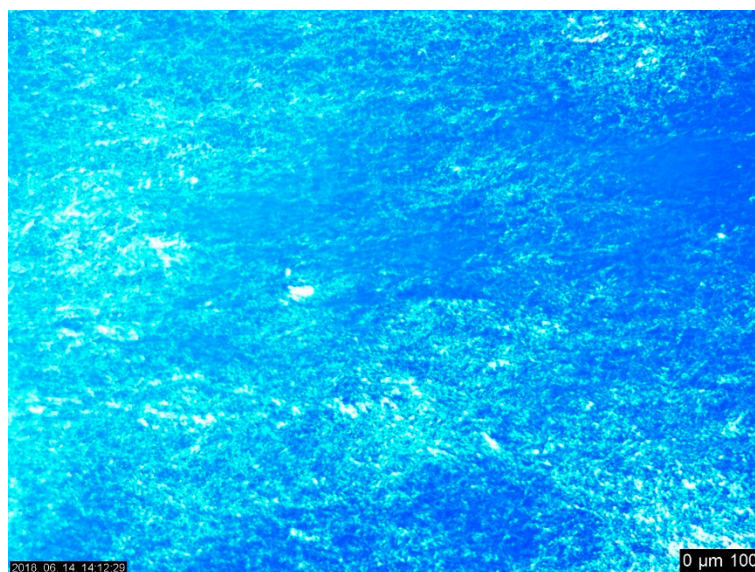


Figure 2. The solid lipid particles (LID-NLC) gel in polarized light at week two. (The magnification was 100 \times).

3.3. Rheological Studies

The LID-NLC gel had a shear thinning behavior (Figure 3A), which means the shear stress increased continuously with the shear rate, but the rate of the increase decreased. Slight thixotropy was observed, meaning that structure regeneration was time-dependent. The viscosity value of the LID-NLC gel at the shear rate of 100 1/s was 6.72 Pa·s at 25 °C. According to the rheological measurements, the consistency of the formulation was suitable for dermal use. The viscosity value of the blank-NLC gel at the shear rate of 100 1/s was 5.58 Pa·s at 25 °C. Based on the rheological curves, it can be stated that incorporation of the API into the formulation made the system more viscous. Viscosity values increased and consistency improved. The frequency sweep test (Figure 3B) showed a viscoelastic behavior, where the elastic characteristic dominated (G' higher than G''); with a relatively large frequency dependence of the moduli (G' and G'') which is a typical feature of a so-called weak gel.

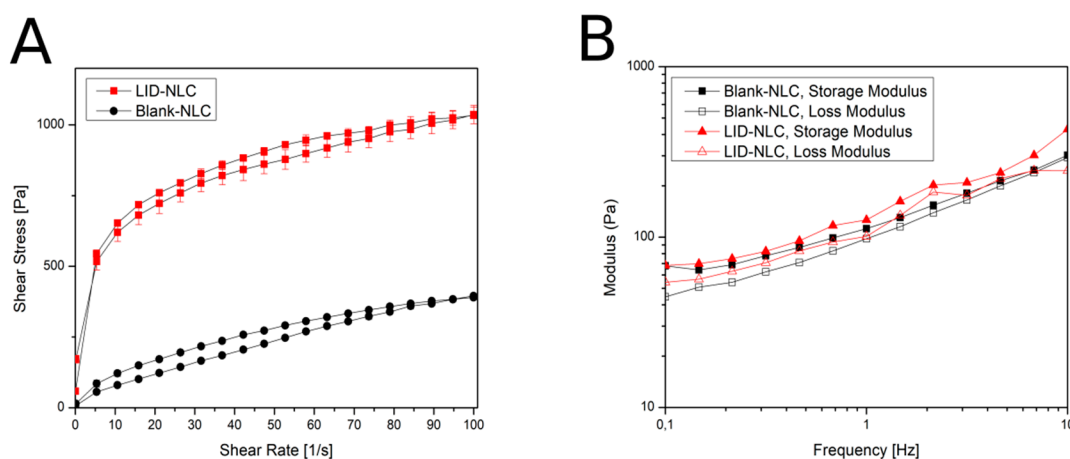


Figure 3. Rheological behavior of the NLC gel. (A): flow curves; (B): frequency sweep test.

3.4. pH Measurement

pH of the blank-NLC dispersion was 5.2 ± 0.2 and the blank-NLC gel 5.3 ± 0.3 . pH of the LID-NLC dispersion was 8.0 ± 0.3 and the LID-NLC gel 7.9 ± 0.4 . Due to its basic characteristics, the active ingredient increased the pH value of the preparation.

3.5. Drug Release, Diffusion and Penetration Studies

The in vitro diffusion/penetration of lidocaine from the LID-NLC gel through the two synthetic and one biological membranes and the Skin-PAMPA membrane were calculated in terms of the mean cumulative amount and percentage diffused/penetrated \pm SD by 6 or 24 h (Table 4).

The cellulose acetate membrane is a non-barrier, non-skin like membrane, which was used to measure the in vitro release of lidocaine from the NLC gel. As expected, a high amount of lidocaine released through this membrane over the course of 24 h from both Franz cell types (Figure 4A). Differences between the Logan and Hanson Franz cell results were not significant, however, a lower standard deviation was observed with the Hanson method.

Table 4. The mean cumulative amount and percentage (%) diffused or penetrated at 6 and 24 h ($\mu\text{g}/\text{cm}^2$).

Time of Experiment	Cellulose		Strat-M [®]		HSE		Skin-PAMPA
	Hanson	Logan	Hanson	Logan	Hanson	Logan	
6 h ($\mu\text{g}/\text{cm}^2$)	3808.82 \pm 448.91	3355.40 \pm 320.70	304.20 \pm 113.40	514.89 \pm 209.69	1778.25 \pm 483.81	670.85 \pm 189.05	696.32 \pm 20.50
6 h (%)	41.35 \pm 18.8	27.73 \pm 0.83	3.45 \pm 1.21	7.72 \pm 2.89	11.61 \pm 2.95	8.785 \pm 2.03	13.93 \pm 0.41
24 h ($\mu\text{g}/\text{cm}^2$)	8014.05 \pm 471.89	6878.13 \pm 1172.21	1079.27 \pm 304.36	1847.08 \pm 335.19	3094.60 \pm 829.73	1222.69 \pm 358.70	-
24 h (%)	70.40 \pm 13.72	58.66 \pm 4.28	12.96 \pm 3.52	27.89 \pm 5.17	19.44 \pm 5.05	16.00 \pm 3.81	-

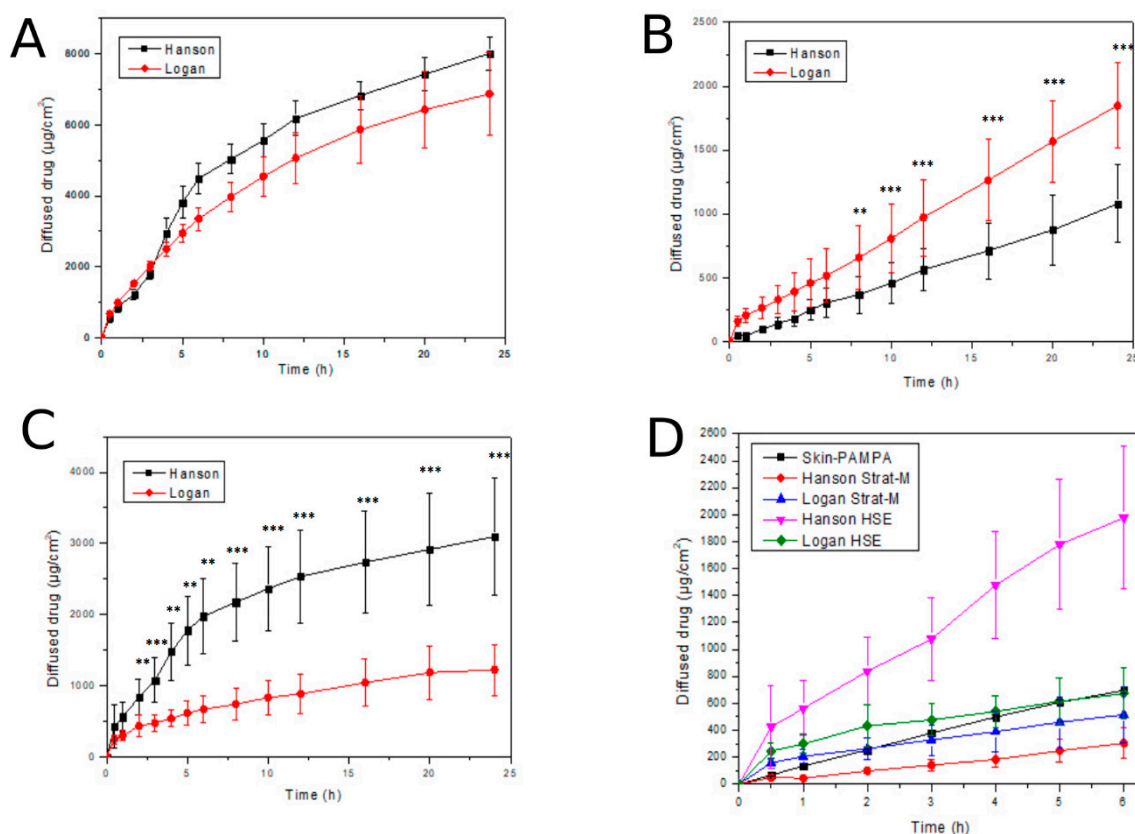


Figure 4. In vitro drug diffusion and ex vivo skin penetration studies. (A): In vitro release of lidocaine through cellulose acetate membrane (24 h); (B): In vitro penetration of lidocaine through Strat-M[®] membrane (24 h); (C): Ex vivo penetration of lidocaine through HSE (24 h); (D): Comparison of various penetration methods with various membranes (6 h). $p < 0.05$ *, $p < 0.01$ ** and $p < 0.001$ *** compared to each other within each one figure.

The Strat-M[®] membrane and HSE were skin-like and acted as barriers to API penetration. Figure 4B shows the penetration of lidocaine via the synthetic Strat-M[®] membrane, which Figure 4C shows the penetration via HSE. As for the Strat-M[®] membrane, differences between the Logan and Hanson Franz cells were significant after eight hours. Penetration via the HSE was higher than via

the Strat-M[®] membrane, especially on Hanson device over the 24 h. In the case of HSE, differences between the Logan and Hanson Franz cells were significant from two hours. This significant difference between the two types of Franz cells can be explained by the difference in structure of the two devices. The Logan cell was open from above, therefore the measurement runs on atmospheric pressure. However, the cell of the Hanson device was closed from the top and the pressure is higher leading to significantly higher penetration. The standard deviation was similar with the two methods. Figure 4D presents the diffusion/penetration data via the three different membranes (Strat-M[®], Skin-PAMPA, HSE) tested on the Franz cells and Skin-PAMPA system. A lower standard deviation was observed with the PAMPA model than with the Franz cell method. This may be caused by the diversity in the membrane structure of the two methods. However, the penetration profiles of the Skin PAMPA and in vitro and ex vivo Franz cell methods were in good balance. If comparing the results at 6 h, the values obtained with Logan cells and Skin-PAMPA method were close to each other. Our results demonstrated that a novel Strat-M[®] synthetic membrane and the Skin-PAMPA method have the potential to be used as an early screening tool to select the best dermal lidocaine-loaded nanoformulation.

4. Conclusions

A lidocaine-loaded NLC dispersion and a lidocaine-loaded, NLC gel were formulated to study their stability at various temperatures and evaluate their in vitro release as well as in vitro and ex vivo skin penetration. The NLC dispersions were found to be stable at room temperature, with acceptable changes in particle characteristics, for two days. Microscopic evaluations further verified the stability of the NLC dispersion at room temperature. It can be concluded that two days is a reasonable time period to create a gel from this NLC dispersion. The microscopic and rheological measurements verified that the consistency of the formulation was well suitable for dermal use, and the gel was stable for at least two weeks at room temperature.

Synthetic membranes are useful tools to examine and determine which formulation is the most promising for in vivo human skin studies. There are numerous commercial membranes available, all of which may have different drug diffusion properties. Cellulose membranes were used to study in vitro drug release, while the Skin-PAMPA membranes and Strat-M[®] membranes were used for modeling in vitro skin penetration. Both the Skin-PAMPA and Strat-M[®] membranes correlated well with HSE in this study, but the Strat-M[®] membranes shared the most similar drug permeability profile to an ex vivo human skin model. Our results can be used to guide formulators in selecting vehicles in early development in the pharmaceutical, personal care and cosmetic industries. Overall, researchers must carefully select the most suitable membrane to be used with Franz cells for topical quality control testing.

Modeling of penetration through the skin is a complex challenge. The drug release profiles of the LID-NLC gel obtained with the different techniques were not fully equivalent. The device and the membrane, along with the properties of the product itself, influence how the system can be tested most effectively. Based on our results, we can select the best in vitro test for modeling human skin penetration of NLC gel systems, but appropriate in vitro/in vivo correlation should be performed to calculate the drug release in vivo. Future studies in this field are still needed to explain the influence of membranes and equipment from other classes on other drug candidates.

Author Contributions: Conceptualization, S.Z. and S.B.; methodology, S.Z. and S.B.; software, M.B.-S.; validation, A.K.; formal analysis, S.Z. and K.C.; investigation, S.Z. and K.C.; writing—original draft preparation, S.Z.; writing—review and editing, G.B., E.C.; visualization, A.G.; supervision, S.B. and E.C.

Funding: This research received no external funding.

Acknowledgments: The authors would like to thank Sasol GmbH, Gattefossé and BASF SE for the gift samples. We are grateful for the financial support of the “GINOP 2.2.1-15-2016-00023” as they have made this article possible.

Conflicts of Interest: The authors declare no conflicts of interest.

References

1. Shah, V.P.; Yacobi, A.; Rădulescu, F.Ş.; Miron, D.S.; Lane, M.E. A science based approach to topical drug classification system (TCS). *Int. J. Pharm.* **2015**, *491*, 21–25. [[CrossRef](#)] [[PubMed](#)]
2. Dragicevic, N.; Maibach, H.I. *Percutaneous Penetration Enhancers Drug Penetration Into/Through the Skin*; Springer Berlin Heidelberg: Berlin/Heidelberg, Germany, 2017; ISBN 978-3-662-53268-3.
3. Ruela, A.L.M.; Perissinato, A.G.; Lino, M.E.D.S.; Mudrik, P.S.; Pereira, G.R. Evaluation of skin absorption of drugs from topical and transdermal formulations. *Br. J. Pharm. Sci.* **2016**, *52*, 527–544. [[CrossRef](#)]
4. OECD. *Guidance Notes on Dermal Absorption, Series on Testing and Assessment No. 156*; OECD: Paris, France, 2011.
5. OECD. *Test Guideline 428: Skin Absorption: In vitro Method*; OECD: Paris, France, 2004.
6. OECD. *Test Guideline 427: Skin Absorption: In vivo Method*; OECD: Paris, France, 2004.
7. OECD. *Guidance Document for the Conduct of Skin Absorption Studies*; OECD: Paris, France, 2004.
8. European Food Safety Authority (EFSA); Buist, H.; Craig, P.; Dewhurst, I.; Hougaard Bennekou, S.; Kneuer, C.; Machera, K.; Pieper, C.; Court Marques, D.; Guillot, G.; et al. Guidance on dermal absorption. *EFSA J.* **2017**, *15*, 4873. [[CrossRef](#)]
9. Shah, V.P.; Elkins, J.; Shaw, S.; Hanson, R. In Vitro Release: Comparative Evaluation of Vertical Diffusion Cell System and Automated Procedure: RESEARCH ARTICLE. *Pharm. Dev. Technol.* **2003**, *8*, 97–102. [[CrossRef](#)] [[PubMed](#)]
10. Hauck, W.W.; Shah, V.P.; Shaw, S.W.; Ueda, C.T. Reliability and Reproducibility of Vertical Diffusion Cells for Determining Release Rates from Semisolid Dosage Forms. *Pharm. Res.* **2007**, *24*, 2018–2024. [[CrossRef](#)]
11. Franz, T.J. Percutaneous Absorption. On the Relevance of in Vitro Data. *J. Invest. Dermatol.* **1975**, *64*, 190–195. [[CrossRef](#)]
12. Bakonyi, M.; Gácsi, A.; Berkó, S.; Kovács, A.; Csányi, E. Stratum corneum lipid liposomes for investigating skin penetration enhancer effects. *RSC Adv.* **2018**, *8*, 27464–27469. [[CrossRef](#)]
13. Flaten, G.E.; Palac, Z.; Engesland, A.; Filipović-Grčić, J.; Vanić, Ž.; Škalko-Basnet, N. In vitro skin models as a tool in optimization of drug formulation. *Eur. J. Pharm. Sci.* **2015**, *75*, 10–24. [[CrossRef](#)]
14. Intarakumhaeng, R.; Alsheddi, L.; Wanasathop, A.; Shi, Z.; Li, S.K. Skin Permeation of Urea Under Finite Dose Condition. *J. Pharm. Sci.* **2019**, *108*, 987–995. [[CrossRef](#)]
15. Trombino, S.; Russo, R.; Mellace, S.; Varano, G.P.; Laganà, A.S.; Marcucci, F.; Cassano, R. Solid lipid nanoparticles made of trehalose monooleate for cyclosporin-A topic release. *J. Drug Deliv. Sci. Technol.* **2019**, *49*, 563–569. [[CrossRef](#)]
16. Soriano-Ruiz, J.L.; Suñer-Carbó, J.; Calpena-Campmany, A.C.; Bozal-de Febrer, N.; Halbaut-Belloua, L.; Boix-Montañés, A.; Souto, E.B.; Clares-Naveros, B. Clotrimazole multiple W/O/W emulsion as anticandidal agent: Characterization and evaluation on skin and mucosae. *Coll. Surf. B Biointerfaces* **2019**, *175*, 166–174. [[CrossRef](#)] [[PubMed](#)]
17. Zhang, Y.; Lane, M.E.; Hadgraft, J.; Heinrich, M.; Chen, T.; Lian, G.; Sinko, B. A comparison of the in vitro permeation of niacinamide in mammalian skin and in the Parallel Artificial Membrane Permeation Assay (PAMPA) model. *Int. J. Pharm.* **2019**, *556*, 142–149. [[CrossRef](#)] [[PubMed](#)]
18. Montenegro, L.; Castelli, F.; Sarpietro, M. Differential Scanning Calorimetry Analyses of Idebenone-Loaded Solid Lipid Nanoparticles Interactions with a Model of Bio-Membrane: A Comparison with In Vitro Skin Permeation Data. *Pharmaceutics* **2018**, *11*, 138. [[CrossRef](#)] [[PubMed](#)]
19. Dahlizar, S.; Futaki, M.; Okada, A.; Yatomi, C.; Todo, H.; Sugibayashi, K. Combined Use of N-Palmitoyl-Glycine-Histidine Gel and Several Penetration Enhancers on the Skin Permeation and Concentration of Metronidazole. *Pharmaceutics* **2018**, *10*, 163. [[CrossRef](#)] [[PubMed](#)]
20. Haq, A.; Goodyear, B.; Ameen, D.; Joshi, V.; Michniak-Kohn, B. Strat-M® synthetic membrane: Permeability comparison to human cadaver skin. *Int. J. Pharm.* **2018**, *547*, 432–437. [[CrossRef](#)] [[PubMed](#)]
21. Balázs, B. Investigation of the Skin Barrier Function and Transdermal Drug Delivery Techniques. Ph.D. Thesis, University of Szeged, Szeged, Hungary, 2016.
22. Simon, A.; Amaro, M.I.; Healy, A.M.; Cabral, L.M.; de Sousa, V.P. Comparative evaluation of rivastigmine permeation from a transdermal system in the Franz cell using synthetic membranes and pig ear skin with in vivo-in vitro correlation. *Int. J. Pharm.* **2016**, *512*, 234–241. [[CrossRef](#)] [[PubMed](#)]

23. Uchida, T.; Kadhum, W.R.; Kanai, S.; Todo, H.; Oshizaka, T.; Sugibayashi, K. Prediction of skin permeation by chemical compounds using the artificial membrane, Strat-MTM. *Eur. J. Pharm. Sci.* **2015**, *67*, 113–118. [[CrossRef](#)] [[PubMed](#)]
24. Kim, K.-T.; Kim, M.-H.; Park, J.-H.; Lee, J.-Y.; Cho, H.-J.; Yoon, I.-S.; Kim, D.-D. Microemulsion-based hydrogels for enhancing epidermal/dermal deposition of topically administered 20(S)-protopanaxadiol: In vitro and in vivo evaluation studies. *J. Ginseng Res.* **2018**, *42*, 512–523. [[CrossRef](#)] [[PubMed](#)]
25. Bakonyi, M.; Berkó, S.; Kovács, A.; Budai-Szűcs, M.; Kis, N.; Erős, G.; Csóka, I.; Csányi, E. Application of quality by design principles in the development and evaluation of semisolid drug carrier systems for the transdermal delivery of lidocaine. *J. Drug Deliv. Sci. Technol.* **2018**, *44*, 136–145. [[CrossRef](#)]
26. Sütő, B.; Berkó, S.; Kozma, G.; Kukovecz, Á.; Budai-Szűcs, M.; Erős, G.; Kemény, L.; Sztojkov-Ivanov, A.; Gaspar, R.; Csányi, E. Development of ibuprofen-loaded nanostructured lipid carrier-based gels: Characterization and investigation of in vitro and in vivo penetration through the skin. *Int. J. Nanomed.* **2016**, *11*, 1201–1212.
27. Sinkó, B.; Garrigues, T.M.; Balogh, G.T.; Nagy, Z.K.; Tsinman, O.; Avdeef, A.; Takács-Novák, K. Skin-PAMPA: A new method for fast prediction of skin penetration. *Eur. J. Pharm. Sci.* **2012**, *45*, 698–707. [[CrossRef](#)] [[PubMed](#)]
28. Köllmer, M.; Mossahebi, P.; Sacharow, E.; Gorissen, S.; Gräfe, N.; Evers, D.-H.; Herbig, M.E. Investigation of the Compatibility of the Skin PAMPA Model with Topical Formulation and Acceptor Media Additives Using Different Assay Setups. *AAPS PharmSciTech* **2019**, *20*, 89. [[CrossRef](#)] [[PubMed](#)]
29. Vizserálek, G.; Berkó, S.; Tóth, G.; Balogh, R.; Budai-Szűcs, M.; Csányi, E.; Sinkó, B.; Takács-Novák, K. Permeability test for transdermal and local therapeutic patches using Skin PAMPA method. *Eur. J. Pharm. Sci.* **2015**, *76*, 165–172. [[CrossRef](#)] [[PubMed](#)]
30. Sinkó, B.; Vizserálek, G.; Takács-Novák, K. Skin PAMPA: Application in practice. *ADMET DMPK* **2015**, *2*, 191–198. [[CrossRef](#)]
31. Luo, L.; Patel, A.; Sinko, B.; Bell, M.; Wibawa, J.; Hadgraft, J.; Lane, M.E. A comparative study of the in vitro permeation of ibuprofen in mammalian skin, the PAMPA model and silicone membrane. *Int. J. Pharm.* **2016**, *505*, 14–19. [[CrossRef](#)] [[PubMed](#)]
32. Bakonyi, M.; Gácsi, A.; Kovács, A.; Szűcs, M.-B.; Berkó, S.; Csányi, E. Following-up skin penetration of lidocaine from different vehicles by Raman spectroscopic mapping. *J. Pharm. Biomed. Anal.* **2018**, *154*, 1–6. [[CrossRef](#)] [[PubMed](#)]
33. Puglia, C.; Sarpietro, M.G.; Bonina, F.; Castelli, F.; Zammataro, M.; Chiechio, S. Development, Characterization, and In Vitro and In Vivo Evaluation of Benzocaine- and Lidocaine-Loaded Nanostructured Lipid Carriers. *J. Pharma. Sci.* **2011**, *100*, 1892–1899. [[CrossRef](#)]
34. Ribeiro, L.N.M.; Breitzkreitz, M.C.; Guilherme, V.A.; da Silva, G.H.R.; Couto, V.M.; Castro, S.R.; de Paula, B.O.; Machado, D.; de Paula, E. Natural lipids-based NLC containing lidocaine: From pre-formulation to in vivo studies. *Eur. J. Pharm. Sci.* **2017**, *106*, 102–112. [[CrossRef](#)]
35. Muller, R.H.; Radtke, M.; Wissing, S.A. Solid lipid nanoparticles (SLN) and nanostructured lipid carriers (NLC) in cosmetic and dermatological preparations. *Adv. Drug Deliv. Rev.* **2002**, *54*, 131–155. [[CrossRef](#)]
36. Rincón, M.; Calpena, A.; Fabrega, M.-J.; Garduño-Ramírez, M.; Espina, M.; Rodríguez-Lagunas, M.; García, M.; Abrego, G. Development of Pranoprofen Loaded Nanostructured Lipid Carriers to Improve Its Release and Therapeutic Efficacy in Skin Inflammatory Disorders. *Nanomaterials* **2018**, *8*, 1022. [[CrossRef](#)]
37. You, P.; Yuan, R.; Chen, C. Design and evaluation of lidocaine- and prilocaine-co-loaded nanoparticulate drug delivery systems for topical anesthetic analgesic therapy: A comparison between solid lipid nanoparticles and nanostructured lipid carriers. *Drug Design Dev. Ther.* **2017**, *11*, 2743–2752. [[CrossRef](#)] [[PubMed](#)]
38. Li, Q.; Cai, T.; Huang, Y.; Xia, X.; Cole, S.; Cai, Y. A Review of the Structure, Preparation, and Application of NLCs, PNPs, and PLNs. *Nanomaterials* **2017**, *7*, 122. [[CrossRef](#)] [[PubMed](#)]
39. *Draft Guideline on Quality and Equivalence of Topical Products*; EMA/CHMP/QWP/708282/2018; European Medicines Agency: Amsterdam, The Netherlands, 2018.



III

Review

Methods to Evaluate Skin Penetration In Vitro

Stella Zsikó^{ID}, **Erzsébet Csányi**^{ID}, **Anita Kovács**, **Mária Budai-Szűcs**^{ID}, **Attila Gácsi** and **Szilvia Berkó** *^{ID}

Institute of Pharmaceutical Technology and Regulatory Affairs, Faculty of Pharmacy, University of Szeged, Eötvös u. 6, H-6720 Szeged, Hungary

* Correspondence: berkosz@pharm.u-szeged.hu

Received: 21 May 2019; Accepted: 31 July 2019; Published: 8 August 2019



Abstract: Dermal and transdermal drug therapy is increasing in importance nowadays in drug development. To completely utilize the potential of this administration route, it is necessary to optimize the drug release and skin penetration measurements. This review covers the most well-known and up-to-date methods for evaluating the cutaneous penetration of drugs in vitro as a supporting tool for pharmaceutical research scientists in the early stage of drug development. The aim of this article is to present various experimental models used in dermal/transdermal research and summarize the novel knowledge about the main in vitro methods available to study skin penetration. These techniques are: Diffusion cell, skin-PAMPA, tape stripping, two-photon microscopy, confocal laser scanning microscopy, and confocal Raman microscopic method.

Keywords: drug release; skin penetration; Franz cell; skin-PAMPA; tape stripping; two-photon microscopy; CLSM; confocal Raman microscopy

1. Introduction

The number of dermal formulations has grown in recent decades. According to a market analysis conducted in 2016, profits from transdermal preparations will increase significantly by 2024 [1]. The basic reason for their success is that they have numerous benefits. These include, for example, non-invasive treatment, gastrointestinal tract protection, and avoiding the first pass metabolism of the liver. Topical semisolid preparations are complex formulations. The physical characteristics of the product depend on numerous factors, including the particle size of dispersed particles, the surface tension between the phases, the fractional distribution of the drug between the phases, and rheological behavior. These attributes collectively determine the in vitro release profile, together with additional characteristics. The quantity of Active Pharmaceutical Ingredients (API) released in vitro is an essential characteristic of a product.

Topical and transdermal formulations are commonly used for carrying drugs to the skin and the underlying tissue, or through the skin for systemic action. The modelling of penetration into a skin layer and permeation through the skin is a complex challenge. The device with the attributes of the formulation influence how the system can be examined the most effectively. There are several types of methods with which the release and penetration of drug carrier systems can be examined.

Semisolid products, including creams, ointments, and gels are regularly well-accepted by patients. Topical formulations deliver the active substance into different layers of the skin, therefore, various diseases can be prevented and/or cured. The start, duration, and depth of the therapeutic effect depend on the efficacy of three consecutive processes: (1) The liberation of the API from the carrier system; (2) the penetration/permeation of the API into the stratum corneum (SC) or other skin layers; (3) the effect at the target point. All these processes determine the safety-efficacy profile of a product [2].

The investigational method is greatly influenced by the predictive ability, time, and labor requirements of the given method and its cost. Human skin examinations give the most appropriate

information but, because of the high cost, it is a commonly accepted way to choose simpler methods in the early stages of formulation development [3]. These investigations also help other industries in addition to pharmaceutical research. In agrochemistry, pesticides and insect repellents are involved, and the veterinary and cosmetic industries also rely on these methods [4].

1.1. Structure and Function of the Skin

The skin is the largest organ of the human body and has a surface area of about 2 m² in healthy grown-ups [5]. The human skin is a complex organ that acts as the first protecting barrier of the body. The clarification of skin structure, mainly in relation to its barrier function, has been studied by many researchers since the 1960s [6–10]. It is a multilayer tissue, and its main function is to guard the body against external circumstances by functioning as an effective barrier to the absorption of exogenous particles [11–13]. The skin is an important target as well as a main barrier for dermal drug delivery [14].

The skin consists of three main layers: The epidermis, the dermis, and the subcutaneous tissue. The epidermis, excluding the stratum corneum, which is its outside layer, is a viable tissue. The epidermis does not have vascularization, and nutrients diffuse from the dermo-epidermal junction to maintain its viability. There are five layers that describe the different steps of cell life in the epidermis (Figure 1) [15]. These sublayers are the following, beginning from the non-viable stratum corneum: Stratum lucidum (clear layer), stratum granulosum (granular layer), stratum spinosum (spinous or prickly layer), and stratum germinativum (basal layer). Providing mechanical protection, the cutaneous barrier protects the body from drying as well as from the penetration of dangerous substances and microorganisms. The stratum corneum acts as a critical part in the barrier function for topical drug penetration. Various models have been recommended for mimicking the SC. The most simplistic model is defined as a “brick and mortar” structure; the stratum corneum includes corneocytes (the “bricks”) and an intercellular lipid matrix (the “mortar”), which is essentially responsible for the barrier function [9]. The SC cells are named corneocytes. There are 15 to 20 layers of corneocytes with a thickness of 10 to 15 µm, but when hydrated, the stratum corneum considerably grows, and its thickness may reach up to 40 µm, showing extended permeability. These cells are dense, functionally dead and anucleated. The lipids form bilayers surrounding the corneocytes. The intercellular lipid consists of a mixture of fatty acids, ceramides, cholesterol, cholesterol esters and a small fraction of cholesterol sulfate [11,16,17]. Considering its barrier qualities and water resistance, the stratum corneum is the main layer that limits drug permeation through the skin [15].

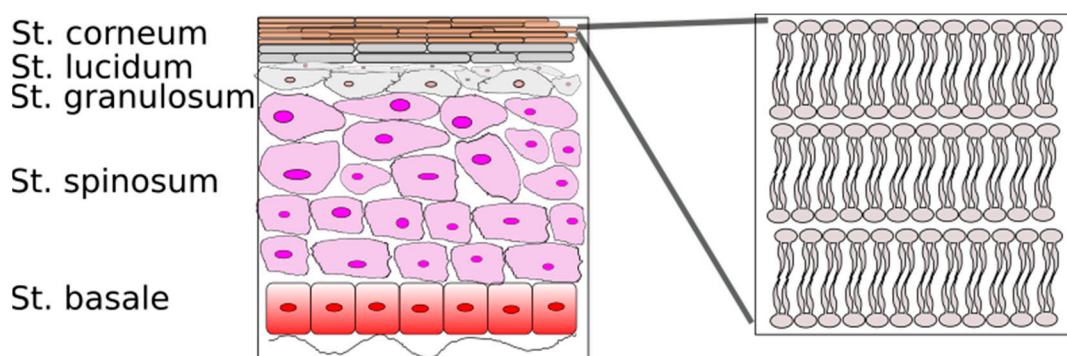


Figure 1. Structure of the epidermis and the intercellular lipid matrix.

There are three different pathways allowing substances to pass through the cutaneous barrier [18]. There are three major routes of penetration for the passive diffusion of a molecule across the SC (Figure 2). The first pathway is the intercellular penetration pathway, which has come to be the most important one for many years. Approximately 15 years ago, the follicular penetration pathway was also found to be a second essential pathway. The transcellular penetration pathway, where the materials pass through both the corneocytes and the lipid layers, seems to be unimportant at present [16,19].

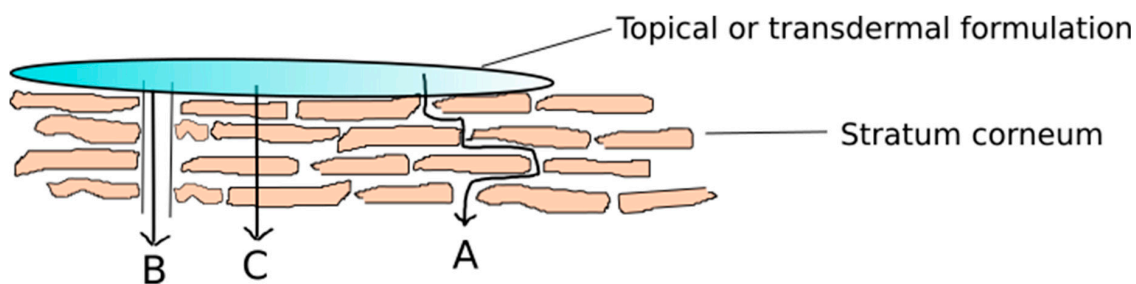


Figure 2. Routes of penetration. A: Intercellular penetration pathway, B: Follicular penetration pathway, C: Transcellular penetration pathway.

The difference between skin penetration and permeation is important. Buist and co-workers have defined them as follows [20]. Dermal penetration: The movement of a chemical from the outer surface of the skin into the epidermis, but not necessarily into the circulatory system. Dermal permeation: The penetration through one layer into another, which is both functionally and structurally different from the first layer.

1.2. Modifying Factors of Skin Penetration

The interactions between the drug, skin, and vehicle determine: (1) The drug release, (2) the penetration through the SC, (3) the penetration through the viable skin layers.

The liberation of an API from a pharmaceutical product applied to the skin and its transport to the systemic circulation is a multistep process which includes (a) the release of API from the preparation, (b) drug partitioning into the stratum corneum, (c) drug diffusion toward the stratum corneum, (d) drug partitioning from the stratum corneum into viable epidermis layers, (e) diffusion across the viable epidermis layers into the dermis, (f) drug absorption by vessels, (g) reaching systemic circulation (Figure 3).

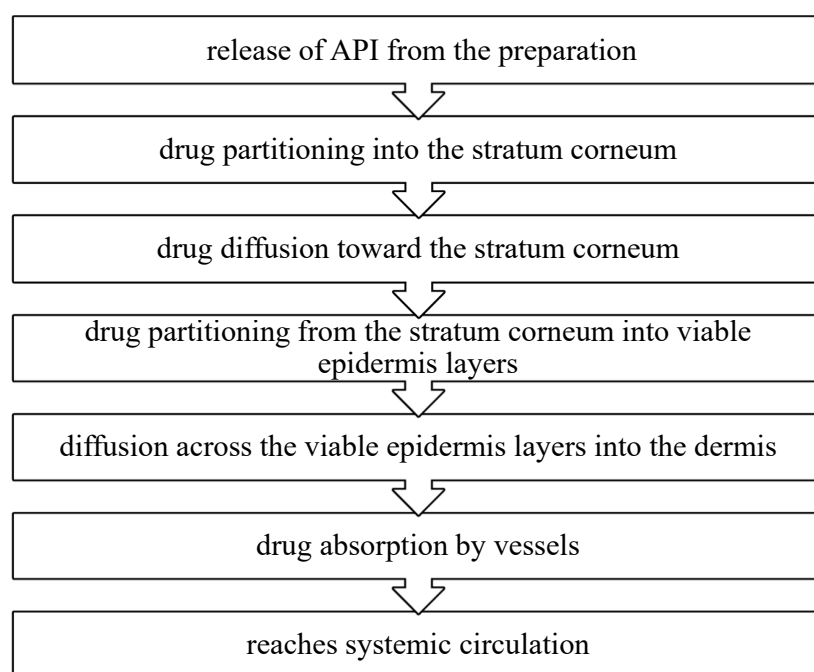


Figure 3. Drug transport across the skin.

The selection of APIs for dermal delivery must be based on many factors, including physicochemical characteristics, drug interactions with the membrane, and pharmacokinetic aspects. The ideal physicochemical characteristics of a drug chosen for cutaneous administration are low

molecular weight (<600 Da); low melting point (<200 °C), which is related to appropriate solubility; a high but stable partition coefficient because very high partition coefficients may increase drug retention, thus inhibiting drug clearance from the skin, and of course, solubility in water and oils to achieve a proper concentration gradient and increase the diffusion force over the skin [21–24].

Percutaneous penetration is affected by biological factors, too. There is basic variability in the skin barrier, due to factors such as skin hydration level, age, gender, site of the skin surface, malformations due to illness or damage and prior treatment [25–29]. To provide the skin with a healthy barrier function, the hydration level of the skin needs to be balanced, and enough volume of water is needed. If hydration increases, permeability may be improved [30]. Age has an impact on penetration into the skin. Baby skin and damaged skin have higher permeability.

The permeability of the drug through the stratum corneum is modulated by the carrier/vehicle, too. A vehicle can improve the physical state and permeability of the skin by the hydration effect or an alteration of the lipid bilayer structure.

1.3. General Guidelines of Skin Penetration Testing

Recently, the regulation of dermal and transdermal preparations has received increasing attention. More and more documents are available for dermal absorption studies from Europe and the United States (Figure 4). These documents promote a harmonized road to conducting dermal and transdermal studies. The Organization for Economic Cooperation and Development (OECD) published several issues about this topic, including the Guidance Notes on Dermal Absorption (No. 156) [20], Test Guidelines 427 (in vivo methods) [31] and 428 (in vitro methods) [32], and the Guidance Document for the Conduct of Skin Absorption Studies [33]. There are some other documents such as the World Health Organization International Programme on Chemical Safety (WHO/IPCS) Environmental Health Criteria 235 [34], the European Centre for Ecotoxicology and Toxicology of Chemicals (ECETOC) Monograph 20 [35], the United States Environmental Protection Agency (USEPA) report on dermal exposure assessment [36], and the European Food Safety Agency (EFSA) Guidance on dermal absorption for plant protection products [20,37]. These documents present rules on and descriptions of how to perform dermal absorption assays, however, the measurements are not properly regulated. There are two suggested methods. One is the widely used diffusion cell and the tape stripping methods. However, in the scientific literature there are a lot of other types of measurements, such as spectroscopic and microscopic methods, to complete the suggested tests.

OECD Guidance Notes on Dermal Absorption (No. 156), 2011
OECD Test Guidelines 427 (in vivo methods), 2004
OECD Test Guidelines 428 (in vitro methods), 2004
OECD Guidance Document for the Conduct of Skin Absorption Studies, 2004
World Health Organization International Programme on Chemical Safety (WHO/IPCS) Environmental Health Criteria 235, 2006
European Centre for Ecotoxicology and Toxicology of Chemicals (ECETOC) Monograph 20, 1993
United States Environmental Protection Agency (USEPA) Report on Dermal Exposure Assessment, 2007
European Food Safety Agency (EFSA) Guidance on Dermal Absorption for Plant Protection Products (PPR), 2017

Figure 4. Guidelines for modelling dermal penetration/permeation.

2. Techniques for Modelling Penetration/Permeation through Human Skin

There are two main types of techniques. Quantitative techniques include the use of diffusion cells and skin-PAMPA. Qualitative or semiquantitative techniques are different microscopic and spectroscopic methods and the combinations thereof. Figure 5 shows the quantitative and qualitative methods for following up skin penetration.

Quantitative in vitro tests are regularly performed to measure the amount of API permeated through a membrane over time in relation to the diffusion area related to the collected quantity of API in an acceptor chamber [11,38–43]. In the case of qualitative techniques, the aim is usually to follow the active substance. The presence or the relative amount of the active ingredient in the different skin layers can be determined. The use of multiple methods together can perfectly complement each other, making the regulatory authorization process easier.

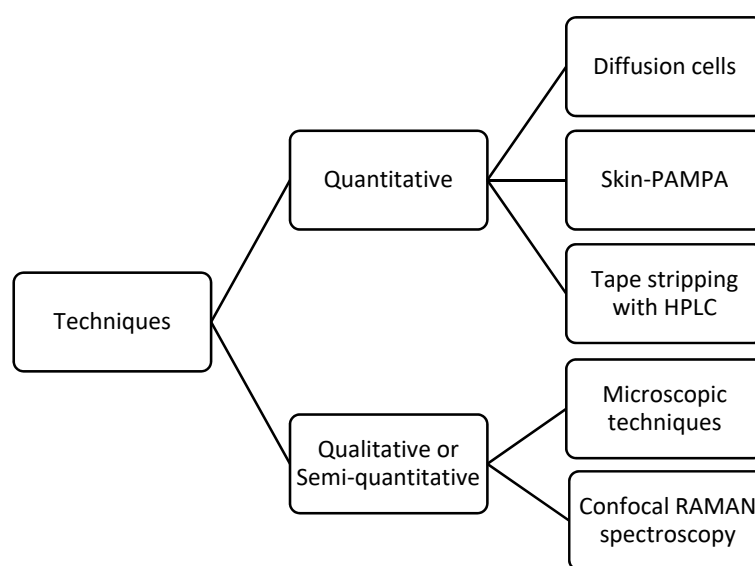


Figure 5. The main quantitative and qualitative methods for following up skin penetration.

2.1. Diffusion Cells

The skin can be considered as a selectively permeable biological membrane of drugs. Diffusion tests working with diffusion cells have become the “gold-standard” model due to the pioneering work of Dr. Thomas J. Franz, who developed the “Franz cell” in 1970. It determines important relationships between skin, API, and formulation [44–46]. The diffusion test models the method of medicine applied to the skin. This tool consists of a cell that holds a chamber for drug application, a membrane within which the drug may diffuse, and an acceptor media chamber from which samples may be investigated [47].

2.1.1. Types and Properties of Diffusion Cells

Diffusion cells can be categorized into two main classes, static and flow-through cells. The cells are normally made of glass. In static cells, the donor, the membrane, and the acceptor may be placed either vertically, as in the popular Franz diffusion cell (Figure 6) [44], or horizontally (Figure 7) [48]. There are Franz cells which open from above, therefore the measurement runs on atmospheric pressure. However, most of the cells are closed from the top, and because of this, the pressure is higher, predicting higher penetration values. Nowadays, the “hand-sampler” Franz diffusion cells have been replaced by systems connected to an automated sampler. Sampling systems facilitate the work of researchers and reduce error from human sampling.

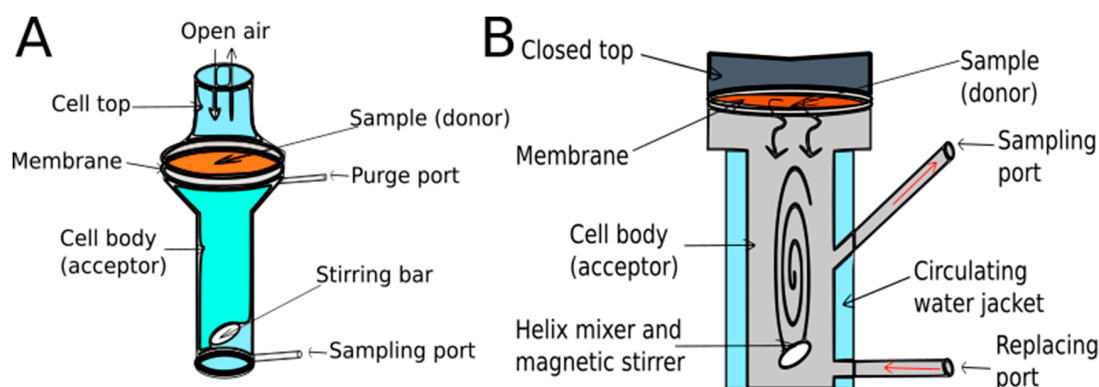


Figure 6. Open (A) and closed (B) vertical Franz diffusion cells.

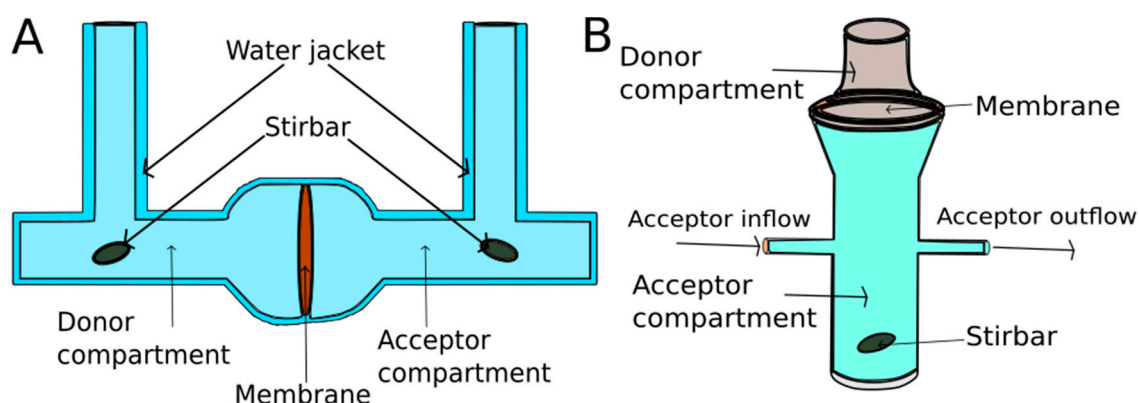


Figure 7. Side-by-side cell (A) and flow-through cell (B).

2.1.2. Diffusion Test Types

In the EMA (2018) document (Draft Guideline on Quality and Equivalence of Topical Products) diffusion tests are grouped as follows. There are in vitro release tests (IVRT) and in vitro skin permeation studies (IVPT).

In the case of IVRT, synthetic membrane (lipid-based or non-lipid based model membranes) should be used. The sample dose must be occluded and infinite. The IVRT study shows the release rate. The detected quantities are in the μg to mg range. In the case of IVPT, human skin should be used in unoccluded circumstances. The sample dose must be finite. The IVPT study shows the flux profile and the detected quantities are in the pg to ng range. In the early stages of development, IVRT should be used, thereafter, IVPT can be used for promising formulations [49]. The main differences are summarized in Table 1.

Table 1. In vitro release tests (IVRT) and in vitro skin permeation studies (IVPT).

IVRT	IVPT
Synthetic membrane	Human skin
Occluded dose	Unoccluded dose
Infinite dose	Finite dose
Release rate	Flux profile
μg to mg range	pg to ng range
Relative consistency	Donor variability

Every year, several papers are published involving the use of a vertical Franz diffusion cell. In the last four months, “Franz Diffusion” as a keyword can be found in 13 articles. The specifications of the publications are summarized in Table 2. Many different APIs and membranes were used.

Table 2. Some Franz diffusion measurements (last 4 months).

Researcher	Membrane/Skin Model	Main Topic
Jung Dae Lee et al. [50]	full-thickness Sprague-Dawley rat skin	permeability of 1-phenoxy-2-propanol in a shampoo and a cream
Yanling Zhang et al. [51]	heat separated human epidermis and full-thickness porcine ear skin; skin-PAMPA membrane	comparison of the Franz cell methods with different membranes and different doses to the skin-PAMPA method
Sonia Trombino et al. [52]	dialysis membranes and rabbit ear skin	cyclosporin-A incorporated in SLN for the topical treatment of psoriasis
Oludemi Taofiq et al. [53]	pig ear skin	studied mushroom ethanolic extracts matrix-type patches for the transdermal delivery of galantamine for the treatment of Alzheimer's disease
Dina Ameen et al. [54]	dermatomed human cadaver skin	oral solution of pioglitazone for the treatment of Alzheimer's disease
Marcelle Silva-Abreu et al. [55]	dialysis membrane and porcine mucosa (buccal, sublingual, nasal and intestinal)	skin permeation of urea at finite dose and comparison to infinite dose condition
Rattikorn Intarakumhaeng et al. [56]	heat-separated torso split-thickness cadaver skin	methotrexate loaded topical nanoemulsion for the treatment of psoriasis
Panonnummal Rajitha et al. [57]	cellophane membrane, isolated pig ear skin and full-thickness pig ear skin	mucoadhesive buccal film containing rizatriptan benzoate and propranolol hydrochloride
Sahar Salehi et al. [58]	rat buccal mucosa	multiple emulsion for the topical application of clotrimazole
José L. Soriano-Ruiz et al. [59]	nylon, cellulose and polysulfone membranes; porcine buccal mucosa, porcine sublingual, vaginal mucosa	permeation profiles of lidocaine and prilocaine across the palatal mucosa without bone
Luciano Serpe et al. [60]	porcine palatal mucosa	fractional CO ₂ laser effect on drug penetration and absorption
Woan-Ruoh Lee et al. [61]	nude mouse skin	amidoalkylating agent and SLNs with antimicrobial activity
Ahmed O.H. El-Nezhawy et al.	cellophane membrane	

2.2. Skin-PAMPA

The Parallel Artificial Membrane Permeability Assay (PAMPA) is a 96-well plate-based method for the fast determination of the passive membrane permeability of molecules [62]. It is a promising method because of its low cost and high throughput. There are different PAMPA models and one for skin penetration. The earlier published skin model combines silicone oil and isopropyl myristate [63].

Sinkó et al. have developed the skin-PAMPA method for the prediction of skin penetration in vitro [64]. Skin-PAMPA has been created to imitate the characteristics of the stratum corneum [25]. Using this new plate, the donor phase contacts the hydrated artificial membrane (approximately 60–70 µL). This amount was ~180–200 µL using a conventional bottom plate. When examining the cross-sectional image of the donor cell of the new plate, the amount of material that is in direct contact with the membrane is about 30 µL. This results in a clear penetration surface (0.3 cm²), leading to 100 µL/cm² of donor per unit area. Compared to the OECD recommendation, this is still one order of magnitude higher, but it is closer to the concept of finite dose [65]. Skin-PAMPA membrane was produced by using cholesterol, free fatty acid, and a ceramide-analogue compound that imitates the features of lipid matrix [66]. The donor plate of the conventional skin-PAMPA procedure requires the use of a large amount of sample, which does not meet the concept of finite dose. The experimental design is shown in Figure 8.

In the past few years, skin-PAMPA as a bio-relevant artificial membrane-based permeability model has been used for the evaluation of skin penetration (Table 3) [67].

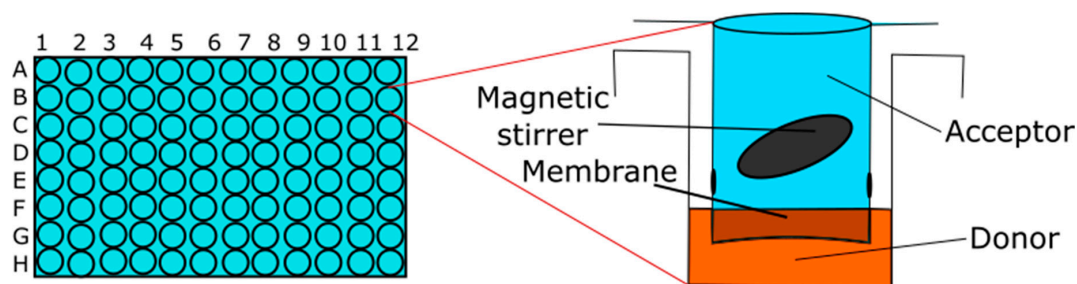


Figure 8. Experimental design of the skin-PAMPA method.

Table 3. Posters and articles related to the skin-PAMPA method [67].

Researcher	Year	Main Topic
Lee et al. [68]	2010	<ul style="list-style-type: none"> homogenous and normalized permeability data for more than 40 compounds
Tsinman et al. [69]	2012	<ul style="list-style-type: none"> investigation of ibuprofen penetration using both the skin-PAMPA model and real human skin mounted in a Franz cell system
Karadzovska and Riviere [65]	2013	<ul style="list-style-type: none"> study of 96-well-based skin penetration models, including skin-PAMPA as well, besides another PAMPA skin model by Ottaviani and Strat-M membrane
Vizserálek et al. [70]	2013	<ul style="list-style-type: none"> the effect of incubation temperature on permeability
Clough et al. [71]	2013	<ul style="list-style-type: none"> the permeability enhancing effect of a series of solvents, lipidic fluids and emulsifiers was investigated
Luo et al. [72]	2014	<ul style="list-style-type: none"> comparison of skin-PAMPA results to porcine skin results measured with the Franz cell method

2.3. The Most Important Experimental Considerations in the Case of Quantitative Methods

In order to obtain reliable dermal permeability data, several parameters have to be considered for the design of the test system, which are influenced by the solubility of the compounds:

- the sink condition
- the incubation time
- the incubation temperature
- the mixing
- the hydration of the membrane
- the amount of dose [73].

In the case of molecules with low solubility, it is not so easy to create the sink condition. Ueda and colleagues have determined the sink condition: To achieve sink conditions, the receptor medium must have a relatively high capacity to dissolve or carry away the drug and the receptor media should not exceed 10% of drug solubility in the releasing matrix at the end of the test [74]. By changing the composition and the pH of the acceptor and donor phases, the suitable sink condition can be created. This means that under certain experimental conditions, the backflow from the acceptor phase can be considered as zero. Alternatively, the sink condition can be achieved by the use of surfactants in the acceptor phase. A further solution is the use of serum albumin because it is capable of binding lipophilic components, thereby keeping the free concentration of the molecule lower. The advantage of using albumin is that it is a sufficiently large molecule to not permeate through the skin.

In the case of the incubation time, it is important to consider the fact that the structure of the skin or the artificial membrane remains unchanged until the end of the experiment. To avoid the overestimation of dermal penetration, different skin integrity tests are needed to eliminate the use of damaged skin preparations. This test should ensure the exclusive use of skin-derived data with an appropriate barrier function in the assays. Several methods can be used to examine skin integrity. Each has advantages and disadvantages. Widely used methods are the measurement of tritium water permeability, the measurement of transepidermal water loss, and the determination of transepidermal electrical resistance. A relatively new method is the use of the tritium-labeled internal reference standard, where integrity testing is performed simultaneously with the measurement [60–64,66,67]. For each method, it can be stated that the measurements are different and not properly regulated. Different labs use different limits and measure under different conditions. In the future, the proper regulation of integrity testing and the clear definition of limit values for the proper evaluation of dermal formulations will be essential.

The incubation temperature affects both the permeability of the compounds and the rheological properties of the product studied. The selected mixing speed should guarantee enough mixing of the acceptor phase during the test [74]. Hydration of the skin affects, among other things, the barrier function of the stratum corneum, therefore, the creation of an optimal hydration state is essential [75].

Depending on the amount of sample in the test cells, two types of experiments can be distinguished: Finite and infinite dose measurements. In the case of the infinite dose, the amount of sample used is in large excess, hence the donor phase (the sample itself) cannot empty under normal circumstances. As a result, when examining a permeability-time profile in this case, the straight line usually rises with a constant slope without experiencing a plateau phase. The opposite of the infinite dose is the finite dose. When finite doses are used, a limited amount of sample (donor phase) is applied to the skin or to the surface of the artificial membrane. It should be noted that the latter experimental circumstance is much closer to the condition when the patient applies a given preparation onto his or her own skin. Based on the recommendation of the OECD (Organization for Economic Co-Operation and Development), a finite dose for a solution-phase sample is recommended if the applied dose does not exceed $10 \mu\text{L}/\text{cm}^2$ or is in the range of 1 to $10 \text{ mg}/\text{cm}^2$ for a semisolid sample [75]. Certainly, it is more advantageous to design the measurement conditions to approach the finite dose requirements as much as possible [64].

There are some measurement parameters which affect drug penetration, such as occlusive or non-occlusive application [76,77]. Dermal and transdermal drug delivery can be performed after occlusive or non-occlusive (open) application. Occlusion can be achieved by covering the skin by impermeable films or others, such as strips, gloves, diapers, textiles garments, wound dressings or transdermal therapeutic systems [78].

2.4. Tape Stripping

The quantification of APIs within the skin is crucial for topical and transdermal delivery examinations. Nowadays, horizontal sectioning, consisting of tape completely stripping the stratum corneum, has become one of the conventional investigation procedures [79]. The method may be quantitative or semiquantitative depending on the analysis.

Tape stripping is a commonly used, minimally invasive method for testing the penetration of topically applied formulations through the stratum corneum, whereby layers of the stratum corneum are removed by an adhesive tape and skin layers residing on the adhesive tape are examined (Figure 9). On the one hand, the protein content of the different layers can be determined by the method, and on the other hand—after the topical application of the composition to be tested—the amount of the active ingredient in the selected layer can be determined. In addition to drug penetration testing, the effect of the substance on skin hydration and skin proteins can be observed, e.g., to modify the secondary structure of keratin. Tape stripping can also be used *in vitro* and *in vivo* on human and animal skin, as well as on appropriate skin models [15,25,80]. The Organization for Economic Co-operation and

Development Test Guideline (OECD TG) 427 describes the use of tape stripping for the removal of upper skin layers and the in vivo penetration of active substances [31], while the OECD TG 428 has been performed with the in vitro application of the method for experiments [32].

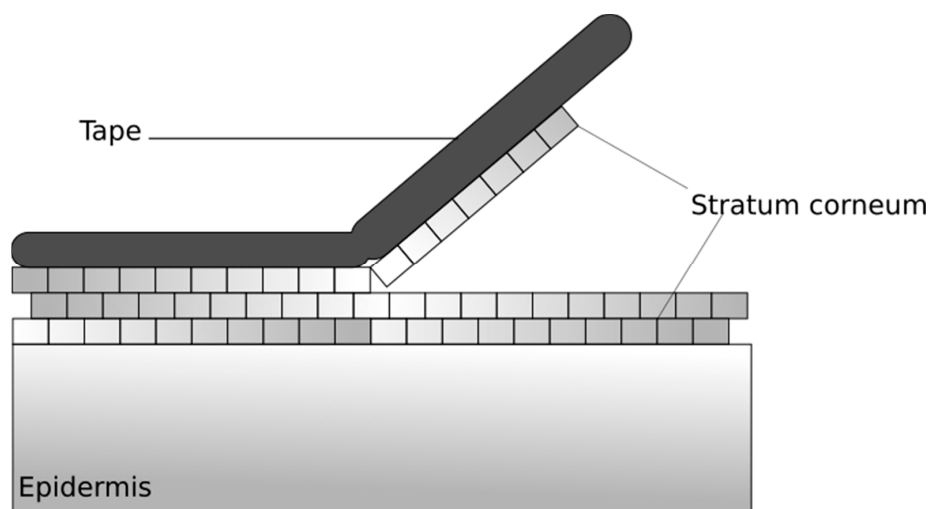


Figure 9. Layers of the stratum corneum are removed by an adhesive tape.

2.4.1. Method Description

The tape stripping process begins after the topical application of the test composition and waiting for an appropriate incubation time. The composition can be removed or left on the skin in order to provide the original amount of the composition used during the measurement. This is of particular importance, for example, when examining sunscreen preparations, where the active substance on the skin surface will exert an effect, so we need to analyze it. The adhesive tape is placed on the skin surface and removed, always from the same selected area. It is important that the adhesive tape is always flattened with the same force as the roller, which eliminates the influence of wrinkles and recesses on tape stripping. In addition, the speed of removal is also an important factor: The slower the removal of the adhesive tape, the greater the adhesion of the stratum corneum to the patch, thus increasing the amount of skin removed from the patch. Removed adhesive tapes will contain both the layers of the SC and the active ingredient of the composition used [25,81,82].

2.4.2. Possibility of Sample Analysis

Several methods can be used to test the sample on the adhesive tape. The HPLC analysis generates a quantitative result, while the spectroscopic method yields semiquantitative results. During the HPLC (High-Pressure Liquid Chromatography) analysis, the test material on the adhesive tape is extracted by a suitable method and chromatographed. In addition, atomic absorption spectrometry may also be used to detect certain active substances, e.g., titanium dioxide. Furthermore, the active ingredients containing chromophore may also be useful for testing vitamin E [83]. However, the most widespread method is Attenuated Total Reflectance Fourier transform infrared spectroscopy (ATR-FTIR) [83]. Spectroscopy measurements are based on the irradiation of the sample, vibrations, and bond angle between the atoms in it, due to absorption or scattering of the infrared radiation. The changes in the radiation passing through the sample are measured by plotting the wavelength/wavenumber to obtain the spectrum that can be analyzed by qualitative and quantitative information. The penetration depth is thus determined by the wavelength of the infrared light, the refractive index of the ATR crystal and the measured material, and the angle of reflection [15,25]. Tape stripping combined with ATR-FTIR spectroscopy may be suitable for detecting various exogenous substances in certain layers of the SC. However, the difficulty of the method is that the characteristic peaks of the substances to be detected are often present and overlap with skin-specific peaks.

2.4.3. Possibilities for Optimizing the Experimental Protocol

The following options may be suitable for standardizing the experimental protocol. The composition should preferably be applied with a latex glove in a defined amount of time. Before applying, it is advisable to cut one finger of the rubber gloves and dip them into the preparation to fill the holes on the latex. Then the glove should be cleaned. This minimizes the amount of drug lost in the rubber glove, thus allowing the same quantities to be applied [84]. It is advisable that parallel measurements should always be carried out by the same person, as this may exclude the potential impact of different application techniques. The intact barrier function of the skin should be checked before starting the experiments. A TEWL test can be used to measure skin integrity. The intact barrier function, suitable for starting tape stripping experiments, indicates a TEWL value of 15–20 g m⁻² h⁻¹ [80]. It is recommended that the adhesive tape be smoothed onto the skin using a roller to eliminate the effects of wrinkles and recesses on the skin [82].

2.5. Microscopic and Spectroscopic Methods Utilised for the Percutaneous Penetration of APIs

Microscopic techniques also give important information about the spatial distribution of the drug inside the different skin layers or explain the mechanism of penetration. Furthermore, these are not destructive in vitro techniques [85–88]. Fluorescence microscopy is a frequently used method, as well. The evaluation of skin treated with fluorescently labeled materials by fluorescence microscopy has shown that the fluorescent labeled material resided in the SC or penetrated deeper in the epidermis [89,90].

Confocal microscopy is a specialized form of standard fluorescence microscopy. It has developed over the last five to six decades and now it is a necessary tool for scientists. The major confocal techniques are two-photon microscopy (2-PFM), confocal laser scanning microscopy (CLSM), and the youngest, Raman microscopic methods. These methods have the possibility to image deeper into a three-dimensional biological sample like skin at high resolution, high speed, in in vitro and in vivo circumstances [15,25,91,92].

2.5.1. Two-Photon Microscopy Method

Two-photon scanning fluorescence microscopy has become an important tool for imaging skin cells. It employs a Ti-sapphire laser excitation source. In single-photon fluorescence, the fluorescence photon is created when a high-energy photon is incident on the fluorophore and increases the energy level of one of the electrons to an excited state. In two-photon excitation, the combined energy shift of the two low-energy photons is enough to raise the same electron to a higher energy level. The setup of a two-photon microscope is quite similar to that of a confocal scanning microscope with two major differences. Two-photon microscopes work with a tunable Ti-sapphire high-frequency pulsed laser. These lasers emit red and near-infrared light in the range from 650 to 1100 nanometers. The other big difference is that there are no pinholes in front of the detector [93].

The most relevant advantages of 2-PFM are that the total energy transferred to the specimen is much lower as compared to other techniques. Furthermore, the two-photon excitation phenomenon occurs only at a very small focal volume and thanks to the fluorophores, a small volume of the specimen is excited, which decreases the possibility of photo-bleaching and photo-damage. The skin samples can be studied without cryofixation and cutting. In the case of imaging of UV absorbing fluorophores, deep tissue imaging is possible with infrared excitation because of less scattering and less absorption. The limitations of a two-photon microscope include the relatively high price of the lasers and the fact that they require a complex cooling system. Additionally, it has a lower lateral resolution compared to other techniques, but in practice, the difference in their resolution is not significant [25,94].

Two-photon microscopes represent a relatively young technology. There are some publications (Table 4) in this area [95–99], but more research is expected in this field in the near future.

Table 4. Two-photon microscopy results.

Researcher	Year	Main Topic
Hanson et al. [99]	2002	<ul style="list-style-type: none"> two-photon fluorescence lifetime imaging of the skin stratum corneum pH gradient the effect of active and passive mechanisms upon the origin of acidic microdomains within the stratum corneum
Plasencia et al. [95]	2007	<ul style="list-style-type: none"> lipid domain coexistence in a broad temperature range (including physiological skin temperatures) using confocal and two-photon excitation fluorescence microscopy
Carrer et al. [98]	2008	<ul style="list-style-type: none"> images of pig skin the presence of a trans-epidermal shunt the junctions between corneocyte clusters accumulate liposomes
Batista et al. [97]	2016	<ul style="list-style-type: none"> all layers of the porcine cornea
Umino et al. [96]	2019	<ul style="list-style-type: none"> the effects of xylitol (a component of some skin-care products) and fructose on lipid dynamics in an epidermal-equivalent model at the single-cell level by means of two-photon microscopy

2.5.2. Confocal Laser Scanning Microscopy Method

Confocal laser scanning microscopy (CLSM) is a non-invasive method developed from fluorescence microscopy. In the last years, CLSM has been widely accepted as a device to visualize the fluorescent model compounds in the skin. CLSM can be used to examine the skin structure without cutting tissue as well as to evaluate the influences of physical and chemical enhancers on skin permeability. It has been used in vivo and in vitro, too. CLSM is used to diagnose general skin dysfunctions and to identify malignant lesions, and it can characterize keratinization and pigmentation disorders as well [100–102].

CLSM can be applied to explain the mechanism by which nanoparticulate formulations promote skin transport. Fluorescent markers (e.g., fluorescein, Nile red, 5-bromodeoxyuridine) may be incorporated in nanostructured formulations, in which they are encapsulated. The therapeutic effect of these formulations can be examined by CLSM to identify the penetration profiles of these fluorescent markers across the skin or skin appendages [15,25]. Table 5 summarizes the most important recent results.

Table 5. Confocal laser scanning microscopy results.

Researcher	Year	Main Topic
Simonetti et al. [103]	1995	<ul style="list-style-type: none"> diffusion pathways across the SC of native and in vitro reconstructed epidermis
Zellmer et al. [104]	1998	<ul style="list-style-type: none"> vesicles made of native human SC lipids interact rapidly with phosphatidylserine liposomes interact weakly with human SC lipid liposomes do not interact with phosphatidylcholine (PC) liposomes
Kuijk-Meuwissen et al. [105,106]	1998	<ul style="list-style-type: none"> flexible liposomes penetrated into the skin in non-occlusive conditions, then after occlusive application
Toutou et al. [107]	2001	<ul style="list-style-type: none"> the penetration of fluorescent probes into fibroblasts and nude mice skin ethosomes promoted the penetration of all probes into the cells
Grams et al. [108,109]	2003 2004	<ul style="list-style-type: none"> follicular accumulation of lipophilic dyes increased when used in combination of surfactant-propylene glycol time-resolved diffusion of a lipophilic dye into the hair follicle of a fresh and unfixed piece of human scalp skin
Alvarez-Roman et al. [101]	2004	<ul style="list-style-type: none"> polystyrene nanoparticles concentrated preferentially in the follicular openings this configuration developed in a time-dependent habit, and the follicular localization was favored by particles of smaller size
Patzelt et al. [19]	2011	<ul style="list-style-type: none"> the follicular penetration for nanoparticles is size-dependent

2.5.3. Confocal Raman Microscopic Method

Spectroscopic methods can produce molecular information about the structure of the skin. Raman spectroscopy is a promising spectroscopic method based on discovering the characteristic vibrational energy levels of a molecule excited by a laser ray and it gives information about the molecular structure of tissue components without the use of fluorescent labels or chemical stains [110–113]. Therefore, this method is promising for discovering modifications in the structure of skin components. In addition, it is good for following up the penetration/permeation of APIs [114,115]. Nowadays, Raman microscopy is a powerful technique to properly understand skin structure and percutaneous drug delivery [111,116–118].

Traditionally, the tape stripping method is used to model the penetration into the stratum corneum. This method is time-consuming, semi-destructive, and difficult to reproduce, and only the stratum corneum can be examined. Important technical developments are custom setting and the confocal microscope combination. This enables chemically selective and non-destructive sample analysis with high spatial resolution in three dimensions and allows multiple components to be monitored at the same time. Confocal Raman microscopy can be used to investigate topical formulations for both penetration and penetration depth in vitro and in vivo [119,120].

Permeation through the skin can be explored by chemical mapping (Figure 10). Chemical mapping is one of the methods of vibration spectrometry; the suitable test apparatus is a vibration spectrometer (e.g., Raman) and a suitable optical unit (e.g., microscope). Raman Spectrometry is highly selective, with a fingerprint spectrum that allows clear molecular identification. The irradiating light can be focused on a very small point ($\sim 1 \mu\text{m}^2$) with a suitable microscope lens, so reliable chemical information can also be obtained from a microscopic area of the sample. The spatial distribution of the fundamental components of the sample can be determined by the spectra that make up the map. Chemical maps contain a huge quantity of data. Although these can be controlled by methods commonly used in spectroscopy, the huge amount of data can be utilized more efficiently by using appropriate mathematical (multivariate data analysis) techniques. Thanks to these advantages, the technology has enormous potential in various applications: From the analysis of the distribution of the physiological components of the skin and tissues through the diagnosis of pathological conditions to biopharmaceutical studies, such as drug penetration kinetics [15,25,120,121]. Table 6 summarizes the most important recent results.

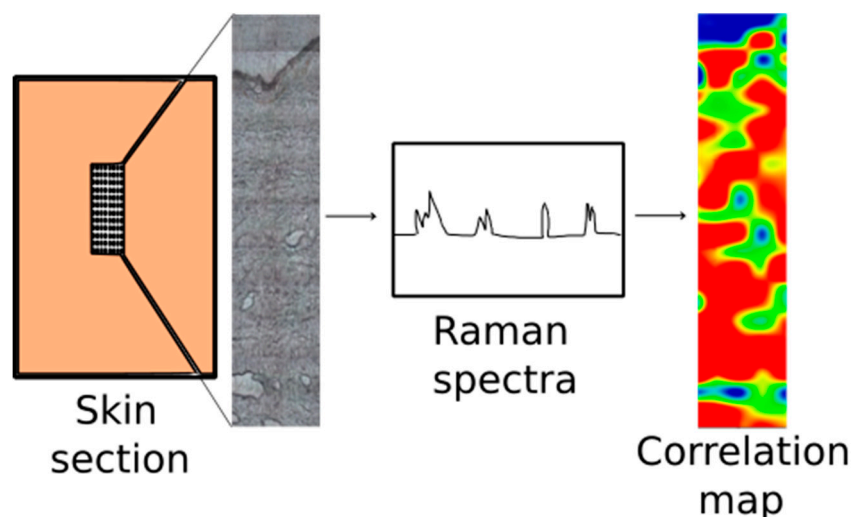


Figure 10. Raman chemical mapping.

Table 6. Confocal Raman microscopic results.

Researcher	Year	Main Topic
Zhang et al. [122,123]	2007	<ul style="list-style-type: none"> the spatial distribution, time-dependent penetration of phosphorylated resveratrol and its transformation into the active form on stratum corneum and live epidermis on pigskin
Freudiger et al. [124]	2008	<ul style="list-style-type: none"> the penetration of dimethyl sulfoxide and retinoic acid in mouse skin by stimulated Raman scattering (SRS) technique the SRS technology makes it much more sensitive and provides better imaging than traditional Raman techniques
Melot et al. [125]	2009	<ul style="list-style-type: none"> the influence of penetration enhancers on the delivery of trans-retinol into human skin the penetration enhancing effect of propylene glycol and oleic acid the penetration enhancement effect of propylene glycol was easy to follow, and propylene glycol was also detected in the deeper layers of the skin
Gotter et al. [126]	2010	<ul style="list-style-type: none"> confocal Raman mapping to measure the amount of dithranol penetration into an artificial acceptor membrane (DDC membrane) at different time points
Saar et al. [127]	2011	<ul style="list-style-type: none"> the penetration of ketoprofen, ibuprofen and co-solvent propylene glycol into mouse skin at different time intervals by SRS the advantage of this technique is that it is uniquely able to provide high-resolution three-dimensional imaging for unlabeled molecules the penetration of the drug through the epidermis and through the stratum corneum can be simultaneously monitored and compared; in addition, crystals of the API can be detected on the surface of the skin
Franzen et al. [128]	2013	<ul style="list-style-type: none"> a semisolid artificial matrix to model the optical properties of human skin deep profiling of skin was performed and a mathematical algorithm was used to describe the modification of the Raman signal in the matrix the algorithm described at the artificial matrix was successfully applied to human skin
Smith et al. [119]	2015	<ul style="list-style-type: none"> the most important measurements made by confocal Raman spectroscopy were summarized
Ilchenko et al. [116]	2016	<ul style="list-style-type: none"> made a quantitative analysis of samples on three-dimensional Raman map of mouse skin on the spectral map of mouse skin, the components of keratin, lipids, water, lactate, urea, and natural hydrating factor (NMF) have been identified the lateral and deep distribution of the major skin components derived from Raman maps correlates with histological information
Berkó et al. [115]	2018	<ul style="list-style-type: none"> semiquantitative analysis of a papaverine hydrochloride containing lyotropic liquid crystal system the Raman correlation maps complete the other skin penetration measurements
Bakonyi et al. [114]	2018	<ul style="list-style-type: none"> four types of formulation: hydrogel, oleogel, lyotropic liquid crystal and nanostructured lipid carrier were investigated the application of Raman spectroscopy provided information about the spatial distribution of the API in the skin

3. Conclusions

The modelling of penetration into a skin layer and permeation through the skin is a complex challenge. Although there are many quantitative and qualitative methods for following up skin penetration/permeation (in vitro and in vivo), the different techniques are not fully equivalent but complement each other. The advantages and disadvantages of the different methods are summarized in Table 7. For the evaluation of drug penetration, pharmaceutical technologists must decide those

properly suited to their examinations. The models give a possibility for rapid screening and faster optimization of products. The selection of the most suitable in vitro model should be based on availability, facility of use, cost, and the respective limitations [30]. The success of topical and transdermal therapy is correlated to the techniques used for the evaluation of the preparations, which facilitate the optimization of the skin penetration of the API so that it can reach sufficient API penetration at the therapeutic site.

Table 7. Advantages and disadvantages of previously discussed methods.

Method	Advantages	Disadvantages
Franz Diffusion	<ul style="list-style-type: none"> gold-standard accepted by authorities quantitative automated (can be) synthetic and biological membranes repeated dosing (open cell) 	<ul style="list-style-type: none"> differences between research labours different types of cells application requires practice
Skin-PAMPA	<ul style="list-style-type: none"> fast several preparations can be tested at the same time small space and instrument demand quantitative near finite quantity 	<ul style="list-style-type: none"> not automated sampling by hand only synthetic membrane
Tape-Stripping	<ul style="list-style-type: none"> in vitro, ex vivo, in vivo minimally invasive accepted by authorities selected layers can be examining 	<ul style="list-style-type: none"> difficult to reproduce not automated sampling by hand
Microscopic and Spectroscopic Methods	<ul style="list-style-type: none"> high resolution in vitro, ex vivo (sometimes in vivo) non-invasive semi-destructive highly selective 	<ul style="list-style-type: none"> difficult to reproduce expensive lasers are needed only qualitative usually the measurement time is long

Funding: This research was funded by GINOP, grant number 2.2.1-15-2016-00023.

Conflicts of Interest: The authors declare no conflict of interest.

References

- Transdermal Drug Delivery Systems Market-Industry Analysis, Market Size, Share, Trends, Application Analysis, Growth and Forecast 2019–2024. Available online: <https://industryarc.com/Research/Transdermal-Drug-Delivery-Systems-Market-Research> (accessed on 1 April 2019).
- Shah, V.P.; Yacobi, A.; Rădulescu, F.S.; Miron, D.S.; Lane, M.E. A science based approach to topical drug classification system (TCS). *Int. J. Pharm.* **2015**, *491*, 21–25. [CrossRef] [PubMed]
- Wiedersberg, S.; Guy, R.H. Transdermal drug delivery: 30+ years of war and still fighting! *J. Control. Release* **2014**, *190*, 150–156. [CrossRef] [PubMed]
- So, J.; Ahn, J.; Lee, T.-H.; Park, K.-H.; Paik, M.-K.; Jeong, M.; Cho, M.-H.; Jeong, S.-H. Comparison of International Guidelines of Dermal Absorption Tests Used in Pesticides Exposure Assessment for Operators. *Toxicol. Res.* **2014**, *30*, 251–260. [CrossRef] [PubMed]

5. Groeber, F.; Holeiter, M.; Hampel, M.; Hinderer, S.; Schenke-Layland, K. Skin tissue engineering—in vivo and in vitro applications. *Adv. Drug Deliv. Rev.* **2011**, *63*, 352–366. [[CrossRef](#)] [[PubMed](#)]
6. Feldmann, R.J.; Maibach, H.I. Absorption of Some Organic Compounds through the Skin in Man. *J. Investig. Derm.* **1970**, *54*, 399–404. [[CrossRef](#)] [[PubMed](#)]
7. Blank, I.H. Factors Which Influence the Water Content of the Stratum Corneum. *J. Investig. Derm.* **1952**, *18*, 433–440. [[CrossRef](#)] [[PubMed](#)]
8. Vinson, L.J.; Singer, E.J.; Koehler, W.R.; Lehman, M.D.; Masurat, T. The nature of the epidermal barrier and some factors influencing skin permeability. *Toxicol. Appl. Pharm.* **1965**, *7*, 7–19. [[CrossRef](#)]
9. Elias, P.M. The permeability barrier in mammalian epidermis. *J. Cell Biol.* **1975**, *65*, 180–191. [[CrossRef](#)] [[PubMed](#)]
10. Sweeney, T.M.; Downing, D.T. The Role of Lipids in the Epidermal Barrier to Water Diffusion. *J. Investig. Derm.* **1970**, *55*, 135–140. [[CrossRef](#)]
11. Anissimov, Y.G.; Jepps, O.G.; Dancik, Y.; Roberts, M.S. Mathematical and pharmacokinetic modelling of epidermal and dermal transport processes. *Adv. Drug Deliv. Rev.* **2013**, *65*, 169–190. [[CrossRef](#)]
12. Bo Forslind. A domain mosaic model of the skin barrier. *Acta Derm. Venereol.* **1994**, *74*, 1–6.
13. Godin, B.; Touitou, E. Transdermal skin delivery: Predictions for humans from in vivo, ex vivo and animal models. *Adv. Drug Deliv. Rev.* **2007**, *59*, 1152–1161. [[CrossRef](#)] [[PubMed](#)]
14. Hadgraft, J. Skin deep. *Eur. J. Pharm. Biopharm.* **2004**, *58*, 291–299. [[CrossRef](#)] [[PubMed](#)]
15. Ruela, A.L.M.; Perissinato, A.G.; de Lino, M.E.S.; Mudrik, P.S.; Pereira, G.R. Evaluation of skin absorption of drugs from topical and transdermal formulations. *Braz. J. Pharm. Sci.* **2016**, *52*, 527–544. [[CrossRef](#)]
16. Jepps, O.G.; Dancik, Y.; Anissimov, Y.G.; Roberts, M.S. Modeling the human skin barrier—Towards a better understanding of dermal absorption. *Adv. Drug Deliv. Rev.* **2013**, *65*, 152–168. [[CrossRef](#)] [[PubMed](#)]
17. Barry, B.W. Novel mechanisms and devices to enable successful transdermal drug delivery. *Eur. J. Pharm. Sci.* **2001**, *14*, 101–114. [[CrossRef](#)]
18. Blume-Peytavi, U.; Massoudy, L.; Patzelt, A.; Lademann, J.; Dietz, E.; Rasulev, U.; Garcia Bartels, N. Follicular and percutaneous penetration pathways of topically applied minoxidil foam. *Eur. J. Pharm. Biopharm.* **2010**, *76*, 450–453. [[CrossRef](#)]
19. Patzelt, A.; Richter, H.; Knorr, F.; Schäfer, U.; Lehr, C.-M.; Dähne, L.; Sterry, W.; Lademann, J. Selective follicular targeting by modification of the particle sizes. *J. Control. Release* **2011**, *150*, 45–48. [[CrossRef](#)]
20. European Food Safety Authority (EFSA); Buist, H.; Craig, P.; Dewhurst, I.; Hougaard Bennekou, S.; Kneuer, C.; Machera, K.; Pieper, C.; Court Marques, D.; Guillot, G.; et al. Guidance on dermal absorption. *EFSA J.* **2017**, *15*, e04873.
21. Kalia, Y.N.; Guy, R.H. Modeling transdermal drug release. *Adv. Drug Deliv. Rev.* **2001**, *48*, 159–172. [[CrossRef](#)]
22. Machado, A.C.H.R.; Lopes, P.S.; Raffier, C.P.; Haridass, I.N.; Roberts, M.; Grice, J.; Leite-Silva, V.R. Skin Penetration. In *Cosmetic Science and Technology*; Elsevier: Amsterdam, The Netherlands, 2017; pp. 741–755. ISBN 978-0-12-802005-0.
23. Moser, K.; Kriwet, K.; Naik, A.; Kalia, Y.N.; Guy, R.H. Passive skin penetration enhancement and its quantification in vitro. *Eur. J. Pharm. Biopharm.* **2001**, *10*, 103–112. [[CrossRef](#)]
24. Delgado-Charro, M.B.; Guy, R.H. Effective use of transdermal drug delivery in children. *Adv. Drug Deliv. Rev.* **2014**, *73*, 63–82. [[CrossRef](#)] [[PubMed](#)]
25. Dragicevic, N.; Maibach, H.I. *Percutaneous Penetration Enhancers Drug Penetration Into/Through the Skin*; Springer: Berlin/Heidelberg, Germany, 2017; ISBN 978-3-662-53268-3.
26. Machado, M.; Hadgraft, J.; Lane, M.E. Assessment of the variation of skin barrier function with anatomic site, age, gender and ethnicity: Assessment of the variation of skin barrier function. *Int. J. Cosmet. Sci.* **2010**, *32*, 397–409. [[CrossRef](#)] [[PubMed](#)]
27. Waller, J.M.; Maibach, H.I. Age and skin structure and function, a quantitative approach (I): Blood flow, pH, thickness, and ultrasound echogenicity. *Skin Res. Technol.* **2005**, *11*, 221–235. [[CrossRef](#)] [[PubMed](#)]
28. Behl, C.R.; Flynn, G.L.; Barrett, M.; Walters, K.A.; Linn, E.E.; Mohamed, Z.; Kurihara, T.; Ho, N.F.H.; Higuchi, W.I.; Pierson, C.L. Permeability of thermally damaged skin II: Immediate influences of branding at 60 °C on hairless mouse skin permeability. *Burns* **1981**, *7*, 389–399. [[CrossRef](#)]
29. Behl, C.R.; Flynn, G.L.; Kurihara, T.; Smith, W.; Gatmaitan, O.; Higuchi, W.I.; Ho, N.F.H.; Pierson, C.L. Permeability of Thermally Damaged Skin: I. Immediate Influences of 60 °C Scalding on Hairless Mouse Skin. *J. Investig. Derm.* **1980**, *75*, 340–345. [[CrossRef](#)] [[PubMed](#)]

30. Flaten, G.E.; Palac, Z.; Engesland, A.; Filipović-Grčić, J.; Vanić, Ž.; Škalco-Basnet, N. In vitro skin models as a tool in optimization of drug formulation. *Eur. J. Pharm. Sci.* **2015**, *75*, 10–24. [[CrossRef](#)] [[PubMed](#)]
31. OECD. *Test Guideline 427: Skin absorption: In Vivo Method*; OECD: Paris, France, 2004.
32. OECD. *Test Guideline 428: Skin absorption: In Vitro Method*; OECD: Paris, France, 2004.
33. OECD. *Guidance Document for the Conduct of Skin Absorption Studies*; OECD Series on Testing and Assessment; OECD: Paris, France, 2004; ISBN 978-92-64-07879-6.
34. Kielhorn, J. *International Programme on Chemical Safety Dermal Absorption*; Environmental Health Criteria; WHO: Geneva, Switzerland, 2006; ISBN 978-92-4-157235-4.
35. European Centre for Ecotoxicology and Toxicology of Chemicals. *Percutaneous absorption, Monograph*; No. 20; European Centre for Ecotoxicology and Toxicology of Chemicals: Bruxelles, Belgium, 1993; ISSN 0773-6347-20.
36. EPAU.S. Environmental Protection Agency (EPA). Dermal Exposure Assessment: A Summary of EPA Approaches. Available online: <http://www.epa.gov/ncea> (accessed on 1 April 2019).
37. Dumont, C.; Prieto, P.; Asturiol, D.; Worth, A. Review of the Availability of In Vitro and In Silico Methods for Assessing Dermal Bioavailability. *Appl. Vitro. Toxicol.* **2015**, *1*, 147–164. [[CrossRef](#)]
38. Anissimov, Y.G.; Roberts, M.S. Diffusion Modelling of Percutaneous Absorption Kinetics: 4. Effects of a Slow Equilibration Process Within Stratum Corneum on Absorption and Desorption Kinetics. *J. Pharm. Sci.* **2009**, *98*, 772–781. [[CrossRef](#)] [[PubMed](#)]
39. Anissimov, Y.G.; Roberts, M.S. Diffusion Modeling of Percutaneous Absorption Kinetics: 3. Variable Diffusion and Partition Coefficients, Consequences for Stratum Corneum Depth Profiles and Desorption Kinetics. *J. Pharm. Sci.* **2004**, *93*, 470–487. [[CrossRef](#)] [[PubMed](#)]
40. Anissimov, Y.G.; Roberts, M.S. Diffusion modeling of percutaneous absorption kinetics: 2. Finite vehicle volume and solvent deposited solids. *J. Pharm. Sci.* **2001**, *90*, 504–520. [[CrossRef](#)]
41. Anissimov, Y.G.; Roberts, M.S. Diffusion modeling of percutaneous absorption kinetics. 1. Effects of flow rate, receptor sampling rate, and viable epidermal resistance for a constant donor concentration. *J. Pharm. Sci.* **1999**, *88*, 1201–1209. [[CrossRef](#)] [[PubMed](#)]
42. Todo, H.; Oshizaka, T.; Kadhum, W.; Sugibayashi, K. Mathematical Model to Predict Skin Concentration after Topical Application of Drugs. *Pharmaceutics* **2013**, *5*, 634–651. [[CrossRef](#)] [[PubMed](#)]
43. Crank, J. *The Mathematics of Diffusion*, 2nd ed.; Clarendon Press: Oxford, UK, 1975; ISBN 978-0-19-853344-3.
44. Franz, T.J. Percutaneous Absorption. On the Relevance of in Vitro Data. *J. Investig. Derm.* **1975**, *64*, 190–195. [[CrossRef](#)] [[PubMed](#)]
45. Franz, T.J. The Finite Dose Technique as a Valid in vitro Model for the Study of Percutaneous Absorption in Man. In *Current Problems in Dermatology*; Simon, G.A., Paster, Z., Klingberg, M.A., Kaye, M., Eds.; S. Karger AG: Basel, Switzerland, 1979; Volume 7, pp. 58–68. ISBN 978-3-8055-2797-2.
46. Sesto Cabral, M.E.; Ramos, A.N.; Cabrera, C.A.; Valdez, J.C.; González, S.N. Equipment and method for in vitro release measurements on topical dosage forms. *Pharm. Dev. Technol.* **2015**, *20*, 619–625. [[CrossRef](#)] [[PubMed](#)]
47. Diffusion Measurements. Available online: www.hansonresearch.com (accessed on 1 April 2019).
48. Bronaugh, R.L.; Stewart, R.F. Methods for In Vitro Percutaneous Absorption Studies IV: The Flow-Through Diffusion Cell. *J. Pharm. Sci.* **1985**, *74*, 64–67. [[CrossRef](#)] [[PubMed](#)]
49. European Medicines Agency. *FDA Draft Guideline on Quality and Equivalence of Topical Products EMA/CHMP/QWP/708282/2018*; European Medicines Agency: Amsterdam, The Netherlands, 2018.
50. Lee, J.D.; Kim, J.Y.; Jang, H.J.; Lee, B.M.; Kim, K.B. Percutaneous permeability of 1-phenoxy-2-propanol, a preservative in cosmetics. *Regul. Toxicol. Pharm.* **2019**, *103*, 56–62. [[CrossRef](#)]
51. Zhang, Y.; Lane, M.E.; Hadgraft, J.; Heinrich, M.; Chen, T.; Lian, G.; Sinko, B. A comparison of the in vitro permeation of niacinamide in mammalian skin and in the Parallel Artificial Membrane Permeation Assay (PAMPA) model. *Int. J. Pharm.* **2019**, *556*, 142–149. [[CrossRef](#)]
52. Trombino, S.; Russo, R.; Mellace, S.; Varano, G.P.; Laganà, A.S.; Marcucci, F.; Cassano, R. Solid lipid nanoparticles made of trehalose monooleate for cyclosporin-A topic release. *J. Drug Deliv. Sci. Technol.* **2019**, *49*, 563–569. [[CrossRef](#)]
53. Taofiq, O.; Rodrigues, F.; Barros, L.; Barreiro, M.F.; Ferreira, I.C.; Oliveira, M.B. Mushroom ethanolic extracts as cosmeceuticals ingredients: Safety and ex vivo skin permeation studies. *Food Chem. Toxicol.* **2019**, *127*, 228–236. [[CrossRef](#)]

54. Ameen, D.; Michniak-Kohn, B. Development and in vitro evaluation of pressure sensitive adhesive patch for the transdermal delivery of galantamine: Effect of penetration enhancers and crystallization inhibition. *Eur. J. Pharm. Biopharm.* **2019**, *139*, 262–271. [[CrossRef](#)] [[PubMed](#)]
55. Silva-Abreu, M.; Gonzalez-Pizarro, R.; Espinoza, L.C.; Rodríguez-Lagunas, M.J.; Espina, M.; García, M.L.; Calpena, A.C. Thiazolidinedione as an alternative to facilitate oral administration in geriatric patients with Alzheimer's disease. *Eur. J. Pharm. Sci.* **2019**, *129*, 173–180. [[CrossRef](#)] [[PubMed](#)]
56. Intarakumhaeng, R.; Alsheddi, L.; Wanasathop, A.; Shi, Z.; Li, S.K. Skin Permeation of Urea Under Finite Dose Condition. *J. Pharm. Sci.* **2019**, *108*, 987–995. [[CrossRef](#)] [[PubMed](#)]
57. Rajithaa, P.; Shammika, P.; Aiswarya, S.; Gopikrishnan, A.; Jayakumar, R.; Sabitha, M. Chaulmoogra oil based methotrexate loaded topical nanoemulsion for the treatment of psoriasis. *J. Drug Deliv. Sci. Technol.* **2019**, *49*, 463–476. [[CrossRef](#)]
58. Salehi, S.; Boddohi, S. Design and optimization of kollicoat ®IR based mucoadhesive buccal film for co-delivery of rizatriptan benzoate and propranolol hydrochloride. *Mater. Sci. Eng. C* **2019**, *97*, 230–244. [[CrossRef](#)] [[PubMed](#)]
59. Soriano-Ruiz, J.L.; Suñer-Carbó, J.; Calpena-Campmany, A.C.; Bozal-de Febrer, N.; Halbaut-Bellowa, L.; Boix-Montañés, A.; Souto, E.B.; Clares-Naveros, B. Clotrimazole multiple W/O/W emulsion as anticandidal agent: Characterization and evaluation on skin and mucosae. *Coll. Surf. B Biointerfaces* **2019**, *175*, 166–174. [[CrossRef](#)] [[PubMed](#)]
60. Serpe, L.; Muniz, B.V. Full-Thickness Intraoral Mucosa Barrier Models for In Vitro Drug- Permeation Studies Using Microneedles. *J. Pharm. Sci.* **2019**, *108*, 1756–1764. [[CrossRef](#)]
61. Lee, W.-R.; Hsiao, C.-Y.; Huang, T.-H.; Wang, C.-L.; Alalaiwe, A.; Chen, E.-L.; Fang, J.-Y. Post-irradiation recovery time strongly influences fractional laser-facilitated skin absorption. *Int. J. Pharm.* **2019**, *564*, 48–58. [[CrossRef](#)]
62. Kansy, M.; Senner, F.; Gubernator, K. Physicochemical High Throughput Screening: Parallel Artificial Membrane Permeation Assay in the Description of Passive Absorption Processes. *J. Med. Chem.* **1998**, *41*, 1007–1010. [[CrossRef](#)]
63. Ottaviani, G.; Martel, S.; Carrupt, P.-A. Parallel Artificial Membrane Permeability Assay: A New Membrane for the Fast Prediction of Passive Human Skin Permeability. *J. Med. Chem.* **2006**, *49*, 3948–3954. [[CrossRef](#)]
64. Sinkó, B.; Garrigues, T.M.; Balogh, G.T.; Nagy, Z.K.; Tsinman, O.; Avdeef, A.; Takács-Novák, K. Skin-PAMPA: A new method for fast prediction of skin penetration. *Eur. J. Pharm. Sci.* **2012**, *45*, 698–707. [[CrossRef](#)] [[PubMed](#)]
65. Karadzovska, D.; Riviere, J.E. Assessing vehicle effects on skin absorption using artificial membrane assays. *Eur. J. Pharm. Sci.* **2013**, *50*, 569–576.
66. Sinkó, B.; Pálfi, M.; Béni, S.; Kökösi, J.; Takács-Novák, K. Synthesis and Characterization of Long-Chain Tartaric Acid Diamides as Novel Ceramide-Like Compounds. *Molecules* **2010**, *15*, 824–833. [[CrossRef](#)]
67. Sinkó, B.; Vizserálek, G.; Takács-Novák, K. Skin PAMPA: Application in practice. *Admet Dmpk* **2015**, *2*, 191–198. [[CrossRef](#)]
68. Lee, P.H.; Conradi, R.; Shanmugasundaram, V. Development of an in silico model for human skin permeation based on a Franz cell skin permeability assay. *Bioorg. Med. Chem. Lett.* **2010**, *20*, 69–73. [[CrossRef](#)] [[PubMed](#)]
69. Tsinman, K.; Tsinman, O.; Schalau, G.; Aliyar, H.; Huber, R.; Loubert, G. Application of Skin PAMPA to Differentiate between Topical Pharmaceutical Formulations of Ibuprofen. (R6058) in AAPS Annual Meeting and Exposition, Chicago, IL, USA, 2012.
70. Vizserálek, G.; Balogh, T.; Takács-Novák, K.; Sinkó, B. PAMPA study of the temperature effect on permeability. *Eur. J. Pharm.* **2014**, *53*, 45–49. [[CrossRef](#)]
71. Clough, M.; Richardson, N.; Langley, N.; Tsinman, K.; Tsinman, O. Assessment of Transdermal Penetration Enhancement by Topical Pharmaceutical Excipients Using Skin PAMPA Method. (T2267) in AAPS Annual Meeting and Exposition, San Antonio, TX, USA, 2013.
72. Luo, L.; Sinkó, B.; Tsinman, K.; Abdalghafor, H.; Hadgraft, J.; Lane, M. A Comparison of Drug Permeation in the Skin PAMPA Model and the Franz Cell Model. (W5104) in AAPS Annual Meeting and Exposition, San Diego, CA, USA, 2014.
73. Vizserálek, G.; Vizserálek, G. Examination of Permeability of Drugs by PAMPA Method in Theoretical and Practical Aspects. Ph.D. Thesis, Semmelweis University, Budapest, Hungary, 13 December 2016.

74. Ueda, C.T.; Shah, V.P.; Derdzinski, K.; Ewing, G.; Flynn, G.; Maibach, H.; Marques, M.; Rytting, H.; Shaw, S.; Thakker, K.; et al. Topical and Transdermal Drug Products. *Dissolution Technol.* **2010**, *17*, 12–25. [[CrossRef](#)]
75. Selzer, D.; Abdel-Mottaleb, M.M.A.; Hahn, T.; Schaefer, U.F.; Neumann, D. Finite and infinite dosing: Difficulties in measurements, evaluations and predictions. *Adv. Drug Deliv. Rev.* **2013**, *65*, 278–294. [[CrossRef](#)] [[PubMed](#)]
76. Zhai, H.; Maibach, H.I. Effects of Skin Occlusion on Percutaneous Absorption: An Overview. *Skin Pharm. Physiol.* **2001**, *14*, 1–10. [[CrossRef](#)] [[PubMed](#)]
77. Treffel, P.; Muret, P.; Muret-D’Aniello, P.; Coumes-Marquet, S.; Agache, P. Effect of occlusion on in vitro percutaneous absorption of two compounds with different physicochemical properties. *Skin Pharm. Physiol.* **1992**, *5*, 108–113. [[CrossRef](#)]
78. Zhai, H.; Maibach, H.I. Occlusion vs. skin barrier function: Occlusion versus skin barrier function. *Skin Res. Technol.* **2002**, *8*, 1–6. [[CrossRef](#)] [[PubMed](#)]
79. Escobar-Chavez, J.J.; Merino-Sanjuán, V.; López-Cervantes, M.; Urban-Morlan, Z.; Piñón-Segundo, E.; Quintanar-Guerrero, D.; Ganem-Quintanar, A. The Tape-Stripping Technique as a Method for Drug Quantification in Skin. *J. Pharm. Pharm. Sci.* **2008**, *11*, 104. [[CrossRef](#)] [[PubMed](#)]
80. Klang, V.; Schwarz, J.C.; Lenobel, B.; Nadj, M.; Auböck, J.; Wolzt, M.; Valenta, C. In vitro vs. in vivo tape stripping: Validation of the porcine ear model and penetration assessment of novel sucrose stearate emulsions. *Eur. J. Pharm. Biopharm.* **2012**, *80*, 604–614. [[CrossRef](#)] [[PubMed](#)]
81. Pailler-Mattei, C.; Guerret-Piecourt, C.; Zahouani, H.; Nicoli, S. Interpretation of the human skin biotribological behaviour after tape stripping. *J. R. Soc. Interface* **2011**, *8*, 934–941. [[CrossRef](#)] [[PubMed](#)]
82. Lademann, J.; Jacobi, U.; Surber, C.; Weigmann, H.-J.; Fluhr, J.W. The tape stripping procedure—evaluation of some critical parameters. *Eur. J. Pharm. Biopharm.* **2009**, *72*, 317–323. [[CrossRef](#)]
83. DB ALM-Tape Stripping. Available online: <https://ecvam-dbalm.jrc.ec.europa.eu/> (accessed on 2 April 2019).
84. Nagelreiter, C.; Mahrhauser, D.; Wiatschka, K.; Skipiol, S.; Valenta, C. Importance of a suitable working protocol for tape stripping experiments on porcine ear skin: Influence of lipophilic formulations and strip adhesion impairment. *Int. J. Pharm.* **2015**, *491*, 162–169. [[CrossRef](#)]
85. Zhang, L.W.; Monteiro-Riviere, N.A. Use of confocal microscopy for nanoparticle drug delivery through skin. *J. Biomed. Opt.* **2012**, *18*, 061214. [[CrossRef](#)]
86. Förster, M.; Bolzinger, M.-A.; Montagnac, G.; Briançon, S. Confocal Raman microspectroscopy of the skin. *Eur. J. Dermatol.* **2011**, 851–863. [[CrossRef](#)] [[PubMed](#)]
87. Schreiner, V.; Pfeiffer, S.; Lanzendörfer, G.; Wenck, H.; Diembeck, W.; Gooris, G.S.; Proksch, E.; Bouwstra, J. Barrier Characteristics of Different Human Skin Types Investigated with X-Ray Diffraction, Lipid Analysis, and Electron Microscopy Imaging. *J. Investig. Derm.* **2000**, *114*, 654–660. [[CrossRef](#)] [[PubMed](#)]
88. Hofland, H.E.J.; Bouwstra, J.A.; Boddé, H.E.; Spies, F.; Junginger, H.E. Interactions between liposomes and human stratum corneum in vitro: Freeze fracture electron microscopical visualization and small angle X-ray scattering studies. *Br. J. Derm.* **2010**, *132*, 853–866. [[CrossRef](#)] [[PubMed](#)]
89. Wang, P.; An, Y.; Liao, Y. A novel peptide-based fluorescent chemosensor for Cd(II) ions and its applications in bioimaging. *Spectrochim. Acta Part A Mol. Biomol. Spectrosc.* **2019**, *216*, 61–68. [[CrossRef](#)] [[PubMed](#)]
90. König, K.; Ehlers, A.; Stracke, F.; Riemann, I. In vivo Drug Screening in Human Skin Using Femtosecond Laser Multiphoton Tomography. *Skin Pharm. Physiol.* **2006**, *19*, 78–88. [[CrossRef](#)] [[PubMed](#)]
91. Ashtikar, M.; Matthäus, C.; Schmitt, M.; Krafft, C.; Fahr, A.; Popp, J. Non-invasive depth profile imaging of the stratum corneum using confocal Raman microscopy: First insights into the method. *Eur. J. Pharm. Sci.* **2013**, *50*, 601–608. [[CrossRef](#)] [[PubMed](#)]
92. Caspers, P.J.; Lucassen, G.W.; Carter, E.A.; Bruining, H.A.; Puppels, G.J. In Vivo Confocal Raman Microspectroscopy of the Skin: Noninvasive Determination of Molecular Concentration Profiles. *J. Investig. Derm.* **2001**, *116*, 434–442. [[CrossRef](#)] [[PubMed](#)]
93. Dunn, K.W.; Young, P.A. Principles of Multiphoton Microscopy. *Nephron Exp. Nephrol.* **2006**, *103*, e33–e40. [[CrossRef](#)] [[PubMed](#)]
94. Imanishi, Y.; Lodowski, K.H.; Koutalos, Y. Two-Photon Microscopy: Shedding Light on the Chemistry of Vision. *Biochemistry* **2007**, *46*, 9674–9684. [[CrossRef](#)]
95. Plasencia, I.; Norlén, L.; Bagatolli, L.A. Direct Visualization of Lipid Domains in Human Skin Stratum Corneum’s Lipid Membranes: Effect of pH and Temperature. *Biophys. J.* **2007**, *93*, 3142–3155. [[CrossRef](#)]

96. Umino, Y.; Ipponjima, S.; Denda, M. Modulation of lipid fluidity likely contributes to the fructose/xylitol-induced acceleration of epidermal permeability barrier recovery. *Arch. Derm. Res.* **2019**, *311*, 317–324. [[CrossRef](#)] [[PubMed](#)]
97. Batista, A.; Breunig, H.G.; Uchugonova, A.; Morgado, A.M.; König, K. Two-photon spectral fluorescence lifetime and second-harmonic generation imaging of the porcine cornea with a 12-femtosecond laser microscope. *J. Biomed. Opt.* **2016**, *21*, 036002. [[CrossRef](#)] [[PubMed](#)]
98. Carrer, D.C.; Vermehren, C.; Bagatolli, L.A. Pig skin structure and transdermal delivery of liposomes: A two photon microscopy study. *J. Control. Release* **2008**, *132*, 12–20. [[CrossRef](#)] [[PubMed](#)]
99. Hanson, K.M.; Behne, M.J.; Barry, N.P.; Mauro, T.M.; Gratton, E.; Clegg, R.M. Two-Photon Fluorescence Lifetime Imaging of the Skin Stratum Corneum pH Gradient. *Biophys. J.* **2002**, *83*, 1682–1690. [[CrossRef](#)]
100. Verma, D.D.; Verma, S.; Blume, G.; Fahr, A. Liposomes increase skin penetration of entrapped and non-entrapped hydrophilic substances into human skin: A skin penetration and confocal laser scanning microscopy study. *Eur. J. Pharm. Biopharm.* **2003**, *55*, 271–277. [[CrossRef](#)]
101. Alvarez-Román, R.; Naik, A.; Kalia, Y.N.; Fessi, H.; Guy, R.H. Visualization of skin penetration using confocal laser scanning microscopy. *Eur. J. Pharm. Biopharm.* **2004**, *58*, 301–316. [[CrossRef](#)] [[PubMed](#)]
102. Vardaxis, N.J.; Brans, T.A.; Boon, M.E.; Kreis, R.W.; Marres, L.M. Confocal laser scanning microscopy of porcine skin: Implications for human wound healing studies. *J. Anat.* **1997**, *190*, 601–611. [[CrossRef](#)] [[PubMed](#)]
103. Simonetti, O.; Kempenaar, J.A.; Ponec, M.; Hoogstraate, A.J.; Bialik, W.; Schrijvers, A.H.G.J.; Boddé, H.E. Visualization of diffusion pathways across the stratum corneum of native and in-vitro-reconstructed epidermis by confocal laser scanning microscopy. *Arch. Derm. Res.* **1995**, *287*, 465–473. [[CrossRef](#)] [[PubMed](#)]
104. Zellmer, S.; Reissig, D.; Lasch, J. Reconstructed human skin as model for liposome–skin interaction. *J. Control. Release* **1998**, *55*, 271–279. [[CrossRef](#)]
105. van Kuijk-Meuwissen, M.E.M.J.; Mougin, L.; Junginger, H.E.; Bouwstra, J.A. Application of vesicles to rat skin in vivo: A confocal laser scanning microscopy study. *J. Control. Release* **1998**, *56*, 189–196. [[CrossRef](#)]
106. van Kuijk-Meuwissen, M.E.M.J.; Junginger, H.E.; Bouwstra, J.A. Interactions between liposomes and human skin in vitro, a confocal laser scanning microscopy study. *Biochim. Et Biophys. Acta (Bba)-Biomembr.* **1998**, *1371*, 31–39. [[CrossRef](#)]
107. Tuitou, E.; Godin, B.; Dayan, N.; Weiss, C.; Piliponsky, A.; Levi-Schaffer, F. Intracellular delivery mediated by an ethosomal carrier. *Biomaterials* **2001**, *22*, 3053–3059. [[CrossRef](#)]
108. Grams, Y.Y.; Alarukka, S.; Lashley, L.; Caussin, J.; Whitehead, L.; Bouwstra, J.A. Permeant lipophilicity and vehicle composition influence accumulation of dyes in hair follicles of human skin. *Eur. J. Pharm. Sci.* **2003**, *18*, 329–336. [[CrossRef](#)]
109. Grams, Y.Y.; Whitehead, L.; Cornwell, P.; Bouwstra, J.A. Time and depth resolved visualisation of the diffusion of a lipophilic dye into the hair follicle of fresh unfixed human scalp skin. *J. Control. Release* **2004**, *98*, 367–378. [[CrossRef](#)] [[PubMed](#)]
110. Chen, G.; Ji, C.; Miao, M.; Yang, K.; Luo, Y.; Hoptroff, M.; Collins, L.Z.; Janssen, H.-G. Ex-vivo measurement of scalp follicular infundibulum delivery of zinc pyrithione and climbazole from an anti-dandruff shampoo. *J. Pharm. Biomed. Anal.* **2017**, *143*, 26–31. [[CrossRef](#)] [[PubMed](#)]
111. Binder, L.; SheikhRezaei, S.; Baierl, A.; Gruber, L.; Wolzt, M.; Valenta, C. Confocal Raman spectroscopy: In vivo measurement of physiological skin parameters—A pilot study. *J. Derm. Sci.* **2017**, *88*, 280–288. [[CrossRef](#)] [[PubMed](#)]
112. Nakagawa, N.; Matsumoto, M.; Sakai, S. In vivo measurement of the water content in the dermis by confocal Raman spectroscopy. *Skin Res. Technol.* **2010**, *16*, 137–141. [[CrossRef](#)]
113. Sigurdsson, S.; Philipsen, P.A.; Hansen, L.K.; Larsen, J.; Gniadecka, M.; Wulf, H.C. Detection of Skin Cancer by Classification of Raman Spectra. *IEEE Trans. Biomed. Eng.* **2004**, *51*, 1784–1793. [[CrossRef](#)]
114. Bakonyi, M.; Gácsi, A.; Kovács, A.; Szűcs, M.-B.; Berkó, S.; Csányi, E. Following-up skin penetration of lidocaine from different vehicles by Raman spectroscopic mapping. *J. Pharm. Biomed. Anal.* **2018**, *154*, 1–6. [[CrossRef](#)]
115. Berkó, S.; Zsikó, S.; Deák, G.; Gácsi, A.; Kovács, A.; Budai-Szűcs, M.; Pajor, L.; Bajory, Z.; Csányi, E. Papaverine hydrochloride containing nanostructured lyotropic liquid crystal formulation as a potential drug delivery system for the treatment of erectile dysfunction. *Drug Des. Dev.* **2018**, *12*, 2923–2931. [[CrossRef](#)]

116. Ilchenko, O.; Pilgun, Y.; Makhnii, T.; Slipets, R.; Reynt, A.; Kutsyk, A.; Slobodianiuk, D.; Koliada, A.; Krasnenkov, D.; Kukharsky, V. High-speed line-focus Raman microscopy with spectral decomposition of mouse skin. *Vib. Spectrosc.* **2016**, *83*, 180–190. [[CrossRef](#)]
117. Pyatski, Y.; Zhang, Q.; Mendelsohn, R.; Flach, C.R. Effects of permeation enhancers on flufenamic acid delivery in Ex vivo human skin by confocal Raman microscopy. *Int. J. Pharm.* **2016**, *505*, 319–328. [[CrossRef](#)] [[PubMed](#)]
118. dos Santos, L.; Téllez, S.C.A.; Sousa, M.P.J.; Azoia, N.G.; Cavaco-Paulo, A.M.; Martin, A.A.; Favero, P.P. In vivo confocal Raman spectroscopy and molecular dynamics analysis of penetration of retinyl acetate into stratum corneum. *Spectrochim. Acta Part A Mol. Biomol. Spectrosc.* **2017**, *174*, 279–285. [[CrossRef](#)] [[PubMed](#)]
119. Smith, G.P.S.; McGoverin, C.M.; Fraser, S.J.; Gordon, K.C. Raman imaging of drug delivery systems. *Adv. Drug Deliv. Rev.* **2015**, *89*, 21–41. [[CrossRef](#)] [[PubMed](#)]
120. Franzen, L.; Windbergs, M. Applications of Raman spectroscopy in skin research—From skin physiology and diagnosis up to risk assessment and dermal drug delivery. *Adv. Drug Deliv. Rev.* **2015**, *89*, 91–104. [[CrossRef](#)] [[PubMed](#)]
121. Vajna, B. Multivariate Curve Resolution and Regression Methods in Raman Chemical Imaging. Ph.D. Thesis, Budapest University of Technology and Economics, Budapest, Hungary, 30 November 2012.
122. Zhang, G.; Moore, D.J.; Sloan, K.B.; Flach, C.R.; Mendelsohn, R. Imaging the Prodrug-to-Drug Transformation of a 5-Fluorouracil Derivative in Skin by Confocal Raman Microscopy. *J. Investig. Derm.* **2007**, *127*, 1205–1209. [[CrossRef](#)]
123. Zhang, G.; Flach, C.R.; Mendelsohn, R. Tracking the dephosphorylation of resveratrol triphosphate in skin by confocal Raman microscopy. *J. Control. Release* **2007**, *123*, 141–147. [[CrossRef](#)]
124. Freudiger, C.W.; Min, W.; Saar, B.G.; Lu, S.; Holtom, G.R.; He, C.; Tsai, J.C.; Kang, J.X.; Xie, X.S. Label-Free Biomedical Imaging with High Sensitivity by Stimulated Raman Scattering Microscopy. *Science* **2008**, *322*, 1857–1861. [[CrossRef](#)]
125. Mélot, M.; Pudney, P.D.A.; Williamson, A.-M.; Caspers, P.J.; Van Der Pol, A.; Puppels, G.J. Studying the effectiveness of penetration enhancers to deliver retinol through the stratum corneum by in vivo confocal Raman spectroscopy. *J. Control. Release* **2009**, *138*, 32–39. [[CrossRef](#)]
126. Gotter, B.; Faubel, W.; Neubert, R.H.H. FTIR microscopy and confocal Raman microscopy for studying lateral drug diffusion from a semisolid formulation. *Eur. J. Pharm. Biopharm.* **2010**, *74*, 14–20. [[CrossRef](#)]
127. Saar, B.G.; Contreras-Rojas, L.R.; Xie, X.S.; Guy, R.H. Imaging Drug Delivery to Skin with Stimulated Raman Scattering Microscopy. *Mol. Pharm.* **2011**, *8*, 969–975. [[CrossRef](#)] [[PubMed](#)]
128. Franzen, L.; Selzer, D.; Fluhr, J.W.; Schaefer, U.F.; Windbergs, M. Towards drug quantification in human skin with confocal Raman microscopy. *Eur. J. Pharm. Biopharm.* **2013**, *84*, 437–444. [[CrossRef](#)] [[PubMed](#)]



© 2019 by the authors. Licensee MDPI, Basel, Switzerland. This article is an open access article distributed under the terms and conditions of the Creative Commons Attribution (CC BY) license (<http://creativecommons.org/licenses/by/4.0/>).

III

Article

Novel In Vitro Investigational Methods for Modeling Skin Permeation: Skin PAMPA, Raman Mapping

Stella Zsikó , Erzsébet Csányi , Anita Kovács, Mária Budai-Szűcs , Attila Gácsi and Szilvia Berkó * 

Institute of Pharmaceutical Technology and Regulatory Affairs, Faculty of Pharmacy, University of Szeged, Eötvös u. 6, H-6720 Szeged, Hungary; zsiko.stella@pharm.u-szeged.hu (S.Z.); csanyi@pharm.u-szeged.hu (E.C.); anita.kovacs@pharm.u-szeged.hu (A.K.); maria.szucs@pharm.u-szeged.hu (M.B.-S.); gacsi.attila@pharm.u-szeged.hu (A.G.)

* Correspondence: berkosz@pharm.u-szeged.hu

Received: 22 July 2020; Accepted: 23 August 2020; Published: 25 August 2020



Abstract: The human skin is marked as a standard by the regulatory agencies in the permeation study of dermal formulations. Artificial membranes can substitute human skin to some extent. Academicians and pharmaceutical corporations are focusing their efforts on developing standardized protocols and safe, reliable options to substitute human skin for carrying out permeability studies. Our research aim was to study the applicability of new techniques in the case of different types of dermal formulations. The skin parallel artificial membrane permeability assay (PAMPA) method and Raman mapping were compared to the gold-standard Franz cell method. A hydrogel and two types of creams were investigated as the most generally used dermal preparations. The values of the diffused drug were closer to each other in PAMPA and Franz cell measurement. The diffused amount of drug showed the same order for the different formulations. These results correlate well with the results of Raman mapping. Our conclusions suggest that all early screening examinations can be performed with model tools such as skin PAMPA supplemented with methods like Raman mapping as a semi-quantitative method.

Keywords: skin PAMPA; Raman mapping; Franz cell; drug release; skin permeation; in vitro release test (IVRT); in vitro permeation test (IVPT)

1. Introduction

The growing number of dermal formulations requires the development of test methods, in particular appropriate in vitro drug permeation tests. There are some in vitro models which are widely used in skin permeation studies, but there is a demand for more rapid and cost-effective studies that better model the real conditions. Permeation tests are usually made to detect the amount of drug permeated through the skin (or skin mimic membrane) over time in connection with the diffusion area and may provide information on drug release, interactions and mechanisms of drug permeation. In the latest European Medicines Agency (EMA) document (Draft Guideline on Quality and Equivalence of Topical Products) Franz diffusion cell tests are classified as follows: in vitro release tests (IVRT) and in vitro permeation tests (IVPT). One of the greatest differences between IVRT and IVPT tests is the membrane used. In the case of IVRT the membrane is synthetic (lipid-based or non-lipid based model membranes), while in the case of IVPT the membrane is biological (e.g., human epidermis). An IVRT using diffusion cells evaluates the rate and extent of release of an active substance from the proposed formulation. An IVPT is used to characterize the permeation profile of the drug, which is an acceptable permeation kinetic test. In the early stages of development, IVRT should be used, thereafter, IVPT can be used for promising formulations [1].

The vertical Franz diffusion cell is generally used for modelling the release and permeation of drugs in the case of dermal drug delivery systems. This device consists of a cell that holds a chamber for drug application, a membrane (it can be synthetic and biological, too) within which the drug may diffuse, and an acceptor media chamber from which samples may be examined [2–7]. The most relevant membrane for assessing the in vitro permeation of drugs is the human skin. Excised human skin layer (epidermis) is the gold standard. The availability of human skin is limited, so artificial membranes are often used [4,8–10]. However, it has been found that simple artificial membranes do not match the characteristics of the skin and, consequently, their use is suggested only in the determination of drug release. Therefore, there is a growing demand for new artificial membranes that model the human skin well to provide relevant and useful results in predicting the permeation of the drug from the dermal drug delivery preparations [1,11].

Artificial skin surrogates have a long history. Nowadays, more and more complex membrane systems have become available. When porous filters are loaded with lipids, these substitutes are more similar to skin attributes [12]. Based on the parallel artificial membrane permeability assay technique (PAMPA), which has been used successfully to predict gastrointestinal and blood-brain barrier absorption, Ottaviani et al. described the use of a skin PAMPA first. This skin PAMPA membrane is filled with an optimized mixture of silicone (70%) and isopropyl myristate (30%) to reduce skin permeability [13]. Recently a novel skin PAMPA model has become available where the membrane contains the special components of the skin barrier such as cholesterol, free fatty acid, and a ceramide-analogue compound which imitates the features of skin lipid matrix [14,15]. This PAMPA is specifically designed for modelling permeation through the skin. It is a 96-well plate-based method so it is a fast, low-cost and high-throughput method. So far, there have been few measurement results, but they are encouraging [16–22].

In addition to permeation studies through different membranes, the Raman microscopy method has been developed as an important technique for a better understanding of skin structure and drug delivery via human skin [23]. Raman spectroscopy can give information about the spatial distribution of the drug in the skin layers based on the characteristic vibrational energy levels of the structure of a molecule. This semi-quantitative technique is suitable for monitoring the permeation of exogenous materials into the skin layers [24–28].

Currently, skin PAMPA is not listed in the official recommendations of skin permeation methods but Raman spectroscopy can be used [1]. Skin PAMPA is a relatively new method still under development. In the future, if there is enough favorable investigation, it might be recommended by authorities. Confocal Raman spectroscopy is not sufficiently established to provide pivotal equivalence data but it may be supportive; thus, research of this area is very important in order to broaden the available methods for more predictable investigation of skin permeation.

The aim of this research was to investigate the applicability of skin PAMPA and Raman mapping methods compared with the widely used gold-standard Franz cell method. The most commonly used dermal preparations such as a hydrogel and two types of creams (containing diclofenac sodium, DFNa) were investigated.

2. Materials and Methods

2.1. Materials

Diclofenac sodium, ethanol, cetyl-stearyl alcohol, liquid paraffin, white petrolatum, microbiological preservative, beeswax, wool fat, oleyl oleate and castor oil were obtained from Hungaropharma Ltd. (Budapest, Hungary). Polysorbate 60 was obtained from Sigma-Aldrich (Budapest, Hungary). MethocelTM E4M (hydroxypropyl methylcellulose) was purchased from Colorcon (Budapest, Hungary). The water used has been filtered and deionized using the Millipore (Milford, MA, USA) Milli-Q method. The skin PAMPA sandwiches (P/N: 120657), hydration solution (P/N: 120706) and stirring bars (P/N: 110066) were purchased from Pion, Inc. (Woburn, MA, USA).

The UV plates were from Greiner Bio-one (Kremsmünster, Austria). UV-star microplate has been used (transparent, flat bottom, half area). The cellulose acetate filter (Porafil membrane filter, cellulose acetate, pore diameter: 0.45 μm) was purchased from Macherey-Nagel GmbH & Co. KG (Düren, Germany). Excised human skin was collected by routine plastic surgery treatment from a Caucasian female patient at the Department of Dermatology and Allergology, Szeged University. The in vitro skin permeation procedure does not require ethical approval or consent of the patient in compliance with Health Act CLIV of 1997, Section 210/A in Hungary. The Ethical Committee of the University of Szeged, Albert Szent-Györgyi Clinical Center was informed about the investigations (Human Investigation Review Board license number: 83/2008).

2.2. Methods

2.2.1. Sample Preparations

The conventional hydrogel was prepared with 1% (*w/w*) DFNa dissolved in the mixture of purified water (65.5%) and ethanol (30%). Methocel E4M (3%) and microbiological preservative (0.5%) were added. In the case of the *o/w* cream, the oily phase consisting of cetyl-stearyl alcohol (4%), liquid paraffin (12%), white petrolatum (20%) and polysorbate 60 (4%) was heated up to 60 °C. Then, hot water (57%) was added to the oily phase under agitation. DFNa (1%) was dispersed in the preparation and it was homogenized until the mixture was cooled. Finally, the microbiological preservative (2%) was added. In the case of the *w/o* cream, the oily phase consisting of beeswax (10%), wool fat (10%), oleyl oleate (5%) and castor oil (40%) was heated up to 60 °C. Then, hot water (29%) was added to the oily phase under agitation. Finally, DFNa (1%) was dispersed in the preparation and it was homogenized.

2.2.2. Drug Release and Permeation Studies

A vertical Franz type diffusion cell (Logan Automated Dry heat sampling system, Logan Instruments Corporation, NJ, USA) was used to model the drug release from the formulations through a synthetic membrane (IVRT) and permeation through human heat-separated epidermis (IVPT). As the synthetic membrane, 0.45 μm cellulose membrane (Porafil membrane filter, cellulose acetate) was used. The heat-separated human epidermis (HSE) was prepared with the following method: the excised human subcutaneous fat-free skin was placed in a water bath (60 ± 0.5 °C, 1 min), and the epidermis was separated from the dermis. A quantity of 0.300 g of the sample was placed on the membrane in the donor chamber. Thermostated phosphate buffer solution (PBS pH 7.4 ± 0.15), made in-house, kept at 32 ± 0.5 °C was used as the receptor phase which was 9 mL. The investigation lasted for 6 h (sampling times: 0.5; 1; 2; 3; 4; 5; 6 h). A Thermo Scientific Evolution 201 spectrometer with a Thermo Insight v1.4.40 software kit (Thermo Fisher Scientific, Waltham, MA, USA) at a wavelength of 275 nm was used to assess the DFNa concentration in the receptor solution.

The skin PAMPA sandwiches were used after 24 h hydration time. A special hydration solution (Pion, Inc., Billerica, MA, USA) was used. As donor phase, 70 μL of the preparations were used in all well of the formulation plate. As receptor phase, phosphate buffer solution (PBS pH 7.4 ± 0.15) was used. The top plate was loaded with a fresh receptor solution of 250 μL , and a stirring bar was also used in each well. The Gut-Box™ from Pion, Inc. was used for stirring; the sandwich was incubated at 32 °C. The receptor solution was analyzed after 0.5, 1, 2, 3, 4, 5 and 6 h of incubation [21]. The quantity of DFNa was measured with UV spectroscopy at 275 nm using a SPECTROstarNano UV plate reader by BMG LABTECH GmbH (Ortenberg, Germany).

Permeation profiles of dermal formulations were obtained. The cumulative amount (*Q*) of DFNa penetrated per cm^2 at 6 h was calculated. The flux (*J*) was the slope of the cumulative amounts of DFNa ($\mu\text{g}/\text{cm}^2$) permeated versus time (h) profiles. Time point correlations between the amounts of drug penetrated through heat-separated human epidermis and skin PAMPA membrane were shown and correlation coefficients (R^2) were calculated.

2.2.3. Investigation of Skin Permeation with Raman Microscopy

Excised human subcutaneous fat-free skin (epidermis and dermis) was used. It was obtained from a Caucasian female patient who underwent abdominal plastic surgery. 1 cm² of the skin surface was treated with the formulations for 3 h at 32 °C. The treated skins were frozen and sectioned (10-µm-thick cross-sections) with a Leica CM1950 cryostat (Leica Biosystems GmbH, Wetzlar, Germany). The microtomed skin samples were placed on an aluminum surface with the SC towards the top of the plate. Raman spectroscopic measurements were made with a Thermo Fisher DXR Dispersive Raman Spectrometer (ThermoFisher Scientific Inc., Waltham, MA, USA) equipped with a CCD camera and a diode laser. A laser light source of 780 nm wavelength was used, with a maximum power of 24 mW, which is the best source for studying biological samples, presenting sufficient energy for the vibrations of protein alternatives in the skin. With the use of this type of laser source, fluorescence had less effect. The microscopic lens used for the measurements was magnified by 50 × and the pinhole aperture was 25 µm. A 200 to 1.800 µm area was explored in the case of chemical mapping; the step size was 50 µm vertically and horizontally. 205 spectra were observed, 16 scans were reported to accumulate each spectrum, and the exposure period was 2 s. When analyzing the treated vs. untreated skin samples, the different spectra of each component of the formulations and diclofenac sodium were used as reference points. A laser light of 532 nm was used to record the different spectra of the components and formulations. 32 scans were registered for each spectrum, with an exposure time of 6 s. The optics magnitude in the Raman microscope was 10 with a 25 µm slit aperture. Data acquisition and analysis were accomplished using OMNICTM8.2 for Dispersive Raman software package (ThermoFisher Scientific Inc., Waltham, MA, USA) [24,27].

2.2.4. Statistical Analysis

Statistical data analysis was performed using Prism for Windows software (GraphPad Software Inc., La Jolla, CA, USA). The values were compared using two-way ANOVA followed by the Bonferroni test. A level of $p \leq 0.05$ was taken as significant, $p \leq 0.01$ as very significant, and $p \leq 0.001$ as highly significant.

3. Results and Discussion

In the case of dermal permeations, there are three main parameters which influence the effect: the characteristics of the active ingredient, the properties of the formulation and the condition of the skin [29,30]. From among the three main parameters, the properties of the preparation were changed in this study, and the measurements were performed with Franz cell, skin PAMPA and Raman spectroscopy. Three most commonly used dermal formulations were compared: a hydrogel and *o/w* and *w/o* creams.

3.1. Comparison Study of Franz Cell and Skin PAMPA

The Franz cell method and the skin PAMPA methods are based on the quantitative measurement of drug permeation through a skin-mimicking membrane. Figure 1. shows the amount of drug passing through the different membranes in 6 h in percentage from the different types of formulations. In the IVRT measurement, most of the DFNa was released from the hydrogel within 6 h, followed by the *o/w* cream, and the least drug was detectable from the *w/o* cream. In the IVPT test (gold-standard method), significantly less drug was delivered to the receptor chamber compared to IVRT, and if the formulations were aligned, different result was obtained. The most diffused active ingredients were detected with the *o/w* cream, followed by the hydrogel and the least with the *w/o* cream. This is due to the barrier function of the skin, which is primarily responsible for the stratum corneum cell layer. It is important to know the extent of release (IVRT), but this does not provide relevant information for penetration. It is clear that it is very important to examine the permeation process through the skin to

know not only the released amount of drug, but also to see the interactions of the drug or the drug delivery system with the skin.

The results of the skin PAMPA method were compared to the results of the IVPT and IVRT methods. The detected DFNa values were closer to the values measured on HSE than the data from the IVRT tests. The diffused amount of drug from the different formulations showed the same order for both the IVPT and the skin PAMPA methods: *o/w* cream > hydrogel > *w/o* cream. In the case of skin PAMPA, the SD values were lower compared with IVPT, where the variability and differences of the human skin membrane are higher.

In addition to the order, it can be concluded that significantly more DFNa penetrated through the cellulose membrane and skin PAMPA vs. HSE, however, the results of skin PAMPA are closer to the results of HSE.

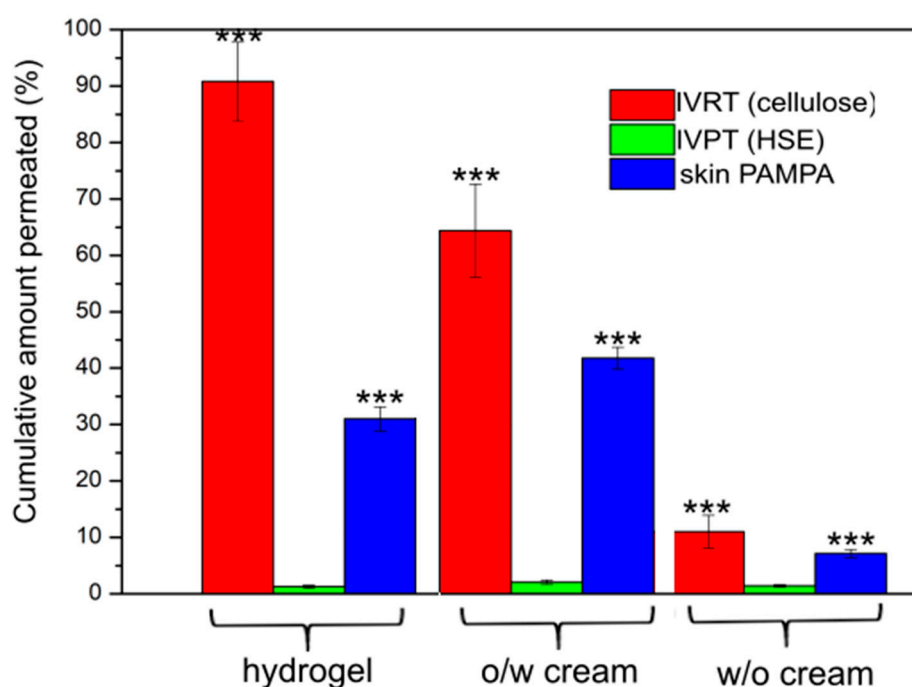


Figure 1. Cumulative amount permeated at the end of 6 h (%). *** $p < 0.001$ vs. HSE.

The mathematical evaluation of the results is shown in Table 1. Permeation parameters (Q , and J) show the differences between the methods and formulations. There were significant differences between the formulations, so it is clear that all methods have good sensitivity to show significant differentiation between the different formulations, so it is a very good tool in the preformulation phase to find the best suited one for the purpose of use. A comparison of the results indicates that the skin PAMPA method was closer to the gold standard (IVPT) method. Its use before IVPT tests may be beneficial as it shows differences between formulations in the same way as HSE. Thus, in pharmaceutical developments, less effective preparations can be excluded quickly and cheaply from the many formulations.

Table 1. Permeation parameters of diclofenac sodium through cellulose membrane, heat-separated human epidermis and skin parallel artificial membrane permeability assay (PAMPA) membrane after 6 h.

Formulation	Q at 6 h (μg/cm²)	J (μg/cm²/h)		
IVRT (cellulose membrane)				
Hydrogel	1552.0 ± 98.9	***	***	76.03
O/W cream	1092.9 ± 98.4			179.13
W/O cream	188.2 ± 48.8			31.36
IVPT (HSE)				
Hydrogel	45.18 ± 4.15	*	***	7.32
O/W cream	56.1 ± 8.6			8.37
W/O cream	31.4 ± 6.0			4.50
skin PAMPA membrane				
Hydrogel	310.1 ± 21.4	***	***	52.59
O/W cream	417.6 ± 19.7			68.51
W/O cream	71.5 ± 7.1			11.85

Q, cumulative amount of diclofenac sodium penetrated per cm^2 at 6 h (mean \pm SD, $n = 6$); J, flux determined from the slope of the cumulative amounts of diclofenac sodium permeated ($\mu\text{g}/\text{cm}^2$) versus time (h) profiles; * $p < 0.05$, ***, $p < 0.001$.

Figure 2 shows the correlation of the skin PAMPA membrane to HSE. The skin PAMPA membrane demonstrates high correlation to HSE in this study. The time point correlation between skin PAMPA and HSE was in the range of 0.93–0.99.

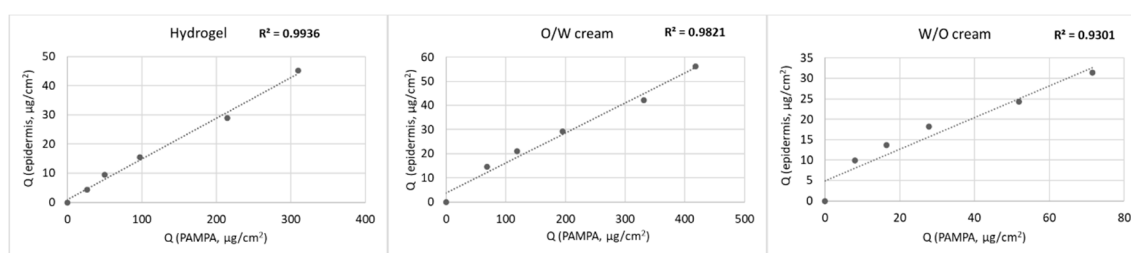


Figure 2. Diclofenac sodium permeation, time point correlations between the amounts of drug penetrated through heat-separated human epidermis and skin PAMPA membrane.

3.2. RAMAN Mapping

The Raman correlation map proves the presence of the penetrated drug formulations in the different regions of the human skin, from the skin surface to the lower layers of the dermis after the treatment with the different compositions. The Raman spectra of the skin are really diverse and consist of numerous bands originating from different skin segments (e.g., nucleic acids, lipids, proteins) [27,31,32]. Several bands are overlapping with the spectra of the examined preparations. During the Raman experiments, the differences in the localization in the skin regions of the formulations were determined and compared with the Franz cell and skin PAMPA results.

The correlation maps, which showed the distribution of DFNa, were produced by fitting the appropriate spectra to the spectra of the treated skin. DFNa is easily determined from the formulations but the intensities of the characteristic DFNa peaks are very low. Therefore, the spectra of the pure API

could not be used to make an acceptable correlation map. In this case, we had to use the spectrum of the whole preparation to make the skin distribution correlation maps, which indicates the presence of DFNa as well. The spectral maps were resolved in order to verify the presence of the formulation in the different regions of the human skin. The fingerprint region of the preparation spectra was related to the spectra of human skin spectra being tested and untreated. The similarity was shown as intensity. The distribution profiles describing the relationship between the map spectra (treated skin specimen) and the defined reference spectrum (fingerprint region) were created. The resulting correlation intensity values of the map spectra are similar to the match values of the reference spectra. A more powerful intensity rate means a higher correlation with the reference spectrum.

The Raman chemical maps of the preparations are shown in Figure 3. In the case of the hydrogel, the most penetrated drugs are found in the upper layers of the skin, the epidermis and the upper dermis. The oil-in-water cream was most penetrated into the deeper layers of the skin. This is due to the emulsifier, which increases permeation. In the case of the water-in-oil cream, most of the composition could be found only in the stratum corneum region, and deeper permeation was blocked. This is due to its really high oil content in the external phase, which cannot pass through the hydrophilic layer of the epidermis.

These results correlate well with the results of IVPT and skin PAMPA. In correlation with these results, the *o/w* cream shows the most effective permeation results where the formulation could be found in the dermis, followed by hydrogel, where the formulation passed through the regions of the epidermis and dermis. The permeation of the *w/o* cream was the lowest with all the methods during the time of the experiment.

In the case of IVRT measurements, the hydrogel showed the highest drug release values. The hydrogel is an aqueous-based system where the drug is in a dissolved form, and diffusion through the synthetic membrane is high. The highest permeation from the *o/w* cream was observed in the IVPT and Skin PAMPA measurements because DFNa is in the outer aqueous phase of the cream, and the emulsifier content of the cream promotes penetration through human skin and special skin-mimicking membrane. The release and permeation of DFNa from the *w/o* cream were extremely low in all measurements. The drug is presumably in the inner phase of the cream, and the low diffusion and penetration can be explained by the fact that the diffusion of DFNa through the oil phase limits the release of the drug.

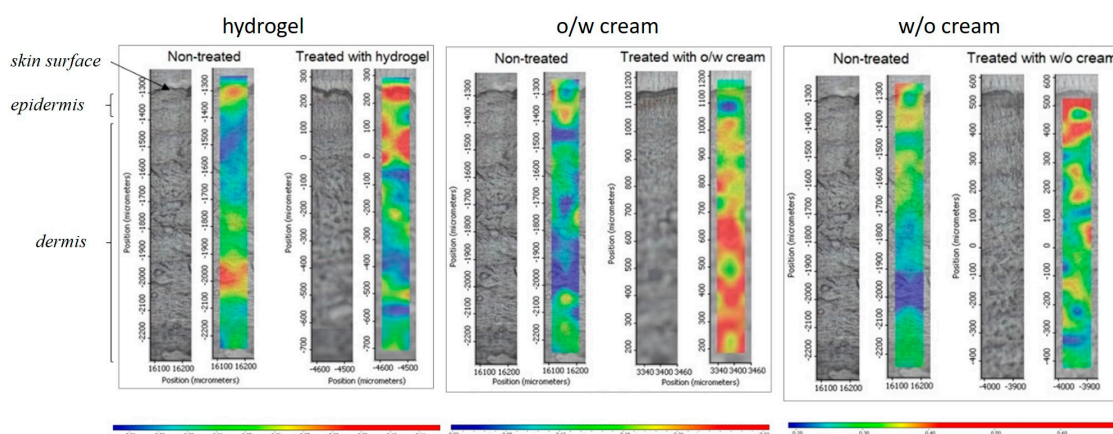


Figure 3. Raman correlation maps for the distribution of diclofenac sodium in human skin specimens after treatment with hydrogel, *o/w* cream and *w/o* cream. Untreated skin is also displayed as a control in all cases. Color coding of drug formulation content: red > yellow > green > blue.

4. Conclusions

The skin PAMPA method was investigated to prove the applicability in skin permeation tests. This method presented high correlations with the IVPT method compared to different dermal formulations. The ranking of the penetrated drug from different formulations was the same, but the permeability rates were different. The skin PAMPA system seems to be an ideal test before IVPT using human skin with a defined thickness. The advantages of PAMPA method are as follows: it is easy to use and store, comparatively low-cost, inert, and gives reproducible results. The main disadvantage of this method is that the measurement time is usually limited (6 h).

This work also highlights the capability of Raman spectroscopy as a nondestructive technique for studying skin distribution and following the active ingredient in the skin layers. It could estimate the relative amounts of preparations penetrated into the different skin layers semi-quantitatively. It is important to understand how different formulations influence the permeation of active agents into/through the skin as this presents relevant information for formulation developers. Like all measurement methods, Raman mapping has its drawbacks. It is difficult to reproduce, expensive lasers are needed, only qualitative information can be extracted, the measurement time is usually long, and not all active substances can be tested with Raman. Its use is recommended for formulations that have previously performed well on IVRT and IVPT tests. Currently, only qualitative (or semi-quantitative) determinations are possible with Raman mapping, but thanks to continuous improvements, quantitative evaluations may also be feasible in the future [25,33,34].

In the current study, the results of Raman mapping have high correlation with the results of skin PAMPA and IVPT methods. Based on our results, the conclusions suggest that all early screening examinations can be performed with model tools such as IVRT and skin PAMPA using cheaper synthetic membranes, and these final formulations should be examined with IVPT to collect permeation data supplemented with qualitative methods like Raman mapping using human skin.

In conclusion, this study has proved that the new skin PAMPA method and the Raman mapping technique have the potential to be used as a screening tool to choose the best dermal formulation in the pharmaceutical, cosmetic, and personal care industries. Future studies in this field are still needed to examine and compare the different methods. Other types of formulations and active substances should also be tested. It would also be useful to study different drug concentrations for the same formulations to support the suitability of the method for monitoring dermal penetration. The development of methodologies to improve the throughput of formulation testing will help to promote a better understanding of preparation variables and mechanisms of skin permeation. Therefore, it is essential to highlight that the investigated in vitro models provide important tools for screening a series of drug formulations, evaluation of skin permeation and mechanism of action of the carrier systems, and evaluation of rank of skin transport.

Author Contributions: Conceptualization, S.Z. and S.B.; methodology, S.Z. and S.B.; software, M.B.-S.; validation, A.K.; formal analysis, S.Z.; investigation, S.Z.; writing—original draft preparation, S.Z.; writing—review and editing E.C.; visualization, S.Z. and A.G.; supervision, S.B. and E.C. All authors have read and agreed to the published version of the manuscript.

Funding: This research received no external funding.

Acknowledgments: We are grateful for the financial support of the Economic Development and Innovation Operational Programme (GINOP 2.2.1-15-2016-00023) as they have made this research possible. This is a tender announced by the Hungarian state, from a European Union source. The tender greatly contributed to the procurement of the instruments. The publication was supported by The University of Szeged Open Access Fund (FundRef, Grant No. 4861).

Conflicts of Interest: The authors declare no conflict of interest.

References

1. *Draft Guideline on Quality and Equivalence of Topical Products*; EMA/CHMP/QWP/708282/2018; European Medicines Agency: Amsterdam, The Netherlands, 2018.
2. Ruela, A.L.M.; Perissinato, A.G.; Lino, M.E.; Mudrik, P.S.; Pereira, G.R. Evaluation of skin absorption of drugs from topical and transdermal formulations. *Braz. J. Pharm. Sci.* **2016**, *52*, 527–544. [[CrossRef](#)]
3. Hauck, W.W.; Shah, V.P.; Shaw, S.W.; Ueda, C.T. Reliability and Reproducibility of Vertical Diffusion Cells for Determining Release Rates from Semisolid Dosage Forms. *Pharm. Res.* **2007**, *24*, 2018–2024. [[CrossRef](#)] [[PubMed](#)]
4. OECD. *Test Guideline 428: Skin Absorption: In Vitro Method*; OECD: Paris, France, 2004.
5. European Food Safety Authority (EFSA); Buist, H.; Craig, P.; Dewhurst, I.; Hougaard Bennekou, S.; Kneuer, C.; Machera, K.; Pieper, C.; Court Marques, D.; Guillot, G.; et al. Guidance on dermal absorption. *EFSA J.* **2017**, *15*. [[CrossRef](#)]
6. Moser, K.; Kriwet, K.; Naik, A.; Kalia, Y.N.; Guy, R.H. Passive skin penetration enhancement and its quantification in vitro. *Eur. J. Pharm. Biopharm.* **2001**, *10*, 103–112. [[CrossRef](#)]
7. Zsikó, S.; Csányi, E.; Kovács, A.; Budai-Szűcs, M.; Gácsi, A.; Berkó, S. Methods to Evaluate Skin Penetration in Vitro. *Sci. Pharm.* **2019**, *87*, 19. [[CrossRef](#)]
8. Machado, A.C.H.R.; Lopes, P.S.; Raffier, C.P.; Haridass, I.N.; Roberts, M.; Grice, J.; Leite-Silva, V.R. Skin Penetration. In *Cosmetic Science and Technology*; Elsevier: Amsterdam, The Netherlands, 2017; pp. 741–755, ISBN 978-0-12-802005-0.
9. OECD. *Guidance Notes on Dermal Absorption, Series on Testing and Assessment No. 156*; OECD: Paris, France, 2011.
10. Abd, E.; Yousuf, S.; Pastore, M.; Telaprolu, K.; Mohammed, Y.; Namjoshi, S.; Grice, J.; Roberts, M. Skin models for the testing of transdermal drugs. *Clin. Pharmacol. Adv. Appl.* **2016**, *8*, 163–176. [[CrossRef](#)]
11. Neupane, R.; Boddur, S.H.S.; Renukuntla, J.; Babu, R.J.; Tiwari, A.K. Alternatives to Biological Skin in Permeation Studies: Current Trends and Possibilities. *Pharmaceutics* **2020**, *12*, 152. [[CrossRef](#)]
12. Flaten, G.E.; Palac, Z.; Engesland, A.; Filipović-Grčić, J.; Vanić, Ž.; Škalko-Basnet, N. In vitro skin models as a tool in optimization of drug formulation. *Eur. J. Pharm. Sci.* **2015**, *75*, 10–24. [[CrossRef](#)]
13. Ottaviani, G.; Martel, S.; Carrupt, P.-A. Parallel Artificial Membrane Permeability Assay: A New Membrane for the Fast Prediction of Passive Human Skin Permeability. *J. Med. Chem.* **2006**, *49*, 3948–3954. [[CrossRef](#)]
14. Sinkó, B.; Kökösi, J.; Avdeef, A.; Takács-Novák, K. A PAMPA Study of the Permeability-Enhancing Effect of New Ceramide Analogues. *Chem. Biodivers.* **2009**, *6*, 1867–1874. [[CrossRef](#)]
15. Sinkó, B.; Garrigues, T.M.; Balogh, G.T.; Nagy, Z.K.; Tsinman, O.; Avdeef, A.; Takács-Novák, K. Skin-PAMPA: A new method for fast prediction of skin penetration. *Eur. J. Pharm. Sci.* **2012**, *45*, 698–707. [[CrossRef](#)]
16. Sinkó, B.; Vizserálek, G.; Takács-Novák, K. Skin PAMPA: Application in practice. *ADMET DMPK* **2015**, *2*. [[CrossRef](#)]
17. Vizserálek, G.; Berkó, S.; Tóth, G.; Balogh, R.; Budai-Szűcs, M.; Csányi, E.; Sinkó, B.; Takács-Novák, K. Permeability test for transdermal and local therapeutic patches using Skin PAMPA method. *Eur. J. Pharm. Sci.* **2015**, *76*, 165–172. [[CrossRef](#)] [[PubMed](#)]
18. Balázs, B.; Vizserálek, G.; Berkó, S.; Budai-Szűcs, M.; Kelemen, A.; Sinkó, B.; Takács-Novák, K.; Szabó-Révész, P.; Csányi, E. Investigation of the Efficacy of Transdermal Penetration Enhancers through the Use of Human Skin and a Skin Mimic Artificial Membrane. *J. Pharm. Sci.* **2016**, *105*, 1134–1140. [[CrossRef](#)]
19. Luo, L.; Patel, A.; Sinko, B.; Bell, M.; Wibawa, J.; Hadgraft, J.; Lane, M.E. A comparative study of the in vitro permeation of ibuprofen in mammalian skin, the PAMPA model and silicone membrane. *Int. J. Pharm.* **2016**, *505*, 14–19. [[CrossRef](#)] [[PubMed](#)]
20. Zhang, Y.; Lane, M.E.; Hadgraft, J.; Heinrich, M.; Chen, T.; Lian, G.; Sinko, B. A comparison of the in vitro permeation of niacinamide in mammalian skin and in the Parallel Artificial Membrane Permeation Assay (PAMPA) model. *Int. J. Pharm.* **2019**, *556*, 142–149. [[CrossRef](#)]
21. Zsikó, S.; Cutcher, K.; Kovács, A.; Budai-Szűcs, M.; Gácsi, A.; Baki, G.; Csányi, E.; Berkó, S. Nanostructured Lipid Carrier Gel for the Dermal Application of Lidocaine: Comparison of Skin Penetration Testing Methods. *Pharmaceutics* **2019**, *11*, 310. [[CrossRef](#)] [[PubMed](#)]
22. Martins, P.P.; Estrada, A.D.; Smyth, H.D.C. A human skin high-throughput formulation screening method using a model hydrophilic drug. *Int. J. Pharm.* **2019**, *565*, 557–568. [[CrossRef](#)] [[PubMed](#)]

23. Dragicevic, N.; Maibach, H.I. *Percutaneous Penetration Enhancers Drug Penetration into/through the Skin*; Springer: Berlin/Heidelberg, Germany, 2017; ISBN 978-3-662-53268-3.
24. Berkó, S.; Zsikó, S.; Deák, G.; Gácsi, A.; Kovács, A.; Budai-Szűcs, M.; Pajor, L.; Bajory, Z.; Csányi, E. Papaverine hydrochloride containing nanostructured lyotropic liquid crystal formulation as a potential drug delivery system for the treatment of erectile dysfunction. *Drug Des. Devel. Ther.* **2018**, *12*, 2923–2931. [[CrossRef](#)]
25. Franzen, L.; Selzer, D.; Fluhr, J.W.; Schaefer, U.F.; Windbergs, M. Towards drug quantification in human skin with confocal Raman microscopy. *Eur. J. Pharm. Biopharm.* **2013**, *84*, 437–444. [[CrossRef](#)]
26. Mao, G.; Flach, C.R.; Mendelsohn, R.; Walters, R.M. Imaging the Distribution of Sodium Dodecyl Sulfate in Skin by Confocal Raman and Infrared Microspectroscopy. *Pharm. Res.* **2012**, *29*, 2189–2201. [[CrossRef](#)] [[PubMed](#)]
27. Bakonyi, M.; Gácsi, A.; Kovács, A.; Szűcs, M.-B.; Berkó, S.; Csányi, E. Following-up skin penetration of lidocaine from different vehicles by Raman spectroscopic mapping. *J. Pharm. Biomed. Anal.* **2018**, *154*, 1–6. [[CrossRef](#)] [[PubMed](#)]
28. Pyatski, Y.; Zhang, Q.; Mendelsohn, R.; Flach, C.R. Effects of permeation enhancers on flufenamic acid delivery in Ex vivo human skin by confocal Raman microscopy. *Int. J. Pharm.* **2016**, *505*, 319–328. [[CrossRef](#)] [[PubMed](#)]
29. Machado, M.; Hadgraft, J.; Lane, M.E. Assessment of the variation of skin barrier function with anatomic site, age, gender and ethnicity: Assessment of the variation of skin barrier function. *Int. J. Cosmet. Sci.* **2010**, *32*, 397–409. [[CrossRef](#)]
30. Jepps, O.G.; Dancik, Y.; Anissimov, Y.G.; Roberts, M.S. Modeling the human skin barrier—Towards a better understanding of dermal absorption. *Adv. Drug Deliv. Rev.* **2013**, *65*, 152–168. [[CrossRef](#)]
31. Synytsya, A.; Alexa, P.; Besserer, J.; De Boer, J.; Froschauer, S.; Gerlach, R.; Loewe, M.; Moosburger, M.; Obstová, I.; Quicken, P.; et al. Raman spectroscopy of tissue samples irradiated by protons. *Int. J. Radiat. Biol.* **2004**, *80*, 581–591. [[CrossRef](#)]
32. Ilchenko, O.; Pilgun, Y.; Makhnii, T.; Slipets, R.; Reynt, A.; Kutsyk, A.; Slobodianiuk, D.; Koliada, A.; Krasnenkov, D.; Kukharsky, V. High-speed line-focus Raman microscopy with spectral decomposition of mouse skin. *Vib. Spectrosc.* **2016**, *83*, 180–190. [[CrossRef](#)]
33. Franzen, L.; Windbergs, M. Accessing Raman spectral variability in human stratum corneum for quantitative in vitro depth profiling: Raman spectral variability in human stratum corneum. *J. Raman Spectrosc.* **2014**, *45*, 82–88. [[CrossRef](#)]
34. Pezzotti, G.; Boffelli, M.; Miyamori, D.; Uemura, T.; Marunaka, Y.; Zhu, W.; Ikegaya, H. Raman spectroscopy of human skin: Looking for a quantitative algorithm to reliably estimate human age. *J. Biomed. Opt.* **2015**, *20*, 065008. [[CrossRef](#)]

